8-30-2011

STIMULATED BRILLOUIN SCATTERING SUPPRESSION VIA TEMPERATURE GRADIENTS IN FIBER AMPLIFIERS

Douglas Nelson

Douglas J. Nelson
Candidate

Optical Science and Engineering
Department

This thesis is approved, and it is acceptable in quality and form for publication:

Approved by the Thesis Committee:

[signature], Chairperson

[signature]

[signature]

[signature]

STIMULATED BRILLOUIN SCATTERING SUPPRESSION VIA TEMPERATURE GRADIENTS IN FIBER AMPLIFIERS

BY

DOUGLAS J. NELSON

B.S. ELECTRICAL ENGINEERING

THESIS

Submitted in Partial Fulfillment of the
Requirements for the Degree of

Master of Science
Optical Science and Engineering

The University of New Mexico
Albuquerque, New Mexico

July, 2011

ACKNOWLEDGMENTS

This thesis was made possible by the hard work of many people. Some helped with lab work and some supplied knowledge or parts, but all are greatly appreciated.

Thanks to Dr. Timothy Newell of the Air Force Research Lab for his continued support, mentoring, and most especially for letting a young lieutenant into his lab.

Thanks to Dr. Wolfgang Rudolf for his patience and instruction.

Thanks to Dane Hult of Trex Enterprises for the countless hours of fiber cleaving and splicing; as well as always having something appropriately inappropriate to say.

Thanks to Andy Lu for supplying the final tap coupler that allowed me to finish my measurements.

Thanks to Chris Vergien for spending the time to teach me how his amplifiers worked.

STIMULATED BRILLOUIN SCATTERING SUPPRESSION VIA TEMPERATURE GRADIENTS IN FIBER AMPLIFIERS

BY

DOUGLAS J. NELSON

ABSTRACT OF THESIS

Submitted in Partial Fulfillment of the
Requirements for the Degree of

Master of Science
Optical Science and Engineering

The University of New Mexico
Albuquerque, New Mexico

July, 2011

STIMULATED BRILLOUIN SCATTERING SUPPRESSION VIA TEMPERATURE GRADIENTS IN FIBER AMPLIFIERS

By

Douglas J. Nelson

B.S., Electrical Engineering, Rose-Hulman Institute of Technology, 2005

ABSTRACT

A method of improving the output power of a 177W narrow linewidth polarization maintaining ytterbium doped fiber amplifier is explored. The limiting factor, Stimulated Brillouin Scattering (SBS), is suppressed with a single-step temperature gradient. A similar fiber amplifier to the 177W amplifier is constructed and tested at various temperatures from 90˚C to -120˚C. The Brillouin frequency is observed to shift with temperature and the Brillouin spectrum splits into two peaks. These peaks correspond to the two temperatures that the fiber amplifier is exposed to and the separation between the peaks determines how strong the SBS suppression will be. Results of the experiment show that output power could be increased to as much as 300W with a temperature gradient of 90˚C.

Table of Contents

List of Figures

List of Tables

1 Introduction

The environment of a fiber amplifier can greatly affect its characteristics. Vibration, pressure, and temperature can each have a beneficial or detrimental effect on a laser system. The goal of this paper is to demonstrate that applying a temperature gradient along a fiber amplifier suppresses Stimulated Brillouin Scattering (SBS) and allows for greater output power. Specifically, we will explore a single step temperature gradient where a portion of gain fiber is either heated or cooled compared to the rest of the fiber.

1.1 Background

Improvements in fiber laser technology will see them replace lasers currently used in semiconductor device manufacturing, surgery, military technology, industrial material processing, remote sensing, imaging, and scientific instrumentation (Galvanauskas, 2004). For narrow spectral linewidth fiber amplifiers, one key obstacle to be overcome is the first nonlinear process capable of damaging or disrupting the laser system, Stimulated Brillouin Scattering (Dajani et al., 2008). Methods currently under investigation to reduce SBS include thermal gradients, polarization effects, large flattened mode area fibers, fibers with modified acoustic properties, and two tone amplification (Dajani et al., 2008).

The United States Air Force, in an attempt to explore coherent beam combining, has developed fiber amplifier chains that are narrow linewidth, polarization maintaining, and output a maximum of 177W. This output power is limited by the onset of SBS. To increase the output power of these amplifiers we will study the effect of applying a temperature gradient on the high power portion of these amplifier chains. While a small temperature gradient is already utilized by slightly heating a portion of the fiber, it is possible that more effective arrangements exist.

The opposite experiment, using SBS to determine a temperature, is useful for both civil and military construction (Zhang et al., 2006). Temperature detection is not directly explored in this work; however, given the similarities in experimental setups, lessons may be learned.

The physics behind SBS will be handled in the Theory section of this work. As a basic introduction, SBS results when the light traveling through a fiber laser reaches a power level that induces an index change in the fiber. The electric field of the light creates a variation in the refractive index of the fiber, a process known as electrostriction (T. Newell, 2011). The fiber changes from a low loss optical path to essentially a Bragg grating (Keiser, 2000). Now a fraction of the light is reflected back down the fiber. This effect is capable of damaging expensive optical components, such as seed and pump laser diodes, and it reduces the total output power of the fiber amplifier.

1.2 Scope

This paper explores the use of a temperature gradient to minimize SBS. The temperatures reached in this experiment range from -120°C to 90°C. There are many characteristics of a laser system to monitor, but the focus of this paper will be on the power level and spectrum of SBS as well as the output power of the fiber amplifiers.

The equipment available to alter the temperature of the fiber lends itself to a single step temperature gradient. Other gradient arrangements such as sinusoidal, multi-step, or continuously increasing will not be explored in this work.

1.3 Road map

The next sections will discuss previous work relating to SBS mitigation via temperature gradients and then cover the theory of SBS generation. From there the experimental setups of the experiments used to explore SBS mitigation will be described followed by the results of these experiments and discussion as to their meaning. Next, conclusions drawn from the experiment and ideas for future research will be listed. All data collected for this thesis can be found in the Appendices.

1.4 Goals

The goal of this work is to determine to what extent a temperature gradient can improve the output power of a fiber amplifier. The fiber amplifier's SBS power and spectrum along with the overall system output power will be explored in answering this question.

2 Literature Review

In this section we will first look at original work in detecting SBS, detecting SBS in optical fiber, and exploring the effect of temperature on SBS. Next we will look at several works concerning mitigating SBS in fiber amplifier systems. Finally we will look at work related to SBS in cryogenic temperature regions.

2.1 Initial studies

SBS was first experimentally observed by Chiao, Townes, and Stoicheff in 1964 (Boyd, 2008). A 694nm ruby laser that output 50MW in a 30ns pulse was focused on both quartz and sapphire and the resulting Stokes light was recorded on a photographic plate (Chiao, Townes, and Stoicheff, 1964). The equivalent experiment used in this paper is to create SBS in optical fibers by using diode lasers.

The first study of SBS in optical fiber was accomplished by Ippen and Stolen in 1972 (Le Floch & Cambon, 2003). They used a 5355 angstrom xenon laser to pump a length of fiber. The backscattered light was passed through a Fabry-Perot interferometer and the Brillouin frequency shift was measured from a photograph of the Fabry-Perot rings. They concluded that SBS can occur at low power levels in optical fiber, that SBS limits the amount of power that can pass through an optical fiber, and that it is possible for an SBS pulse to increase in power well above the input power thus damaging the fiber (Ippen & Stolen, 1972).

In 1989 the thermal effects on SBS in optical fiber were first studied by Kurashima, Horiguchi, and Tateda (Le Floch & Cambon, 2003). They observed that SBS frequency was affected by temperature and strain in an optical fiber. In their experiment the fiber under test was exposed to -30, 20, and 60°C temperatures. For fiber with an ultraviolet curable resin coated 250µm jacket there was a 1.22 MHz/°C shift in Brillouin frequency, and for a fiber with a nylon coated 900µm jacket there was a 3.68 MHz/°C shift in Brillouin frequency (Kurashima, Horiguchi, & Tateda, 1990).

2.2 SBS and temperature gradients

There has been more recent research focused on using SBS for sensing purposes and reducing SBS when it is unwanted. The following paragraphs will describe this work.

In 1993 Imai and Shimada studied the dependence of SBS on temperature distributions in polarization maintaining fiber. They utilized a length of fiber with a sinusoidal temperature gradient that repeated every 1.1m. The heater used in the experiment was adjusted between 23°C and 63°C. As the temperature was adjusted a 2.8MHz/°C shift was observed in the Brillouin frequency. They discovered that a temperature gradient of 37°C was all that was needed to mitigate SBS for their setup. This change in temperature shifted the Brillouin frequency further than the Brillouin gain bandwidth (Imai & Shimada, 1993). The power levels in this experiment were on the order of milliwatts and the fiber core size was 7.5µm.

In 1996 Nikles et al studied Brillouin gain spectrums. From their experiment they concluded several ideas. First, the linewidth of the Brillouin gain decreases as temperature increases. Second, that a broader Brillouin gain spectrum at room temperature was either due to a higher absorption peak or the maximum absorption was at a higher temperature. Third, the Brillouin gain multiplied by the Brillouin gain linewidth is a constant. Finally, from -30°C to 100°C the Brillouin frequency changes with temperature in a linear manner (Nikles, Thevenaz, & Robert, 1997).

Hansryd, Dross, Westlund, Andrekson, and Knudsen (2001) studied several temperature distribution setups and reported on their findings. They conclude that theoretically a temperature gradient of 350°C can result in an 8dB increase in the SBS threshold. Experimentally they are able to prove a 4.8dB increase with a 140°C gradient (-20°C to 120°C). The maximum temperature in their study is limited by the fiber coating. The various gradients studied and the results from each are presented below.

Figure 1 shows the temperature gradients used by Hansryd et al (2001).

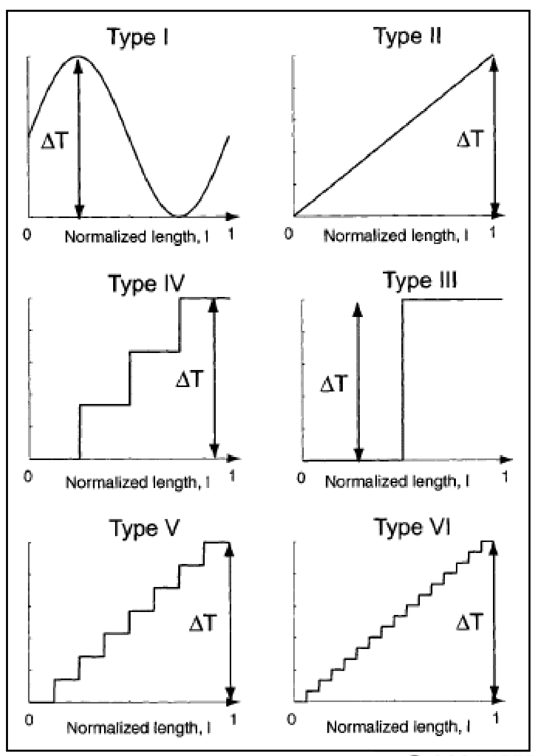

Figure 1: Various temperature gradients[1]

[1] From "Increase of the SBS Threshold in a Short Highly Nonlinear Fiber by Applying a Temperature Distribution," by Hansryd et al., 2001, *Journal of Lightwave Technology*, 19, p. 1693. Copyright 2001 by the IEEE. Reprinted with permission.

In Figure 1 the Type III temperature gradient represents the temperature gradient used in this thesis.

Figure 2 shows the resulting increase in the SBS threshold from each temperature gradient. Note that for a Type III gradient the expected increase in power is 3dB.

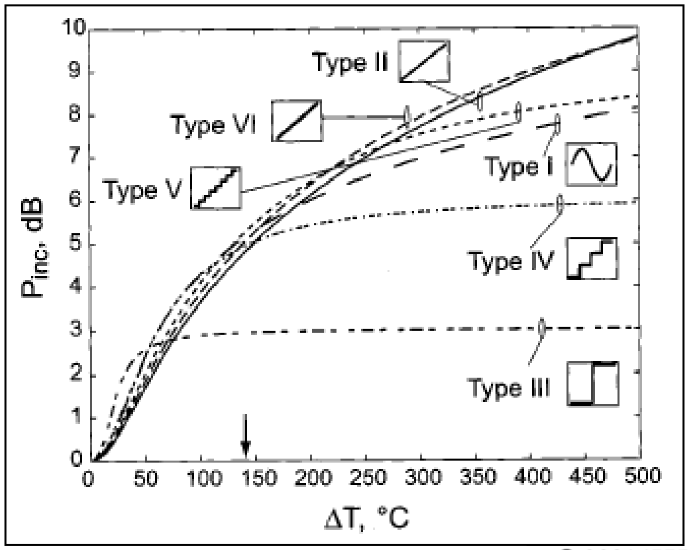

Figure 2: Calculated SBS threshold increase, Pinc, vs temperature gradient[2]

Figure 3 below shows the spectrum of the SBS resulting from gradient types II through V.

Jeong et al. (2005) built and studied a single-frequency single-mode plane-polarized ytterbium-doped fiber master oscillator power amplifier source with 264W of output power. They determined that the output power was limited by the available pump power, not SBS. From their study they determine that temperature gradients can broaden the Brillouin gain. This broadening reduces the Brillouin gain and mitigates SBS (Jeong et

[2] From "Increase of the SBS Threshold in a Short Highly Nonlinear Fiber by Applying a Temperature Distribution," by Hansryd et al., 2001, *Journal of Lightwave Technology*, 19, p. 1693. Copyright 2001 by the IEEE. Reprinted with permission.

al., 2005). They believe that by increasing their temperature gradient, from 100°C to 160°C, they could scale the output power beyond 400W.

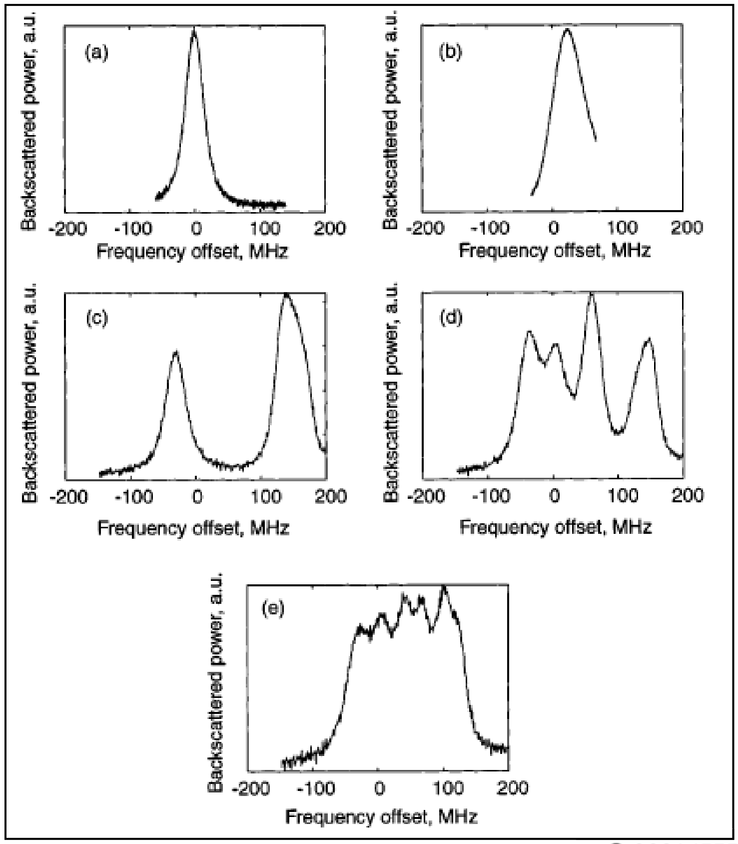

© 2001 IEEE

Figure 3: Measured backscattered light spectra. (a) No gradient. (b) Type II. (c) Type III. (d) Type IV. (e) Type V.[3]

Work by Kovalev and Harrison (2006) presents a theoretical look at using heating from the pump laser to mitigate SBS. By modeling a high-power end-pumped double-clad fiber amplifer with laser gain, SBS gain, and with a pump-induced temperature gradient they conclude that SBS is not the limiting factor in their system. This is assuming that the

[3] From "Increase of the SBS Threshold in a Short Highly Nonlinear Fiber by Applying a Temperature Distribution," by Hansryd et al., 2001, *Journal of Lightwave Technology*, 19, p. 1695. Copyright 2001 by the IEEE. Reprinted with permission.

temperature gradient is greater than 300°C and that the fiber length is less than 6m (Kovalev & Harrison, 2006).

Hildebrandt, Büsche, Weßels, Frede, and Kracht (2008) explored Brillouin scattering in a high-power single-frequency polarization-maintaining ytterbium doped fiber amplifier. Both co-pumping and counter-pumping setups were studied. In the co-pumping setup 32W of output power were achieved before SBS began to exponentially increase. In the counter-pumping setup 80W were achieved prior to SBS exponentially increasing. A summary of this data is shown in Figure 4 below.

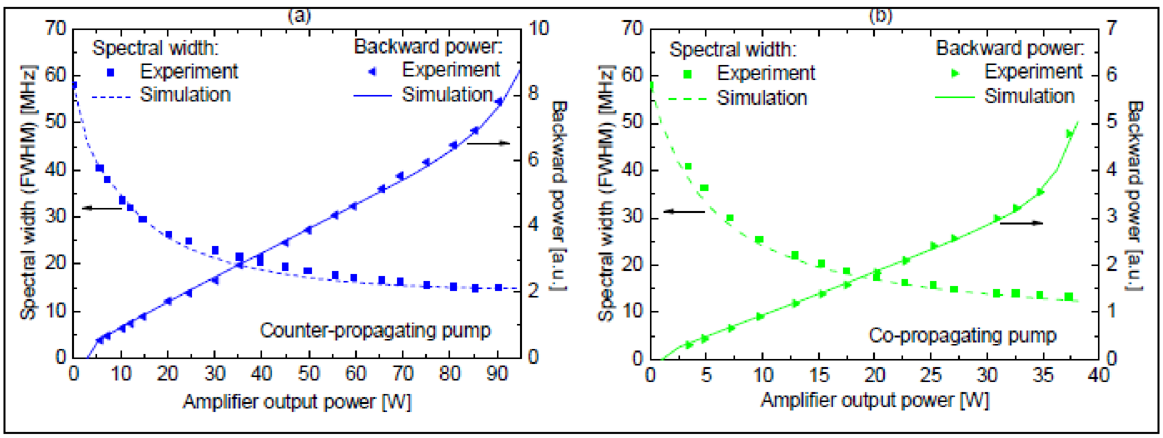

Figure 4: Brillouin scattering spectral width (FWHM) and backward propagating light power as a function of amplifier output power for counter- and co-pumping configurations.[4]

This data was taken with a temperature gradient due entirely to the pump laser. This gradient was roughly 20°C and Hildebrandt et al. (2008) calculated its effect to be a .5dB increase in power over having no gradient.

Figure 5 shows the result of placing 2m of the fiber amplifier on a hot plate. Notice that there are now two Brillouin frequency peaks. When the hot plate is off there is only one

[4] From "Brillouin scattering spectra in high-power single-frequency ytterbium doped fiber amplifiers," by Hildebrandt et al., 2008, *Optics Express, 20* p. 15977. Copyright 2008 by the Optical Society of America. Reprinted with permission.

peak at roughly 1.29GHz. Also shown in part B of Figure 5 is the frequency shift due to temperature changes.

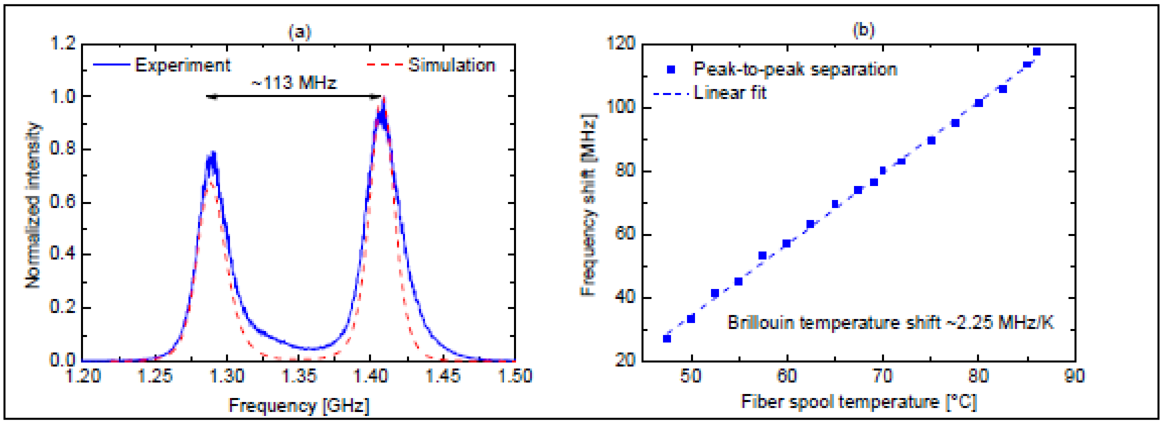

Figure 5: (a) Measured and simulated Brillouin scattering spectra at 70W of amplifier output power at 85°C hot plate temperature. (b) Frequency separation between Brillouin scattering spectral peaks with respect to temperature of heated fiber section[5]

Figure 6 shows where a hot plate was added to the setup to increase the temperature gradient in the counter-pumped setup. Part B of Figure 6 shows how backward power and relative intensity noise change versus output power with and without the temperature gradient.

Hildebrandt et al. (2008) conclude that with a temperature gradient their fiber amplifier could reach 115W without significant SBS.

[5] From "Brillouin scattering spectra in high-power single-frequency ytterbium doped fiber amplifiers," by Hildebrandt et al., 2008, *Optics Express, 20* p. 15978. Copyright 2008 by the Optical Society of America. Reprinted with permission.

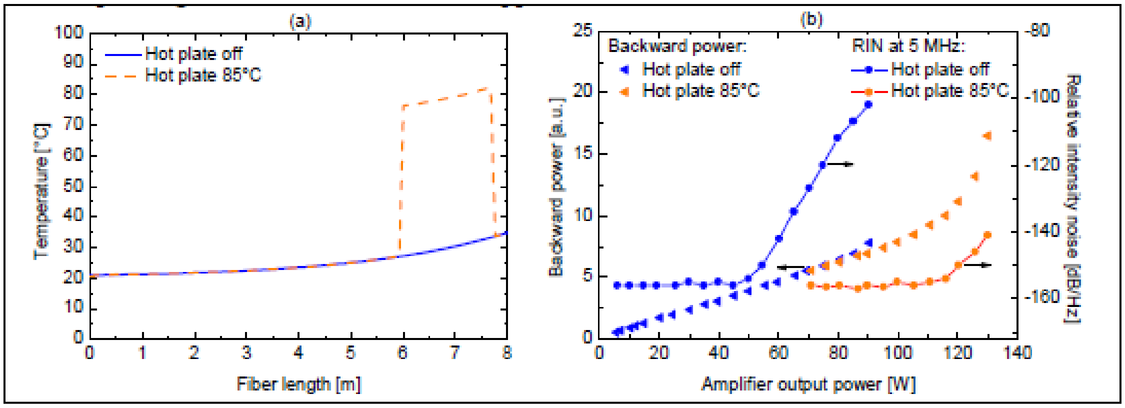

Figure 6: (a) Diagram of temperature distrubtion along fiber. (b) Backward propagating light power and amplifier RIN at 5MHz as a function of amplifier output power[6]

2.3 Low temperature work

Le Floch and P. Cambon (2003) experimentally verified the Brillouin linewidth from 1.4K to 370K. As seen in Figure 7 below from 110K to 370K the Brillouin linewidth increases linearly. This temperature range encompasses the temperature range used in the experiments of this thesis.

Fellay et al. (2005) researched the use of SBS as a temperature sensor in environments down to 1K. They state that from -25°C to 80°C the Brillouin shift changes linearly.

Figure 8 shows the Brillouin gain at 60k and at 4.2k. There is a definite change with temperature.

Figure 9 shows how the Brillouin shift changed as sections of the setup were cooled to 2k. The fiber in this experiment was detecting the temperature along a magnet as it was cooled from 300k to 2k.

[6] From "Brillouin scattering spectra in high-power single-frequency ytterbium doped fiber amplifiers," by Hildebrandt et al., 2008, *Optics Express, 20* p. 15978. Copyright 2008 by the Optical Society of America. Reprinted with permission.

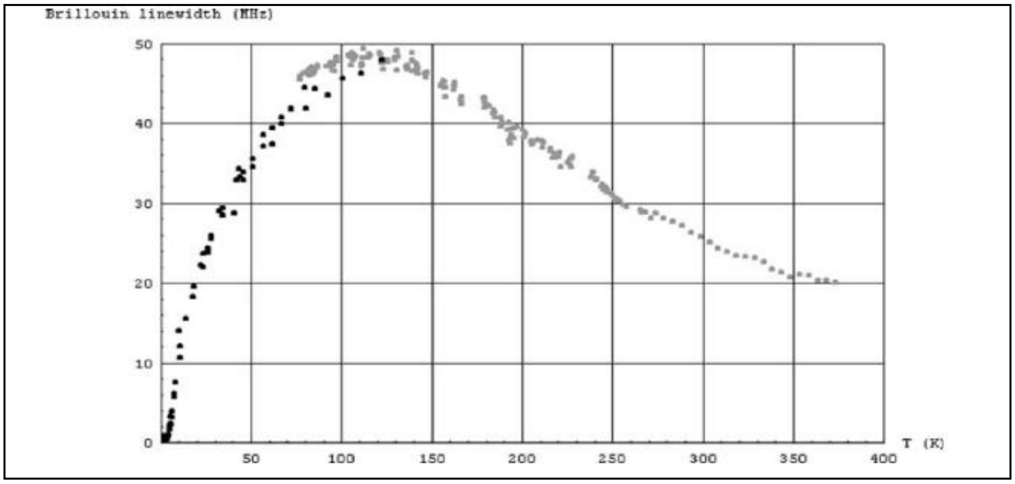

Figure 7: Brillouin linewidth measurements. Black dots - helium cooled. Grey dots - nitrogen cooled[7]

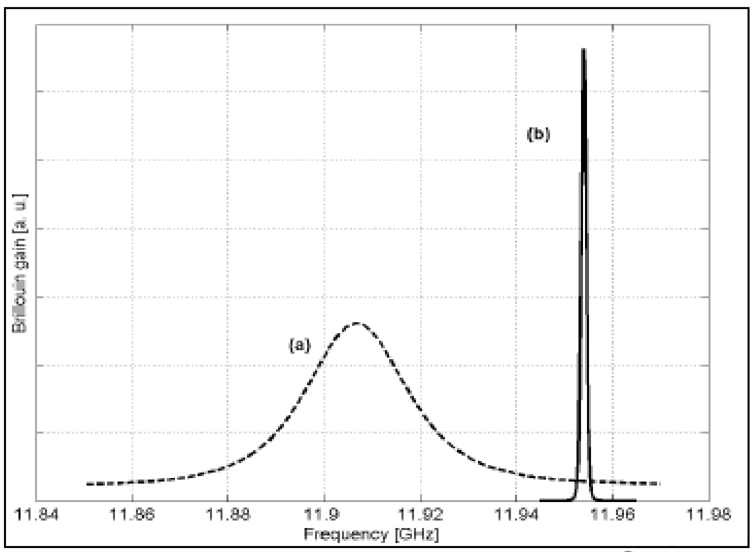

Figure 8: Typical Brillouin gain curves at 1319nm (a) T=60k. (b) T=4.2k.[8]

---

[7] From "Study of Brillouin gain spectrum in standard single-mode optical fiber at low temperatures (1.4-370 K) and high hydrostatic pressures (1-250 bars)," by S. Le Floch and P. Cambon, 2003, *Optics Communications*, 219, p. 402. Copyright 2003 by Elsevier. Reprinted with permission.

[8] From "Brillouin-based temperature sensing in optical fibres down to 1 K," by Fellay et al., 2002, *Optical Fiber Sensors*, 1, p. 302. Copyright 2002 by the IEEE. Reprinted with permission.

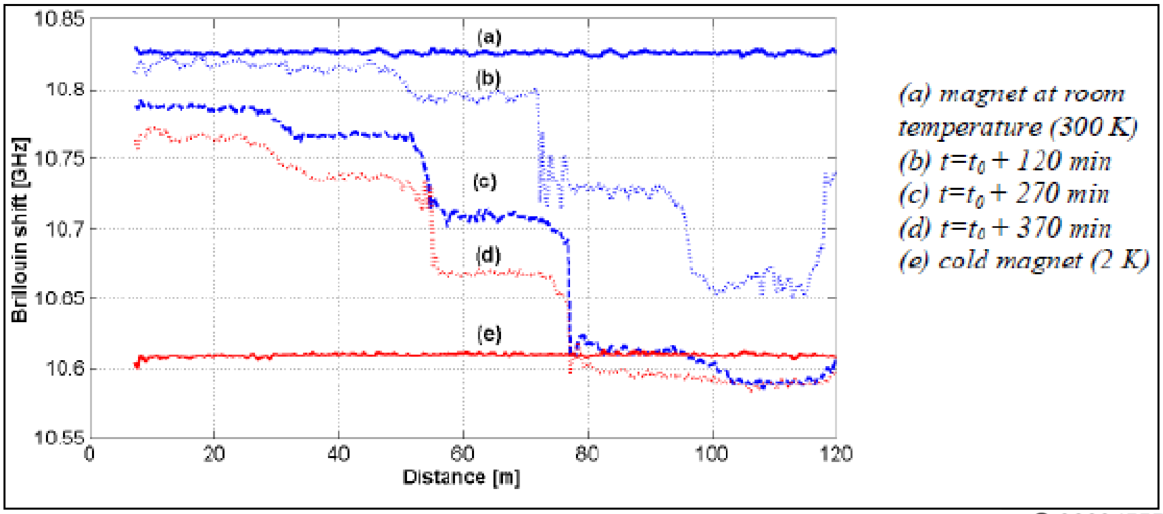

Figure 9: Brillouin shift during cooling[9]

[9] From "Brillouin-based temperature sensing in optical fibres down to 1 K," by Fellay et al., 2002, *Optical Fiber Sensors*, 1, p. 304. Copyright 2002 by the IEEE. Reprinted with permission.

3 Theory

3.1 The basics

Stimulated Brillouin scattering is a process where an incident wave excites an acoustic wave that acts as a Bragg reflector (Massey, 2008). This acoustic wave reflects a portion of the incident wave at a downshifted frequency. The beat note of the incident wave and the reflected light reinforces the acoustic wave. The beat note of the incident light and the acoustic wave reinforces the reflected light (Boyd, 2008).

The acoustic wave travels at the speed of sound in the same direction as the incident light in an optical fiber. This forward motion is the cause of the downshifted Brillouin frequency (Chiao, Townes, and Stoicheff, 1964). In Figure 10 below I_i, k_i, and ω_i are the forward traveling wave's intensity, wavevector, and angular frequency, respectively; I_r, k_r, and ω_r are the backwards traveling wave's intensity, wavevector, and angular frequency, respectively; also ρ, Ω, and q are the sound wave's amplitude, frequency, and wavevector, respectively; and z=0 is the input end of the fiber while z=L is the output end of the fiber. The conservation of energy dictates that the sum of ω_r and Ω is equal to ω_i.

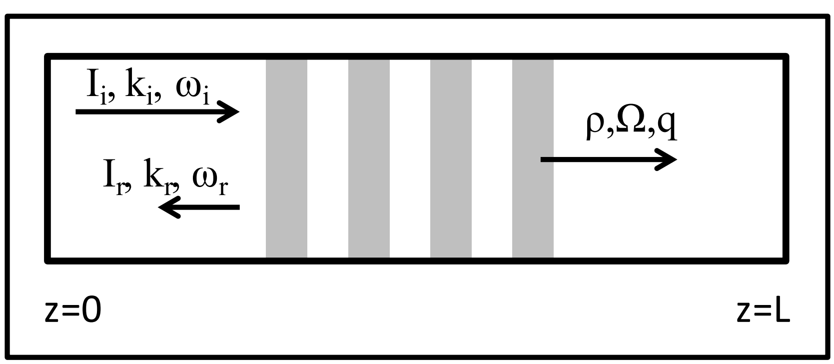

Figure 10: Schematic of SBS in optical fiber[10]

[10] From *Nonlinear Optics* (p. 436), by R.W. Boyd, 2008, Burlington, MA: Academic Press. Copyright 2008 by Elsevier. Adapted with permission.

3.2 Spontaneous versus stimulated

Both spontaneous and stimulated Brillouin scattering can occur in an optical fiber. In spontaneous Brillouin scattering an incident wave is reflected off of an acoustic wave, where the acoustic wave is caused by a thermal process (Boyd, 2008). Stimulated Brillouin scattering occurs when an incident wave is reflected off of an acoustic wave that was created from the interaction of the incident wave and the optical fiber. This interaction takes place in the form of electrostriction (Key and Harrison, 1972).

Electrostriction is a coupling mechanism where electric fields create areas in a material of increased density. In optical fiber this process creates areas of increased density where the optical field is strongest. These density fluctuations excite an acoustic mode that interacts with an incident wave to produce stimulated Brillouin scattering (Stolen, 1980).

The reflected wave mixes with the forward wave to produce an acoustic wave identical to the acoustic wave created by electrostriction. This acoustic wave adds to the initial acoustic wave. The now stronger acoustic wave mixes with the forward wave to produce more of the reflected wave (Tang, 1966).

3.3 Equations

The equations governing SBS are described in this section.

Boyd (2008) uses the following equations to describe SBS due to electrostriction. In steady state conditions the coupled intensity equations are given as seen below.

$$\frac{dI_1}{dz} = -gI_1I_2 \qquad \textbf{Equation 1}$$

$$\frac{dI_2}{dz} = -gI_1I_2 \qquad \textbf{Equation 2}$$

I_1 and I_2 are the intensities of the forward and backward light, respectively. The length along the medium in which SBS occurs is z and g is the SBS gain factor. Note that I_2 propagates in the opposite direction as I_1.

$$g = g_0 \frac{(\Gamma_B/2)^2}{(\ \ _B - \Omega)^2 + (\Gamma_B/2)^2} \qquad \textbf{Equation 3}$$

Here g_o is the line-center gain factor, Γ_B is the Brillouin linewidth, Ω_B is the Brillouin frequency, and Ω is the acoustic wave frequency.

$$g_0 = \frac{{\gamma_e}^2\omega^2}{nvc^3\rho_0\Gamma_B} \qquad \textbf{Equation 4}$$

In the equation above γ_e is the electrostrictive constant, ω is the frequency of the forward traveling light, n is the index of refraction of the medium, *v* is the speed of sound in the medium, c is the speed of light, and ρ_0 is the mean density of the medium.

The Brillouin frequency is the important parameter in this work and is defined below.

$$\Omega_B = 2\pi\frac{2nv}{\lambda} \qquad \textbf{Equation 5}$$

In Equation 5 λ is the wavelength of the forward traveling light and v, the speed of sound in the medium, is temperature dependant (T. Newell, 2009).

The intensity of the reflected light can be found from the equation below, assuming I_1 is constant and $I_2(L)$ is known.

$$I_2(z) = I_2(L)e^{gI_1(L-z)} \qquad \textbf{Equation 6}$$

The total length of the medium is given as L and $I_2(z)$ describes the intensity of the wave traveling in the –z direction. In Equation 6 z is equal to 0 at the beginning of the fiber where the incident wave enters and z is equal to L at the end of the fiber where the incident light exits.

3.4 SBS turn on

As the power of a fiber amplifier increases so does the SBS power. As the power of the fiber amplifier continues to increase the SBS will eventually reach a point where it becomes significant to the operation of the amplifier. This is called the SBS threshold. The SBS threshold has been defined in several different ways. These include when SBS reaches 1% of the output power; when SBS is 20dB higher than Rayleigh power; when SBS crosses a predetermined power level; and when SBS changes from linearly increasing to exponentially increasing (Smith, 1972; Hildebrandt et al., 2008; T. Newell, 2009).

4 Experimental Setup

In order to collect data regarding SBS it was necessary to design two experiments. The first experiment to be discussed, the high power experiment, covers the high power setup in which we attempt to extract the maximum amount of power from our fiber amplifier. We discover that SBS does not appear in significant amounts at low temperatures (-40°C to -120°C) so a second experimental setup is designed to collect SBS data where the first setup was unable. This second experiment will be referred to as the low power experiment.

4.1 High power experiment

To keep the setup diagram simple only the optical train and key components are included in the drawing, refer to Figure 12 and Figure 13. In Appendix A all parts used are listed, and they are separated into optical train components and then all other components consisting of parts used for production, control, and measurement. Appendix A also contains detailed schematics of each setup. The following sections will discuss how all components work together.

The symbols used in the following diagrams are explained in Figure 11 below.

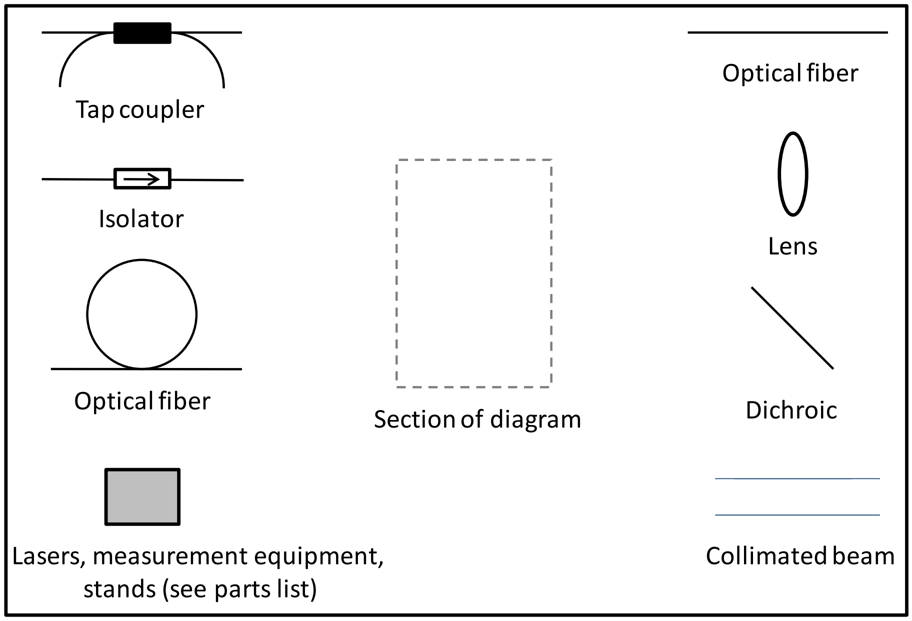

Figure 11: Component descriptions

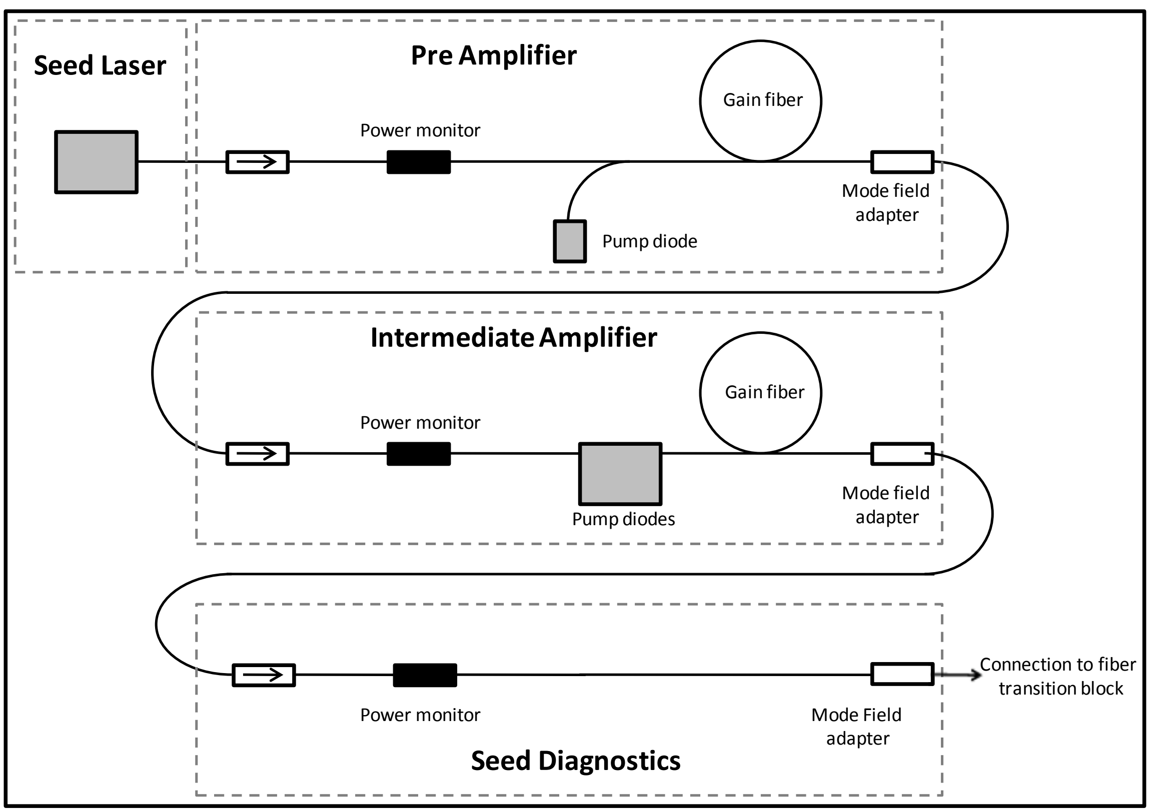

Figure 12: High power experiment setup part 1

4.1.1 Seed laser

A fiber coupled 1064nm NP Photonics laser with a linewidth of 5kHz was used as the seed laser for this amplifier system. Its standard wavelength is 1064.175nm but this is variable with temperature. We maintain the seed laser at 1064.4nm. It has a max output of 50mW and is coupled to 6/125μm fiber.

4.1.2 Pre amplifier

The seed laser is connected to the pre amplifier stage through a Novawave technologies fiber isolator. This isolator connects to a tap coupler which allows for monitoring the forward light from the seed laser and the reflected light from the rest of the system. After the tap coupler the seed light reaches a tapered fiber bundle where the pre amplifier pump light meets the seed light. The pump laser for this stage is an Alfalight 980nm pump diode that produces roughly 2.5W. From here the pump and seed light enter the pre amplifier gain fiber, which is a 6/125μm ytterbium doped Nufern fiber. The last component of the pre amplifier is a mode field adapter which strips any pump light that is not in the core region of the fiber. It also acts as an adapter to change the fiber core diameter from 6μm to 10μm. After the mode field adapter the light enters the intermediate amplifier stage.

4.1.3 Intermediate amplifier

The intermediate amplifier begins with a fiber isolator capable of handling roughly three watts of power in the reverse direction. Next up is another tap coupler such that the forward light from the preamplifier can be monitored, as well as the reflected light from the rest of the system. After the tap coupler, light from the pre amplifier enters an Alfalight pump module. The module is a tapered fiber bundle with 6 Alfalight pump diodes attached. It is capable of pumping with 21W of 976nm light. After the Alfalight module there is 10/125µm Nufern gain fiber. The light then enters a mode field adapter which strips out any light not in the core region of the fiber.

4.1.4 Seed diagnostics

The first component of the seed diagnostics stage is a fiber isolator capable of handling 10W of light in the reverse direction. Next is another tap coupler that allows the forward and backward light to be monitored. The reverse signal port of this tap coupler is spliced to another tap coupler so that the stimulated Brillioun scattering power and spectrum could be measured at the same time. The ends of this 50/50 tap coupler are connected to a power meter and an optical spectrum analyzer. After the initial tap coupler of the seed diagnostics stage there is a section of fiber that is tapered to change the core size from 10µm to 25µm. This allows for a better match between the seed fiber and the gain fiber of the high power stage. Next in line is the fiber transition stage.

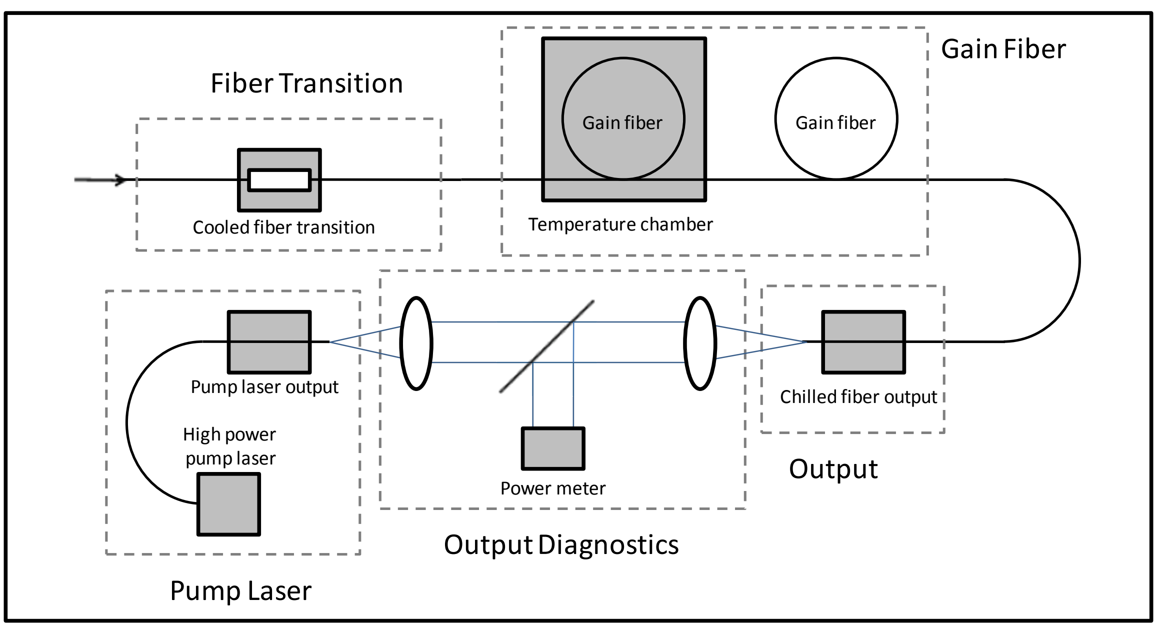

Figure 13: High power experiment setup part 2

4.1.5 Fiber transition

The seed diagnostics stage ends with 25/400µm fiber which feeds into another mode field adapter in the fiber transition stage. This 25/400µm fiber serves as an extension cord for the seed laser to reach the high power stages and allow flexibility in the arrangement of parts on the optical table. Since the 976nm pump is counter-propagating, the mode field adapter of the fiber transition stage has to strip light from the cladding that is left over from the high power stage, and is therefore subject to high power levels and high temperatures. Because of this it is actively cooled with water via a thermocube chiller. The splice from the 25/400µm "extension cord" fiber to the high power gain fiber, also 25/400µm, is covered in high index material that can later be UV cured to form a solid coating. This high index material acts to strip light from the cladding of the fiber and as a glue to hold the splice in place. The splice and high index material are placed between two glass V grooves and the index material is then cured. The glass V grooves, index material, and splice are then placed in a water cooled aluminum clamp to prevent the structure from starting on fire. The water in the chiller is maintained at 19°C.

4.1.6 Gain fiber

After the fiber transition stage we have the gain fiber for the high power stage. A portion of the gain fiber is housed inside a temperature chamber, and the rest is kept on a spool at room temperature. 3.6m of gain fiber are inside the temperature chamber. Outside the chamber at room temperature there is 1m between the chamber and the end facet, and another .7m between the chamber and the splice with the passive fiber. This arrangement is due to the size of the temperature chamber, location of its ports, and not being able to place it on the optical table. The temperature chamber is controlled by a sigma systems controller and requires liquid nitrogen to operate at its full capacity.

4.1.7 Output

After the temperature chamber the fiber is placed in a water cooled aluminum clamp that is attached to a five axis stage that is controlled by micrometers. The setup of the aluminum clamp is similar to the clamp used in the fiber transition stage. The gain fiber is stripped back from the tip approximately 2cm. A drop of high index material is placed over the area where the buffer starts, and then the end of the fiber is placed in glass V grooves. Once the index material is cured the V grooves are placed in the clamp and the fiber tip is aligned to the pump light. Figure 14 below details this setup.

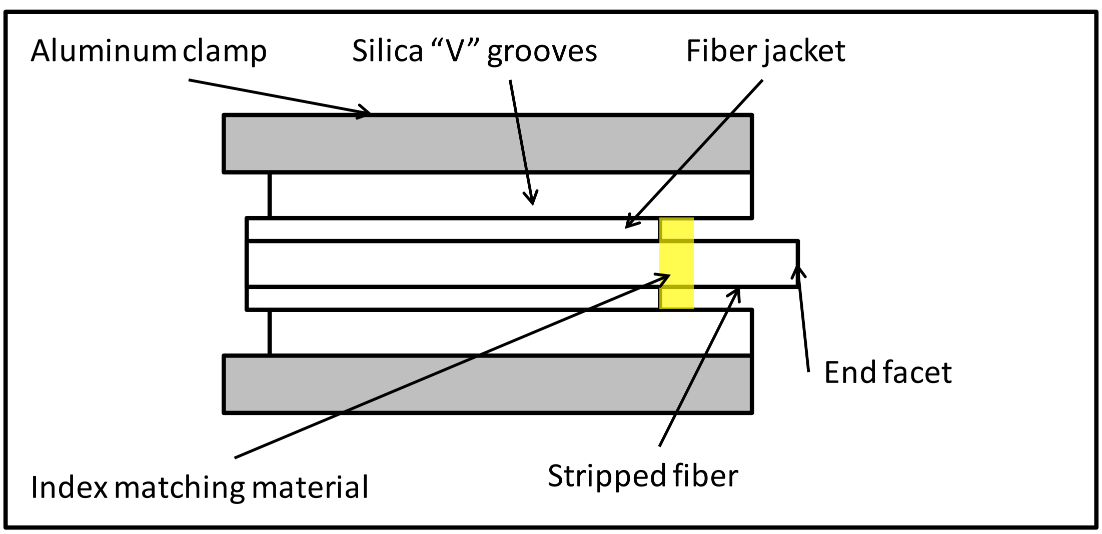

Figure 14: Fiber output setup

4.1.8 Pump laser

The pump laser for the high power stage is a Nuvonyx laser diode system capable of pumping with 800W of 976nm light from a 400μm fiber with a .22 NA. A Melles-Griot

40mm focal length lens is used to collimate the pump light and a Lightpath 40mm focal length lens is used to focus the collimated pump light into the amplifier system.

4.1.9 Output diagnostics

Between the collimating lenses there is a dichroic that transmits the pump light, but reflects the amplified light at 1064nm. The reflected light is collected by a 5kW detector.

4.2 Procedure

Once the components are set up, data can be taken. This involves aligning the pump and seed laser outputs, setting the temperature chamber, and then using Labview to automate adjusting the pump laser power and recording power levels.

4.2.1 Alignment

The end facet of the gain fiber was angled at 8 degrees rather than 0 degrees. This angled facet serves to reduce reflections from the end facet. Creating an end facet at a smaller angle could lead to power oscillations throughout the amplifier system. This was accomplished by using a dry polisher so that the procedure could be accomplished at the optical table rather than dismantling the entire setup.

The pump laser exits a 400µm core fiber, is collimated by a 40mm focal length lens, passes through a dichroic, is focused by a 40mm lens, and then enters a 25µm core fiber.

The backward traveling light at the cooled mode field adapter is monitored for maximum power while the seed laser is off. This is accomplished at low power such that no damaging oscillations are created.

After maximizing the pump power into the gain fiber the seed laser is turned on and the amplified light is directed onto the detectors. A power meter measures the amplified power and a fast photodetector monitors the amplified light for fluctuations that correspond to oscillations within the amplifier. This is a safety precaution because a large oscillation can destroy the fiber end facet.

4.2.2 Temperature chamber

The temperature chamber had a range of 200°C to -120°C. It was possible to take data from -120°C to 90°C, but any warmer and the risk of damaging the fiber was too great. An attempt at 120°C resulted in burning of the acrylic coating of the gain fiber during testing.

The temperature chamber was set at +80°C and then ramped down to -120°C in 20° intervals. The temperature was allowed to settle for ten minutes before data was taken.

4.2.3 Automation/data collection

Labview was used to automate the data collection process. The power meters, optical spectrum analyzers, and the high power pump laser were all controlled by Labview. A program was written to collect data from the power meters while ramping the pump laser power.

It was found that the gain fiber could only handle roughly 250W of output power before catastrophic damage occurred. This limited our data collection abilities. The damage was due to an imperfect end facet. Either micro fractures from the cleaving process or dust particles accumulating on the facet caused a gradual build up of heat. At output powers near 250W these imperfections caused the facet to fail.

At cooler temperatures we found that SBS did not reach an appreciable level before damage occurred to the fiber end facet. Because of this we developed a second experimental setup that allowed the turn on of SBS to be viewed at temperatures reaching -120°C.

From the High Power Experiment we have several data sets. These include output power as temperature and input power are varied; SBS power as temperature and input power are varied; and SBS spectrum data as temperature and input power are varied. The scattered power difference is defined as the Rayleigh power subtracted from the SBS power.

4.3 Low power experiment

To observe significant SBS at low temperatures and the spectrum of each SBS signal we conduct the low power experiment. In this experiment we reuse many of the components from the first experiment. The same seed laser and pre-amplifier parts are used. We deviate from the High Power Experiment in that after the intermediate amplifier pump source we introduce a new gain fiber. The new gain fiber has a smaller core size, 6µm, and is 8m long. These changes will help to observe SBS prior to the laser system melting. This new fiber will be the fiber under test in the temperature chamber and its max output is roughly 12W. This experiment is accomplished in two phases. In the first phase we measure output power and the resulting SBS power. In the second phase we investigate the spectrum of the SBS.

4.4 Phase I: SBS power

Figure 15 shows the configuration of the equipment used in this experiment. Again, all equipment used is listed in9 Appendix A.

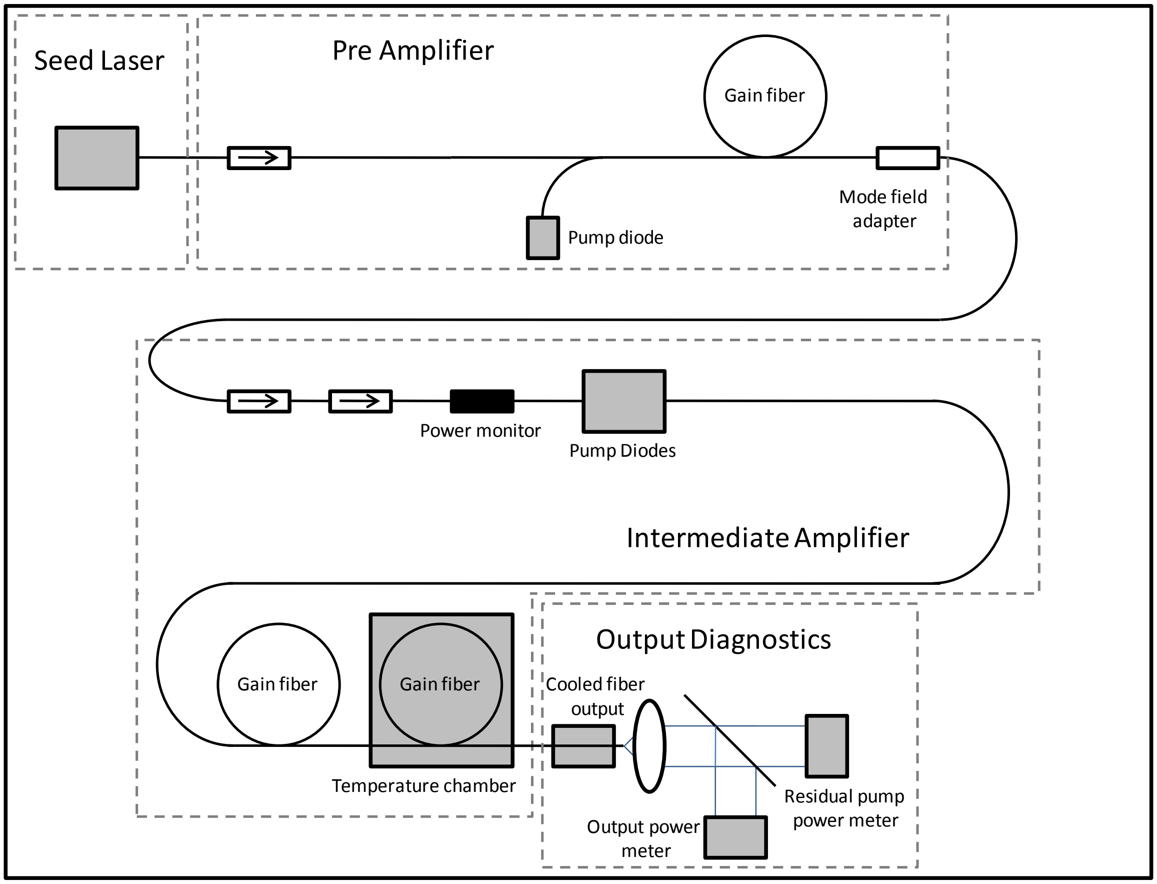

Figure 15: Low power experiment phase I setup

4.4.1 Seed laser

The same seed laser is used as in the high power experiment.

4.4.2 Pre amplifier

The seed laser is connected to the pre amplifier stage through a Novawave technologies fiber isolator. To reduce system instabilities we have removed the tap coupler that existed between the seed laser and the preamplifier pump laser. The rest of the pre amplifier is identical to the high power experiment.

4.4.3 Intermediate amplifier

The intermediate amplifier begins with a fiber isolator capable of handling roughly three watts of power in the reverse direction. A single isolator was not enough to mitigate feedback from SBS that caused spiking and power fluctuations. To further reduce system instabilities we add a second 3W isolator after the first. Next is a 90/10 tap coupler such that the forward light from the preamplifier can be monitored as well as the reflected light from the rest of the system. This is where the SBS from the fiber under test will be monitored. After the tap coupler, light from the pre amplifier enters an Alfalight pump module. This is the same module from the high power experiment. After the Alfalight module there is 6/125µm Nufern gain fiber. This fiber is 8m long. The first 4m are spooled and are at room temperature, roughly 20°C. The next 3.5m are inside the temperature chamber and then .5m run from the chamber to the output diagnostics section.

4.4.4 Output diagnostics

The gain fiber is cleaved at an 8 degree angle to minimize reflections and is held on a Newport 3-axis stage. A 40mm focal length lens collimates the output of the system. A dichroic is used to separate the amplified 1046nm light from the 976nm pump light and both paths are measured.

4.5 Phase I procedure

After setting up the equipment according to the diagrams we need only set the temperature chamber to the desired temperature and use Labview to automate the data collection process.

4.5.1 Temperature chamber

The temperature chamber was set at +80°C and then ramped down to -120°C in 20° intervals. The temperature chamber took roughly ten minutes to change 20°C and the setup was allowed to settle for an additional ten minutes before data was taken after the desired temperature was reached.

4.5.2 Automation/data collection

The power levels we are interested in from this experiment are the 1064nm output level and the SBS level. Labview was used to automate the data collection process in a similar manner as the high power experiment. After performing the low power phase I experiment data is available on output and SBS powers at various input power levels and at various temperatures.

4.6 Phase II: SBS spectrum

In the second phase of this experiment we remove the power meter from the SBS measurement and connect the tap coupler to a second tap coupler so that we can mix the SBS with the forward travelling seed light. Figure 16 shows how the equipment is configured.

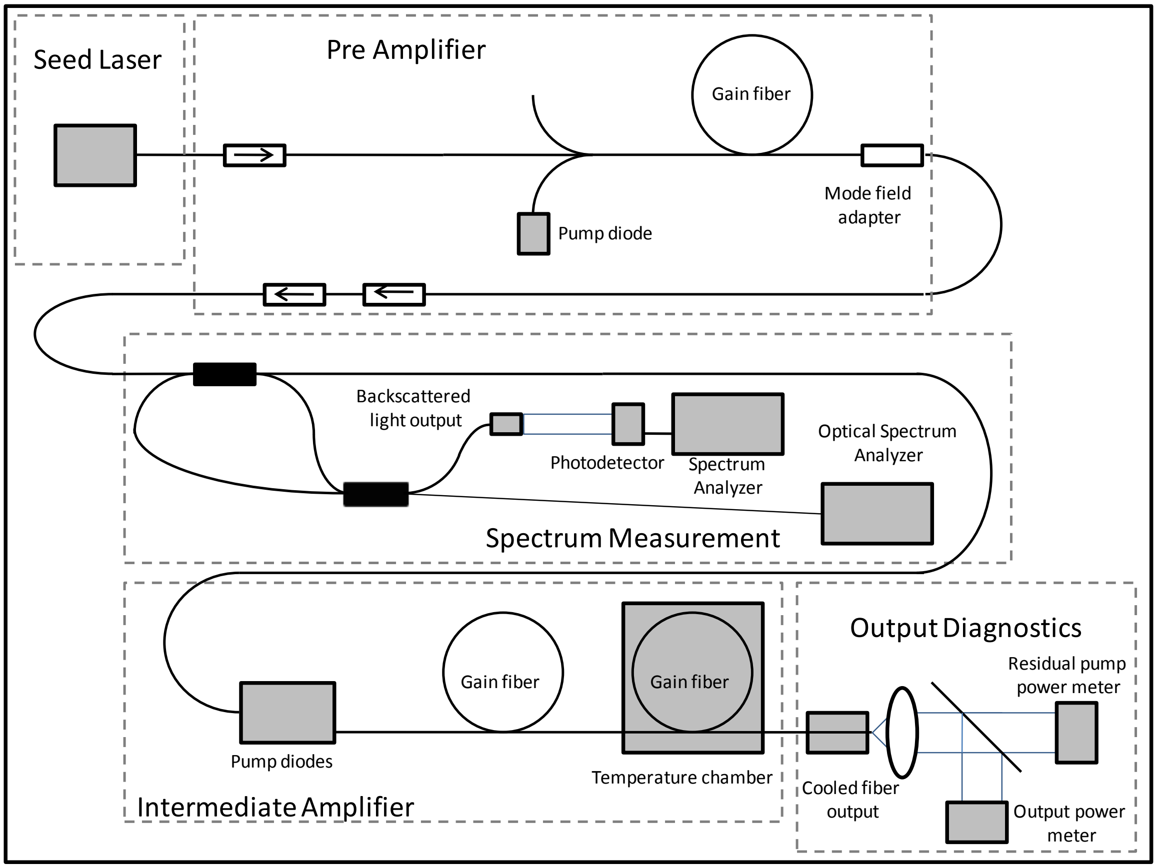

Figure 16: Low power experiment phase II setup

4.7 Procedure

After setting up the equipment according to the diagrams we need only set the temperature chamber to the desired temperature, use Labview to collect data from the Spectrum Analyzer, and manually collect data from the laser output.

4.7.1 Temperature chamber

The temperature chamber was set at +90°C and then ramped down to -120°C in 10° intervals from 90°C to -60°C, and then 20° intervals from -60°C to -120°C. The temperature chamber took roughly ten minutes to change 20°C and the setup was allowed to settle for an additional ten minutes before data was taken after the desired temperature was reached.

4.7.2 Data collection

Only the spectrum analyzer portion of the experiment was automated. After the temperature chamber reached the desired temperature and a ten minute settling period was up the intermediate amplifier pump laser level was adjusted. An optical spectrum analyzer was utilized where the Rayleigh and total SBS levels could be monitored. To keep measurements similar the pump laser was adjusted such that the SBS power level was equal to the seed laser power. Once this was accomplished the spectrum analyzer was adjusted to view the beat notes of the SBS, one signal from the fiber at room temperature and one signal from the fiber inside the temp chamber, with the forward traveling seed light. This process was repeated from 90°C to -120°C.

After performing the low power phase II experiment data is available on the spectrum of beat notes resulting from two SBS signals and the seed laser at various temperatures.

5 Results

A temperature gradient on the gain fiber of a fiber amplifier changed the power level and spectrum of stimulated Brillouin scattering.

5.1 High power experiment

SBS has been successfully mitigated at temperatures below 40°C. In this experiment we see that as the temperature of the temperature chamber varies away from 60°C that the SBS power changes. Note that 60°C is not the ambient temperature of the room. Both increasing and decreasing the temperature away from 60°C reduces the power of the SBS. From the data in Figure 17 we see that at temperature chamber temperatures of less than 40°C we cannot observe SBS levels above 1mW. While we can still make estimates as to the behavior of the SBS we cannot see it physically turn on. Results of SBS and Output power levels versus input power at each temperature are available in Appendix A.

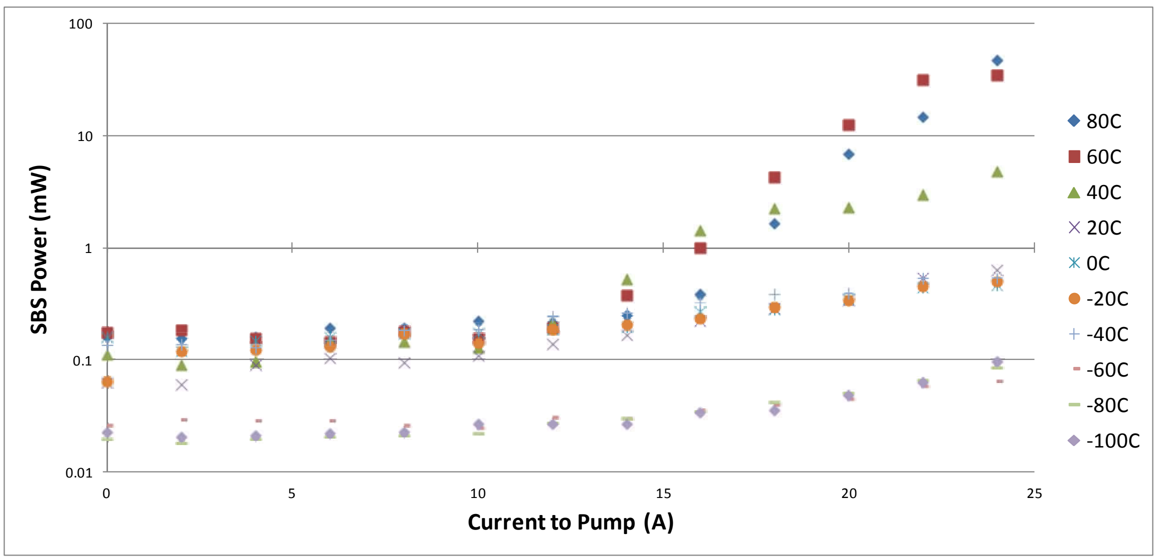

Figure 17: SBS power vs current to pump

From the spectrum data in Figure 18 we see, at the highest output power measured, that the Rayleigh light, at 1064.41nm, differs by 5.6dBm while the Stokes light, at 1064.475, differs by 28.6dBm. This all occurs as the temperature is varied from 80°C to -100°C. All data from the spectrum measurements are available in Appendix B.

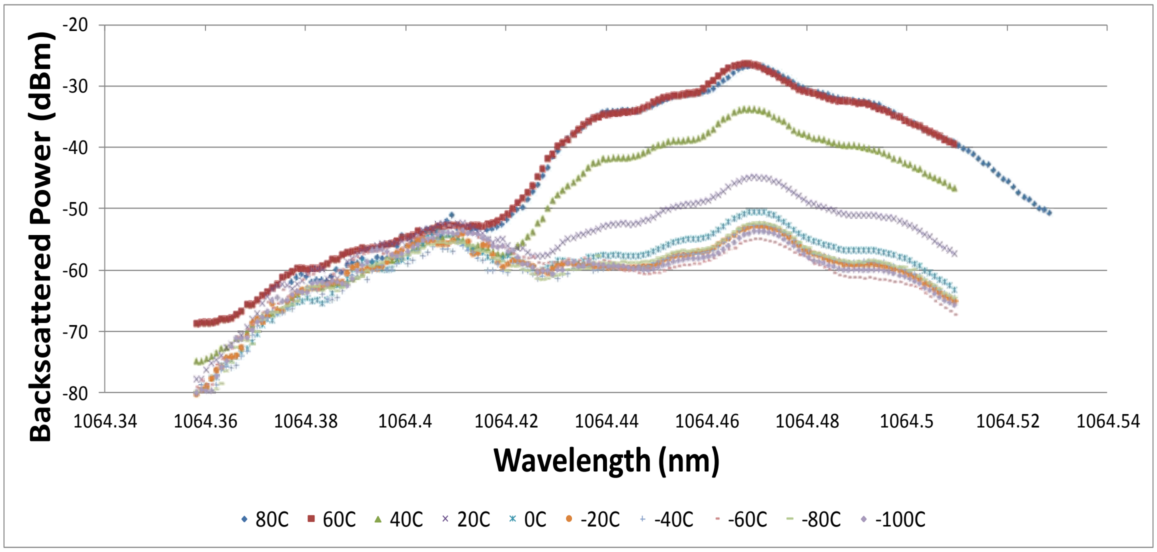

Figure 18: Backscattered spectra at various temperatures

5.2 Low power experiment phase I

In this experiment we see that as the temperature of the temperature chamber varies away from 28°C that the power of the SBS changes. As the temperature in the chamber decreases so does the power of the SBS. At temperatures of 20°C and 40°C we see the lowest power level that causes SBS to turn on. As temperatures increase or decrease away from these two it takes an increasing amount of power to turn on the SBS. This is evident in Figure 19.

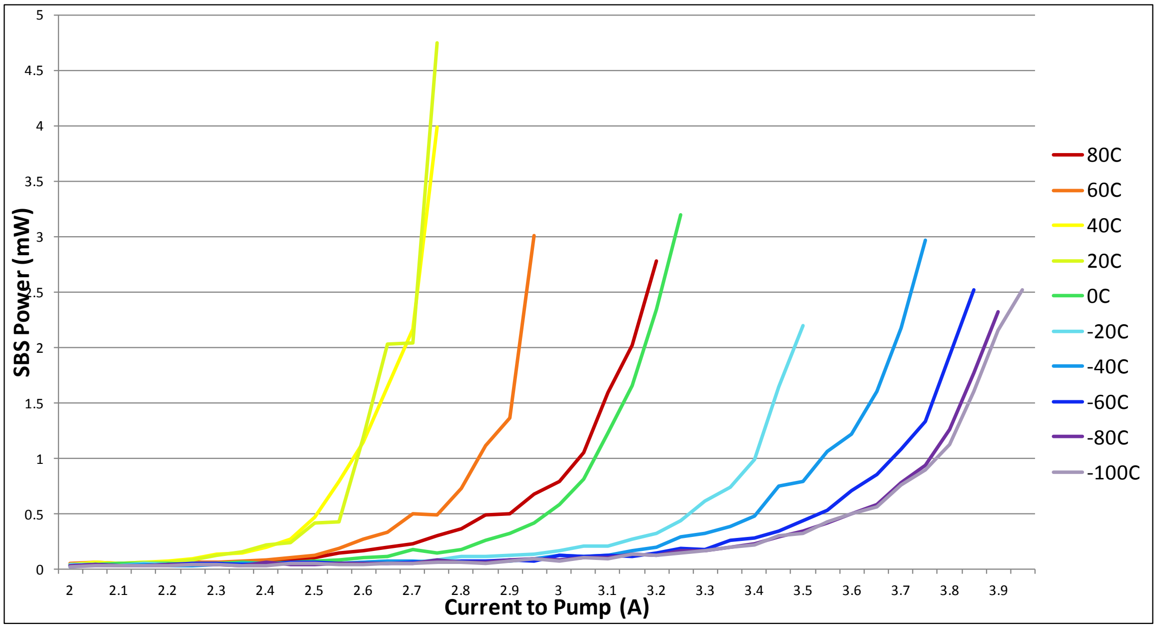

Figure 19: SBS power vs current to pump

Figure 20 and Figure 21 show results at 20°C and -100°C of Output power and SBS power versus input power. All of the data collected can be found in Appendix C.

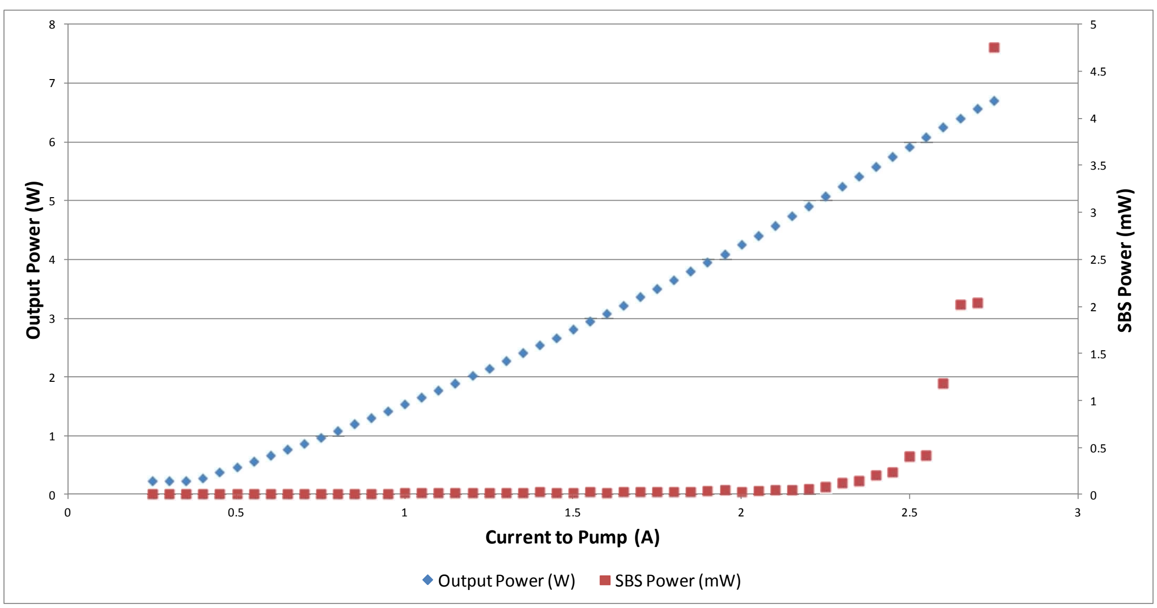

Figure 20: Output and SBS power vs current to pump at 20°C

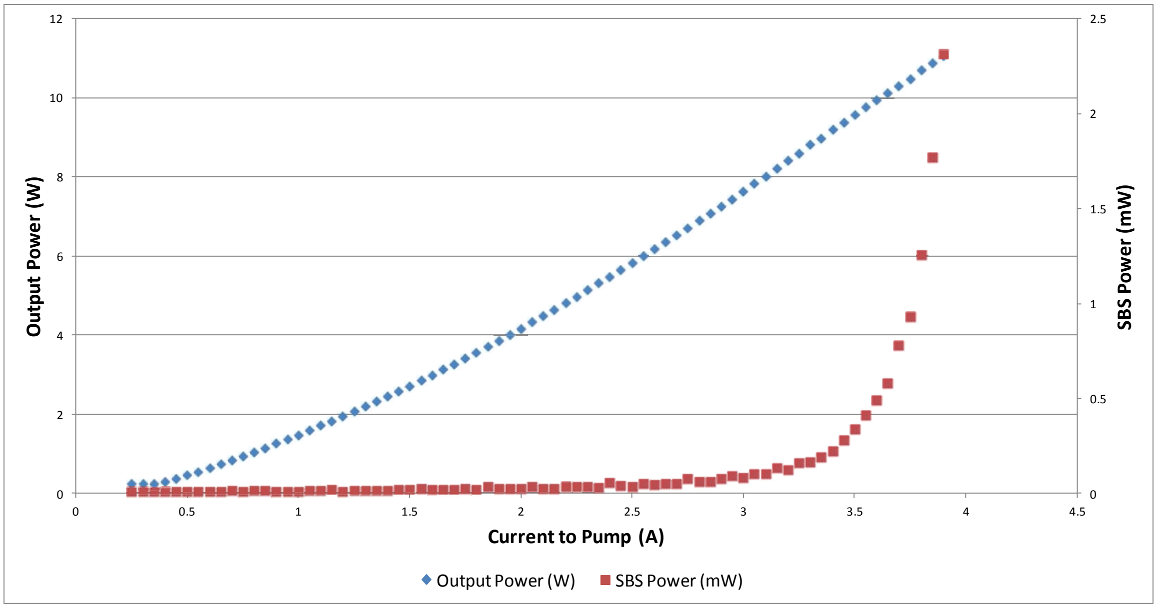

Figure 21: Output and SBS power vs current to pump at -100°C

5.3 Low power experiment phase II

In this experiment we see similar changes in output power level due to temperature changes in the temp chamber as we observed in the Low Power Experiment phase I. However, we also observe the SBS spectrum splitting into two separate peaks. One peak varies with the temperature chamber temperature at 1.6MHz/°C and another peak varies with the temp chamber temperature at .02MHz/°C. Comparing the two peaks it appears as though one stays put at roughly 16.116GHz and the other peak shifts by 1.6MHz/°C with a change in temperature. There is a section of data that cannot be properly analyzed most likely due to the SBS peaks combining on the spectrum analyzer. These data points are from 0°C to 40°C.

Figure 22 shows all results for the low power experiment phase II. The stationary peak at 16.116GHz is made evident. However, other signals are lost to the overlapping data points. Figure 29 in the discussion section shows each data set separated from other data sets. For individual results see Appendix D.

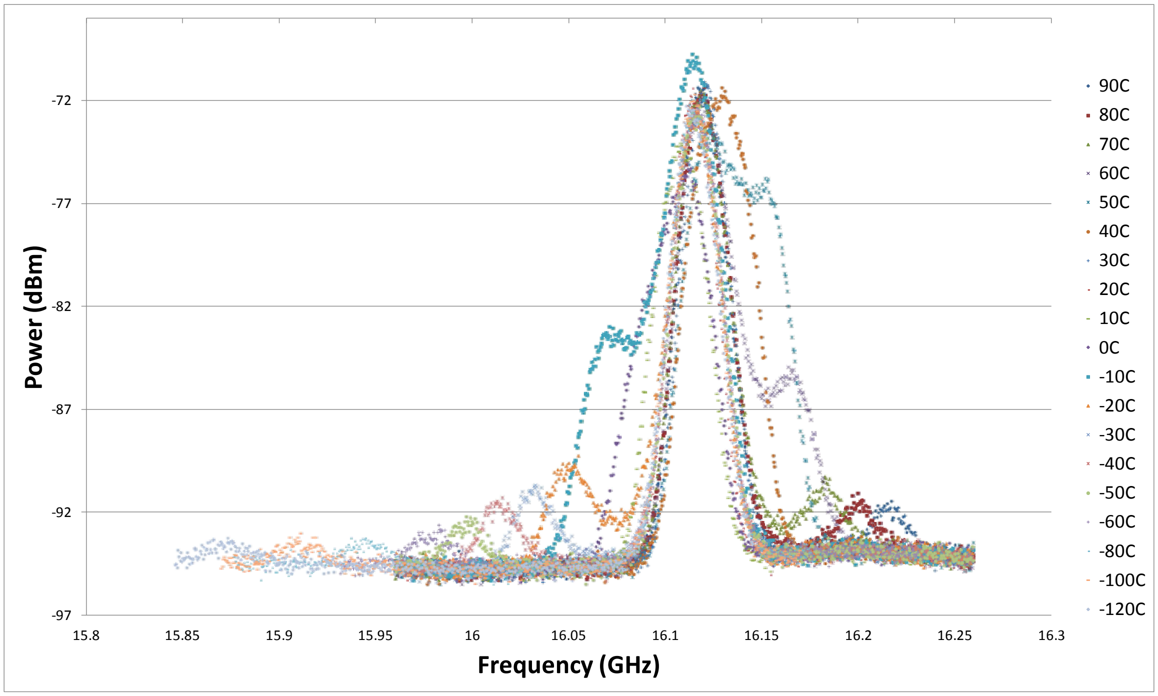

Figure 22: Beat note power vs frequency

6 Discussion

6.1 Summary of important results

In the high power experiment SBS is reduced to the point where the limit on output power is the quality of the end facet. SBS is reduced from 47mW to .1mW. In the low power experiment SBS is mitigated such that the output power can increase from 6.16W to 10.79W. The high power experiment showed that by varying the temperature SBS can be mitigated at power levels where it used to cause damage. The low power experiment showed that the SBS frequency shifts linearly with temperature by 1.6MHz/°C and that as the two SBS peaks move apart the SBS grows weaker.

6.2 The high power experiment

First, a look at the output power of the fiber amplifier in Figure 23. We see that the power level at each input stage is consistent across the temperature range. This shows that the change in SBS is not due to amplifier power variations. The only variable that was changed is the temperature inside the temperature chamber.

By comparing the Stokes power level to the Rayleigh power level in the spectrum plots we can further analyze our results. We take the point at which the Stokes power is 20dBm higher than the Rayleigh power to be the threshold for saying that SBS has turned on (T. Newell, January 2009). Plotting the difference between the Stokes power and the Rayleigh power versus output power results in Figure 24 below.

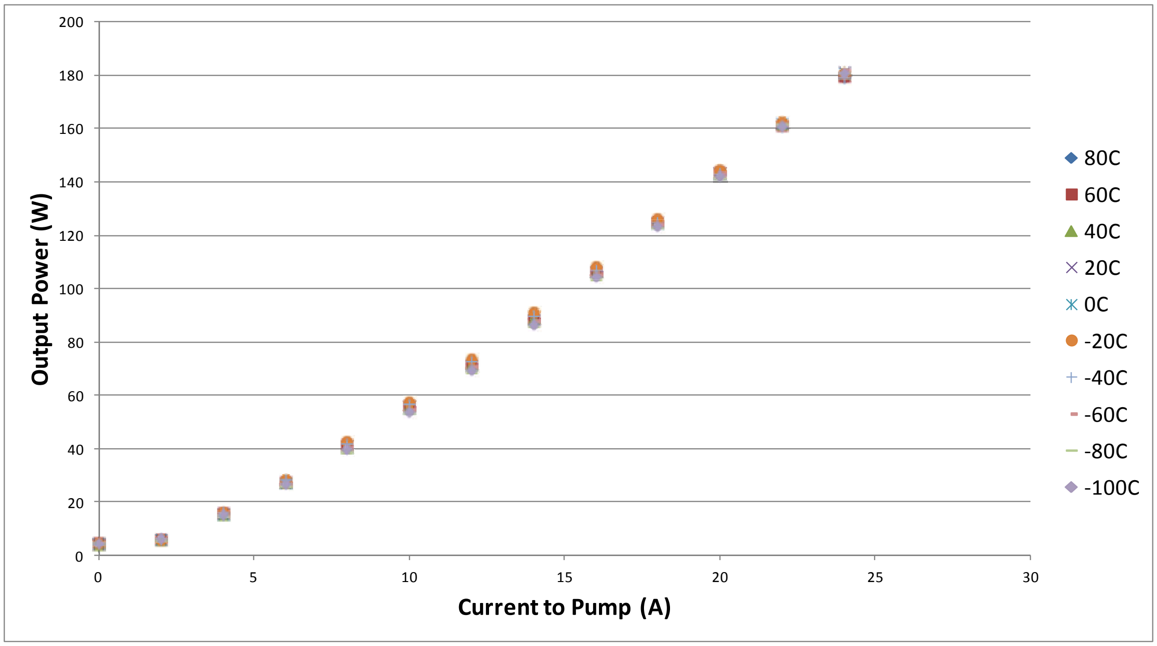

Figure 23: Output power of fiber amplifier vs current to pump at various temperature chamber settings

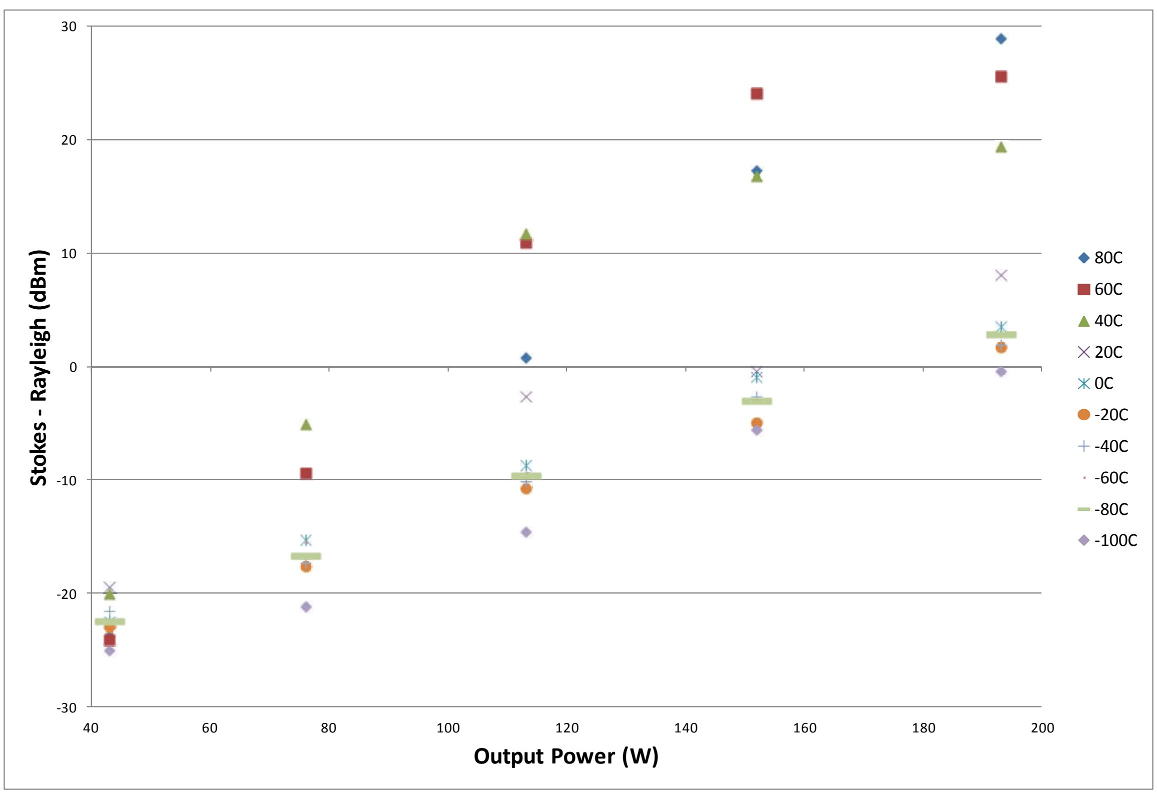

Figure 24: Stokes - Rayleigh power vs output power at various temperature chamber settings

Figure 24 allows us to make a linear fit of the data points and develop an equation to predict when the SBS power will reach 20dBm more than the Rayleigh power. This equation is simply the linear fit solved for Output Power when Stokes – Rayleigh is set to 20. Now we have data that tells us the estimated max output of the fiber amplifier at each temperature based on the SBS power level. Plotting this results in Figure 25 below.

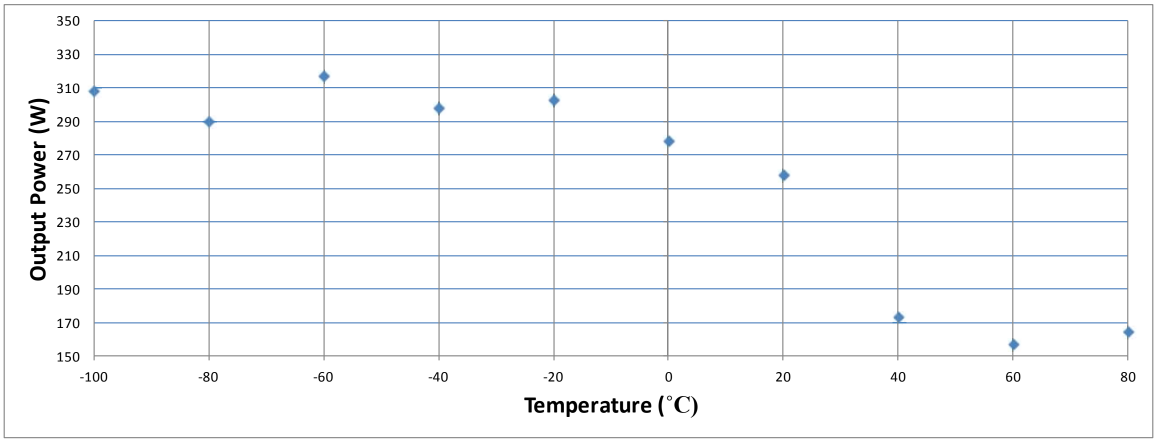

Figure 25: Output power vs temperature

From Figure 25 we see that the lowest estimated output power level is 155W and it is reached at 60°C. The highest estimated output power level is 318W and it is reached at -60°C. The data points from -20°C to -100°C most likely make a gradual slope where the effects of SBS mitigation are slowly used up. This is expected from the results of a type III gradient from Figure 2.

Constructing Figure 26 is accomplished by finding the maximum power output at each temperature level. The lowest of these, found at 60°C in this experiment, is subtracted from each of the maximum power levels. The total from these calculations are then divided by the number we subtracted to give a percent change. The purpose of this figure is to clearly show the change in power levels and to point out the magnitude of temperature gradients necessary for SBS suppression.

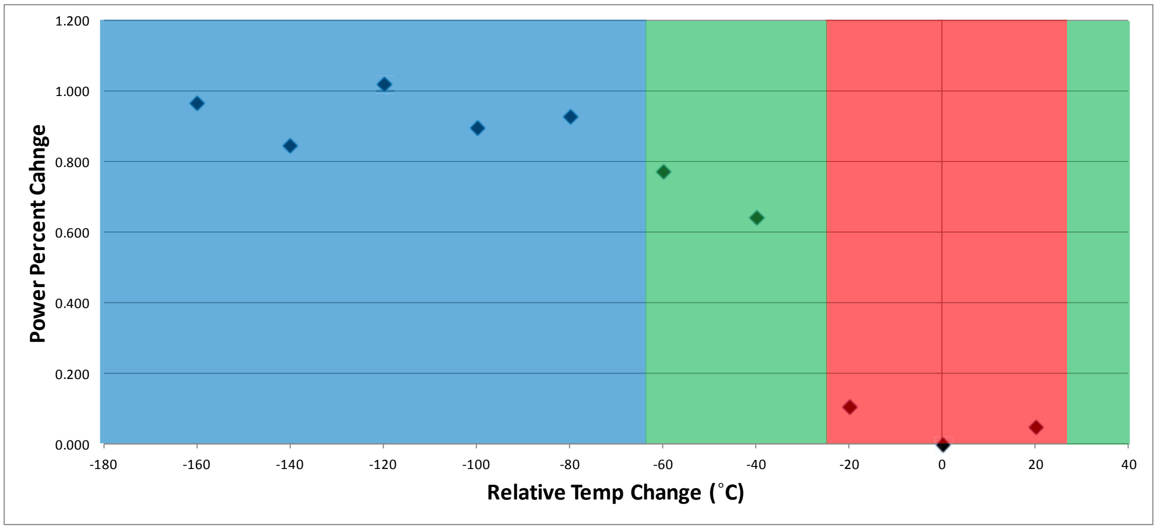

Figure 26: High power experiment power change vs temperature

Figure 26 shows three distinct regions of SBS suppression. These regions are rather arbitrary; however they serve to show where the temperature gradient does and does not have a significant effect. The first region in red is where the temperature shift is not large enough to significantly alter the SBS. The next region, in green, is where the temperature change is affecting the SBS. This is due to the SBS frequency produced by the fiber at ambient temperature sharing gain with the SBS frequency produced by the temperature controlled fiber (Hildebrandt et al., 2008). Since these frequencies do not match, their ability to amplify is reduced. The third region, seen in blue, is where there is no more significant benefit to moving the two SBS frequencies apart.

From the data points available in this experiment we cannot determine whether cooling or heating the fiber is more advantageous. A 100% increase in power is achieved at a temperature gradient of -90°C. A 50% increase in power is achieved at -30°C, and a 10% increase is seen at -15°C and 24°C.

6.3 The low power experiment

The data collected on SBS power and Output power can be used to make a similar analysis as the High Power Experiment. We do not have data on the Rayleigh power levels; however, we can pick the point where the SBS power reaches 1% of the output power to call the SBS threshold power.

Figure 27 shows that at 20 and 40˚C the output power reached 6W. The minimum power, roughly 5.8W is most likely reached at 30˚C. At -80˚C the output power reaches it maximum of 10.8W. The increase of the output power does not reach the 3dB observed by Hansryd et al (2001) for a single step temperature gradient, but this may be due to the co-pumped configuration used for this experiment (Hildebrandt et al., 2008). In the co-pumped configuration the added benefit of a temperature gradient from pump heating occurs in a short length of fiber where the fiber is also already warm. Counter pumping places this extra temperature gradient in a strategic location, at the end of the fiber, where it can do the most to SBS mitigation.

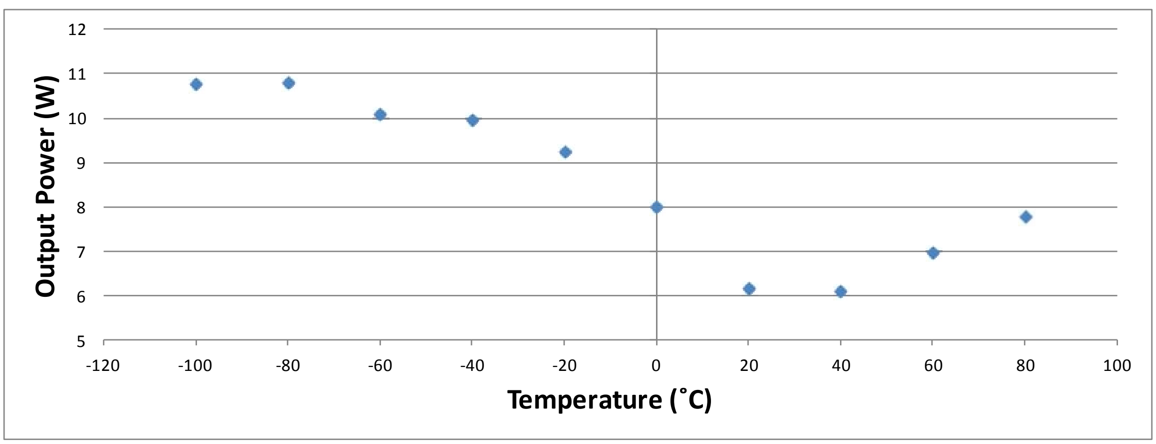

Figure 27: Output power at 1% SBS threshold vs temperature

Figure 28 is constructed in the same was as Figure 26 and it serves to show the magnitude of the output power change. It also points out the necessary temperature gradient required for a desired power increase.

The same SBS suppression regions appear, although they are now centered around 30°C. This is due to the temperature in the core of the ambient temperature fiber being at roughly 30°C. It has been shown by Hansryd et al (2001) that the low point of SBS mitigation is when no temperature gradient is present. In Figure 28 the red region is where the temperature change is not large enough to shift the SBS frequencies a significant amount. The green region shows where the SBS frequencies are pulling apart such that they must share the amplifier gain. The blue region shows where there is no more significant benefit to moving the two SBS frequencies apart.

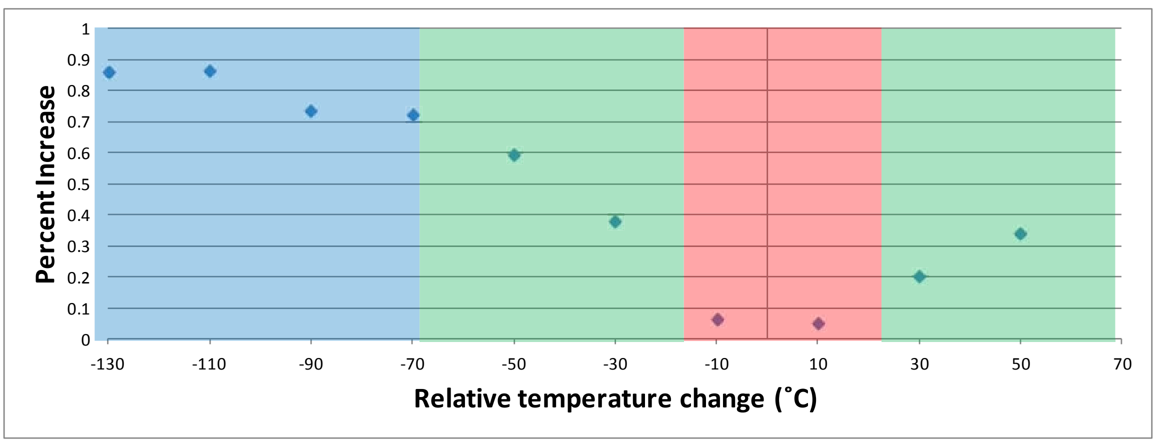

Figure 28: Low power experiment power change vs temperature

Also from Figure 28 we see that the maximum output power, and therefore the most SBS suppression, occurs at a gradient of -110°C. A 50% power increase occurs at a gradient of -40°C. A 10% increase at both -16°C and 22°C. Continuing in the positive direction the highest positive temperature gradient, 50°C, gives a 33% increase in output power. From the data collected, cooling the fiber suppressed SBS more so than heating the fiber. In Figure 28 from gradients of -68 to -16˚C the power increases at a higher rate than from 22 to 50˚C.

The splitting of the SBS spectrums can be seen from Figure 29 below. Figure 29 is simply Figure 22 with each temperature series pulled vertically apart. The SBS from the fiber at ambient temperature is seen as the stationary peak. The SBS from the fiber in the temperature chamber is seen as the peak that traverses the graph as temperature changes (Fellay, 2002). It can be seen that from 0°C to 40°C the SBS peaks are completely overlapping and cannot be accurately measured.

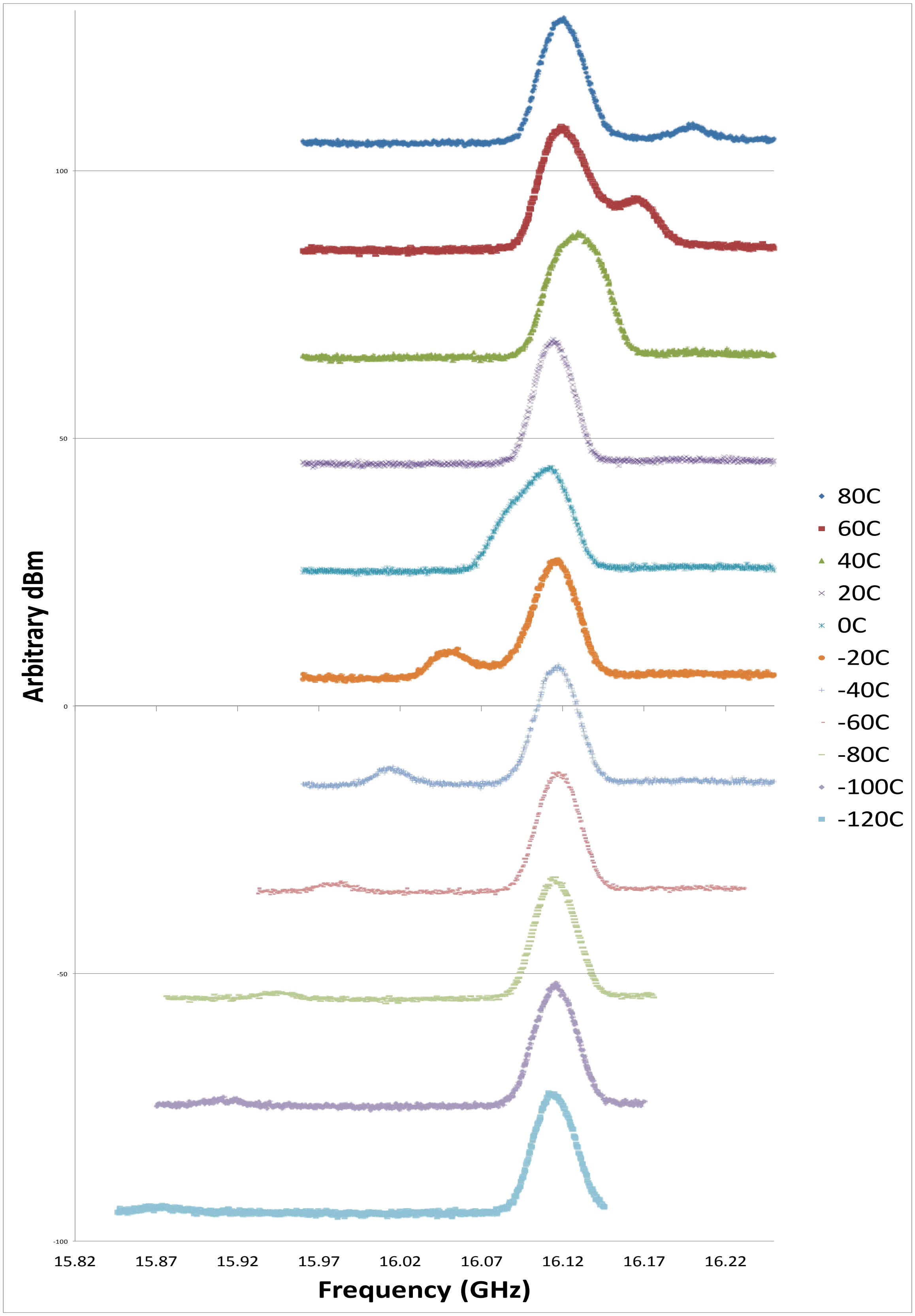

Figure 29: Beat notes vs frequency

Figure 29 can be broken down into the two graphs below by taking the center value of the SBS peak spectrum and plotting against temperature. The first graph below, Figure 30, is for the beat frequency due to the fiber in the temperature chamber. The second graph below, Figure 31, is from the fiber held at room temperature.

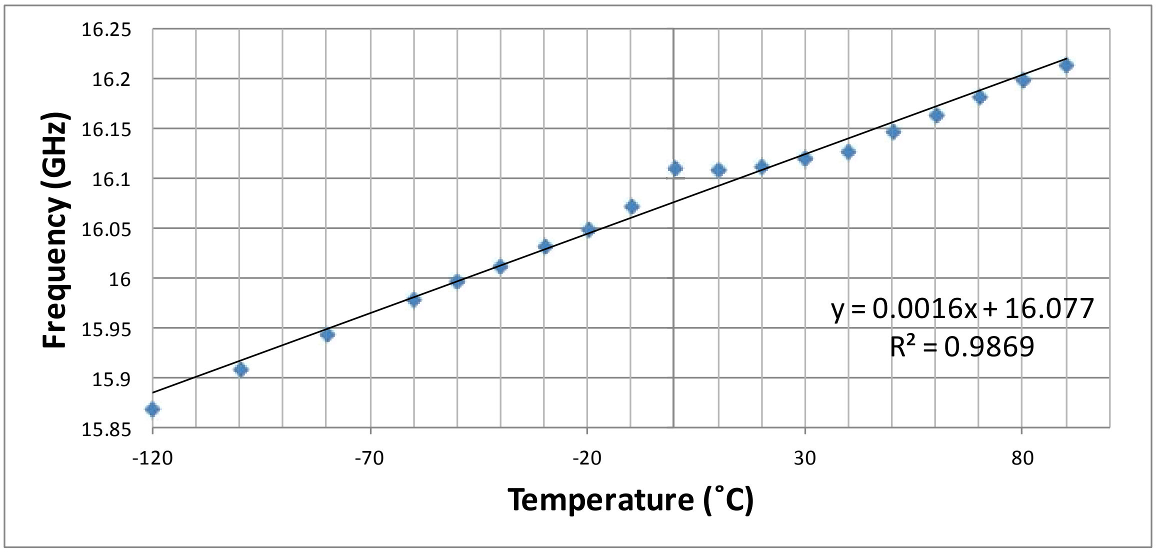

Figure 30: Beat frequency from temperature controlled fiber vs temperature

The first thing to notice on Figure 30 is that the data taken from 0°C to 40°C doesn't fit with the rest of the data points. This is because the two SBS peaks are not perfectly overlapping or completely separate. The data points from 0 to 40°C are taken from a peak made from the addition of the two SBS peaks. Data points above and below this region are taken when the SBS peaks are further apart, allowing a more accurate reading. By fitting a line to the data points we can get a sense for how much the SBS frequencies move with respect to temperature. The fiber used in this experiment shows a 1.6MHz/°C shift.

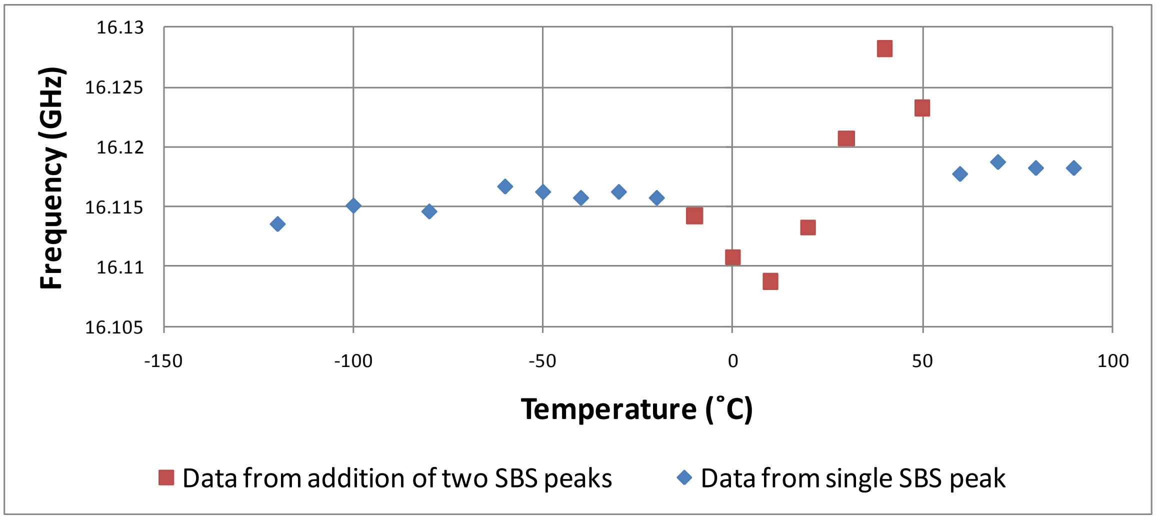

Figure 31: Beat frequency from ambient temperature fiber vs temperature

Figure 31, Beat Freq (temp const) versus Temp, displays data taken from the fiber held at ambient temperature. Due to the .02MHz/°C shift in frequency we see that the fiber was not at a constant temperature. This is most likely due to the temperature of the fiber in the temperature chamber leaking into this portion of the fiber. A shift of .02MHz/°C is significantly smaller than the 1.6MHz/°C from the temperature shifted fiber.

The data points marked as red squares represent where the spectrum was affected by the combining of the two SBS spectrums. We see here that the peak of the spectrum deviates from the norm even when the two SBS signals can be resolved at -10 and 50°C. Data used for this analysis is available in Appendix D.

7 Conclusion

To meet the goal of this work I have conducted a high and low power experiment in which the power and spectrum of SBS along with the overall output power of a fiber amplifier are explored at various temperature gradients.

I have shown that the application of a temperature gradient to the gain fiber of a fiber amplifier will suppress stimulated Brillouin scattering and allow for increased output powers. In the high power experiment, utilizing counter-pumping, SBS is reduced such that the output power is doubled. In the low power experiment, utilizing co-pumping, SBS is reduced such that output power is increased by 85%.

Using a heterodyne measurement technique allows the observation of the splitting of the SBS power into two separate frequencies. These SBS "peaks" are observed to pull apart as SBS is increasingly suppressed. In both the high and low power experiments a temperature gradient of 90°C achieves the maximum SBS mitigation.

In conclusion, when utilizing a temperature gradient to suppress SBS there are three possible suppression regimes to occupy: no suppression when the two SBS frequencies are not far enough apart; increasing suppression when the SBS frequencies are pulling apart from each other; and maximum suppression when the two SBS frequencies have completely separated.

It has been discovered that temperature gradients from 25 to 65˚C are capable of improving the power output of a fiber amplifier from 20 to 80%. Smaller gradients will not have a significant affect and larger gradients will have a diminishing return on investment. The 177W fiber amplifiers in use by the Air Force Research Laboratory can be further engineered to produce approximately 300W of output power.

8 Recommendations

8.1 Applying the results

The Air Force Research Lab could utilize this technique to increase the output power of their 177W fiber amplifiers to approximately 300W. The output facet may still fail at 250W, but the power is no longer limited by SBS. The setups used in the high and low power experiments share several characteristics with the Air Force's amplifier chains such as the seed laser, pump lasers, spooling methods, fiber lengths, and fiber types. So, all that would need to be added is the temperature gradient.

8.2 Future experiments

In the high power experiment SBS mitigation worked so well that significant SBS was not observed at low temperatures. Future research should begin with using fiber that can withstand large temperature shifts and high output powers. The high power experiment could be repeated at higher temperatures to determine if there is a difference in SBS mitigation when heating or cooling a portion of the fiber.

The temperature gradient was limited to what the single temperature chamber could create. Developing alternate setups with more temperature control would allow for the exploration of more gradient types, rather than just the single step gradient.

9 Appendix A: Detailed Setups and Equipment

Detailed setup schematics and equipment lists are described in this appendix. Numbers correspond to associated tables

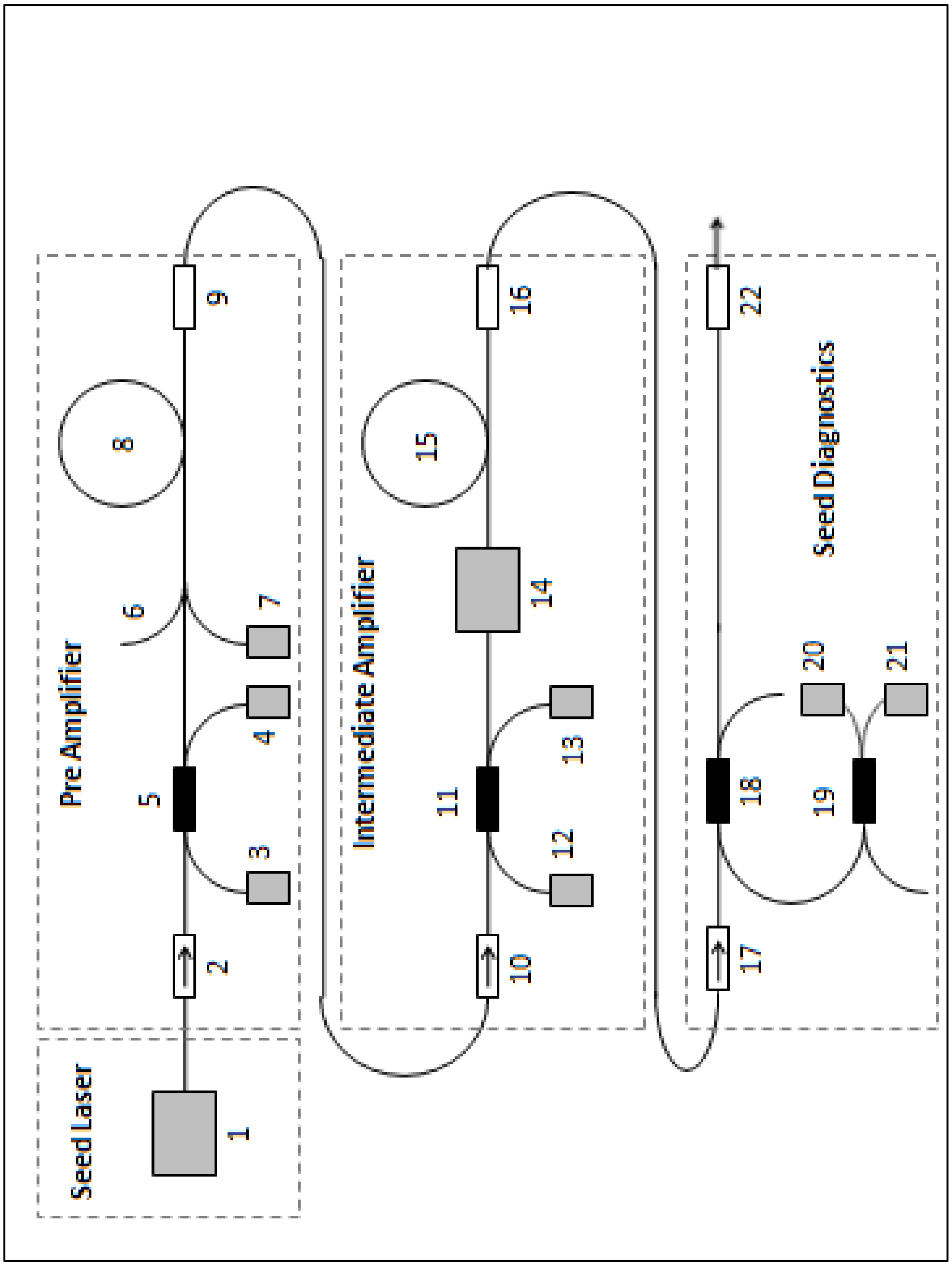

Figure A1: High power experiment detailed setup part 1

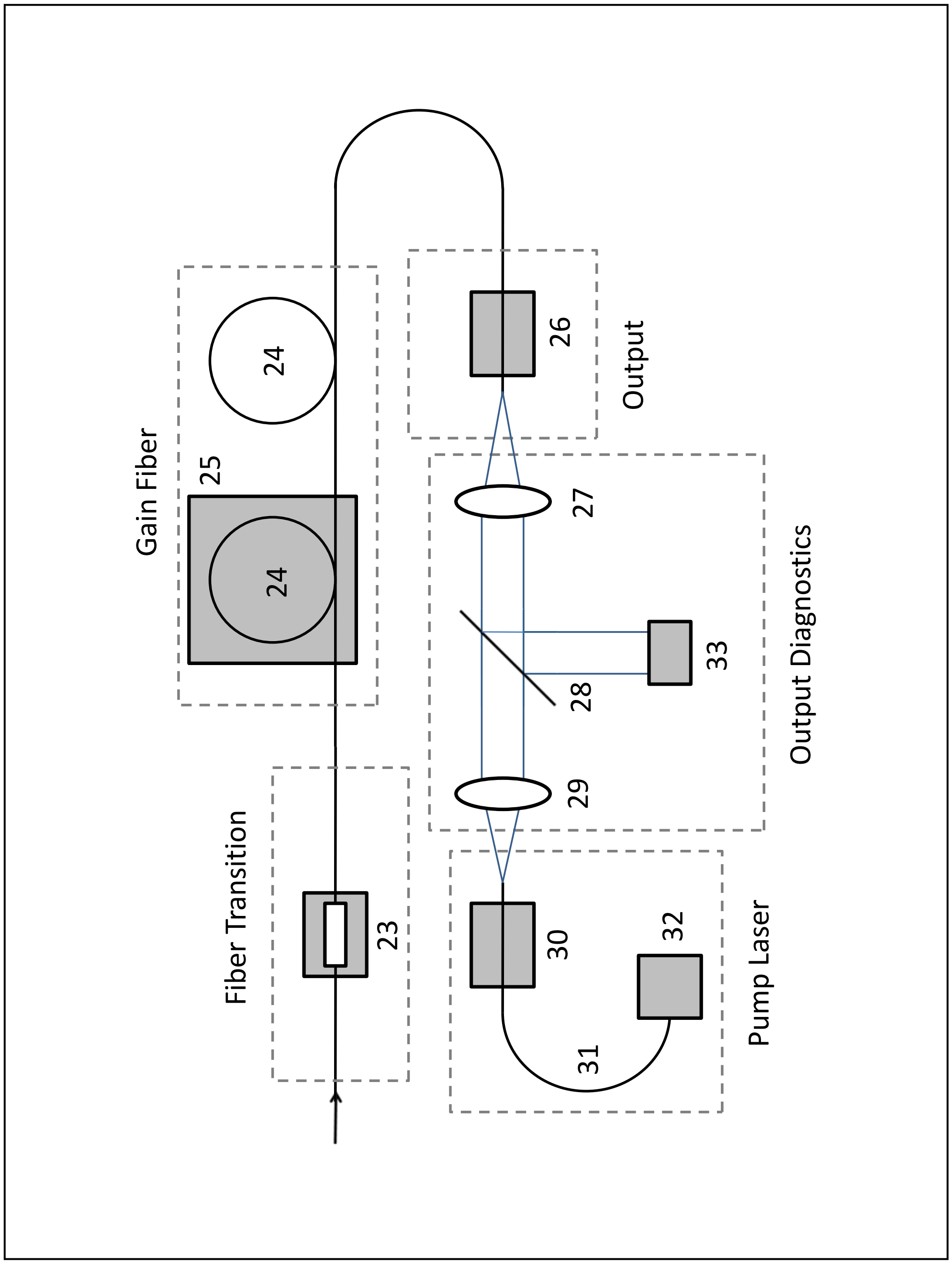

Figure A2: High power experiment detailed setup part 2

High Power Experiment		
Number	**Name**	**Description**
1	Sead laser	NP Photonics FLM-50-0-1064.175-1, 5kHz lindewidth
2	Novawave technologies isolator	300mW
3	Pre amp backward power monitor	Newport 818-sl
4	Seed laser monitor	Newport 818-sl
5	Tap coupler	99/1
6	Tapered fiber bundle	OFS tapered fiber bundle (6 legs)
7	Pre amp pump laser	Alfalight 980nm pump diode, 4007 B30386, 1.2-2.5W
8	Pre amplifier fiber	Nufern PLMA-YDF-6/125µm, 7.5m
9	Mode field adapter	5µm to 10µm
10	Isolator	3W Isolator
11	Tap coupler	99/1
12	Intermediate amplifier backwards power monitor	Newport 818-sl
13	Pre amplifier power monitor	Newport 818-sl
14	Intermediate amplifier pump laser	Alfalight CPM-II 20W pump unit
15	Intermediate amplifier fiber	Nufern PLMA-YDF-10/400µm, 4.5m
16	Mode field adapter	10µm to 10µm
17	Isolator	OFR 10W Isolator
18	Tap coupler	99/1, ITF
19	Tap coupler	50/50
20	Integrating sphere	Newport 5.3" with 818P
21	Optical spectrum analyzer	Anritsu MS9780A
22	Tapered fiber	10µm to 25µm
23	Mode field adapter/chilled splice	Glass V-grooves, aluminum clamp
24	High power fiber	Nufern PLMA-YDF-25/400µm, 5.3m
25	Temp chamber	Sigma systems corporation, M10g, "temp chamber"
26	Fiber mount	Water cooled bracket with silica-grooved rods
27	Lens	LightPath f=40mm lens
28	Dichroic	LayerTec dichroic, Rmax 976nm, Tmax 1064nm
29	Lens	Melles-Griot f=40mm lens
30	Fiber mount	Newport 3-axis stage
31	Pump fiber	HighYag .22 NA delivery fiber
32	High power pump laser	Nuvonyx 1kW laser diode
33	Output power monitor	Coherent Power Max M# PM5k

Table A1: High power experiment equipment

High Power Experiment	
Support Equipment	**Details**
Oscilloscope	Tektronix TDS7704B
Power meter	Multi function optical meter, Newport Model 2835-C
Power meter	Molectron EPM 2000
Optical spectrum analyzer	Anritsu MS9780A
Current source	ILX Lightwave, LDX-3565
Temperature controller	ILX Lightwave, LDT-5910
Current source	ILX Lightwave, LDX-3670
Power backup	APC 500
Temp chamber controller	Sigma systems Corporation, C4, controller
Current source	ILX Lightwave LDX-3565
intermediate amplifier temp control	ILX Lightwave, LDT-5910, Temperature Controller
Intermediate amplifier pump control	ILX Lightwave, LDX-3670, High power laser diode current source
Data collection software	Labview 8.0
Data collection hardware	National Instruments I/O box
Water chiller	Thermocube, 19.2°C
Piping	Tubes (1/4”)
Liquid nitrogen containment	Cryo-cyl, 160LP
Water chiller	Lytron, RC009G03BB2M028, chiller
Fiber finishing	Krell Technologies, dry polisher
Fiber viewing	Edmund optics, “microscope adapter”
Fiber viewing	CIDTEC, camera-video
Fiber holding	Newport 5 axis stage
5 axis stage holder	Magnetic base
Fiber cleaving	Vytran, LDC-200, cleaver
Fiber fusing	Vytran, FFS-2000 splicer
Fiber fusing	Vytran, GPX 3000, splicer
Ultrasonic cleaner	Branson 200
Light curing system	ELC-410
Low noise photoreceiver	IR-DC-125MHz New Focus 1811

Table A2: High power experiment support equipment

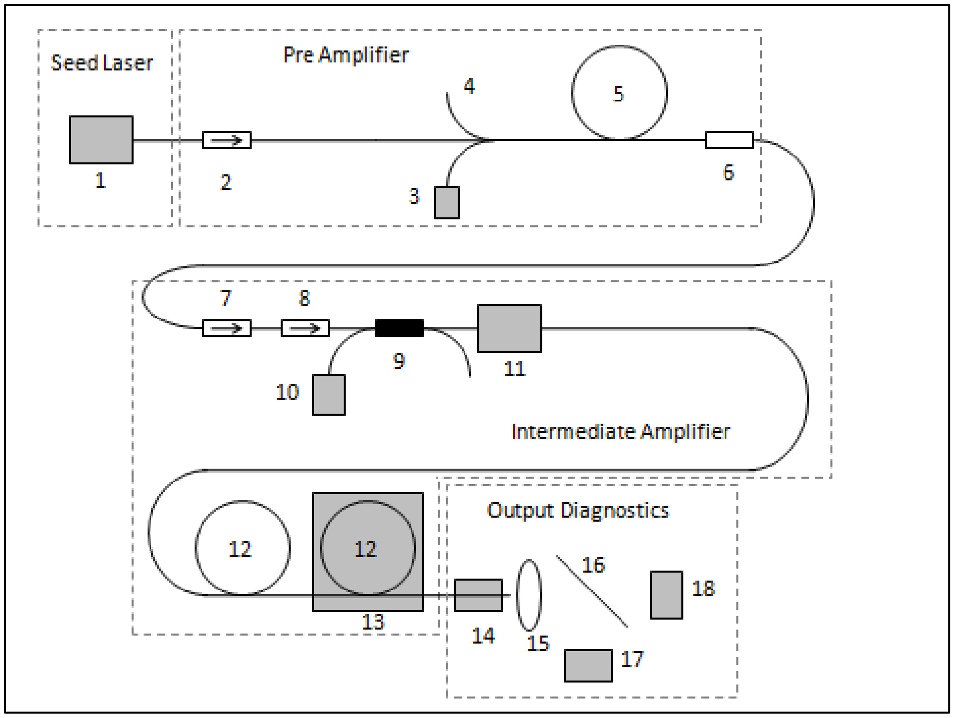

Figure A3: Low power experiment phase I detailed setup

Low Power Experiment: phase I		
Number	**Name**	**Description**
1	Seed laser	NP Photonics FLM-50-0-1064.175-1, 5kHz lindewidth
2	Isolator	Novawave tech PM1-06-P
3	Pre amp pump laser	Alfalight 980nm pump diode, 4007 B30386, 1.2-2.5W
4	Tapered fiber bundle	OFS tapered fiber bundle (6 legs)
5	Pre amp fiber	Nufern PLMA-YDF-6/125μm, 7.5m
6	Mode field adaptor	6μm to 10μm
7	Isolator	OFR IO-J-1064, 3W
8	Isolator	OFR IO-J-1064, 3W
9	Tap coupler	CIR 90/10
10	Integrating sphere	Newport 818-sl, 2W
11	Int amp pump laser	Alfalight CPM-II 20W pump unit
12	Int amp fiber	6/125μm PM YB gain fiber
13	Temp chamber	Sigma systems corporation, M10g, “temp chamber”
14	Fiber mount	Newport 3 axis stage
15	Lens	LightPath f=40mm lens
16	Dichroic	LayerTec dichroic, Rmax 976nm, Tmax 1064nm
17	Power sensor	Newport 818P 30W
18	Power sensor	Newport 818P 30W

Table A3: Low power experiment phase I equipment

Low Power Experiment: phase I	
Support Equipment	**Details**
Water chiller	Thermocube (19.2°C)
Laser diode controller	ILX Lightwave LDC-3900
Fiber cleaver	PKTech FK12
Laser diode controller	ILX Lightwave LDX 36000
Power backup	APC 500
Temp chamber controller	Sigma systems Corporation, C4, controller
Data collection software	Labview 8.0
Data collection hardware	National Instruments I/O box
Piping	Tubes (1/4")
Fiber viewing	Edmund optics, "microscope adapter"
Fiber viewing	CIDTEC, camera-video
Fiber cleaving	Vytran, LDC-200, cleaver
Fiber fusing	Vytran, FFS-2000 splicer
Fiber fusing	Vytran, GPX 3000, splicer
Ultrasonic cleaner	Branson 200
Optical power measurement	Newport 2835-C
Optical power measurement	Newport 2935-C

Table A4: Low power experiment phase I support equipment

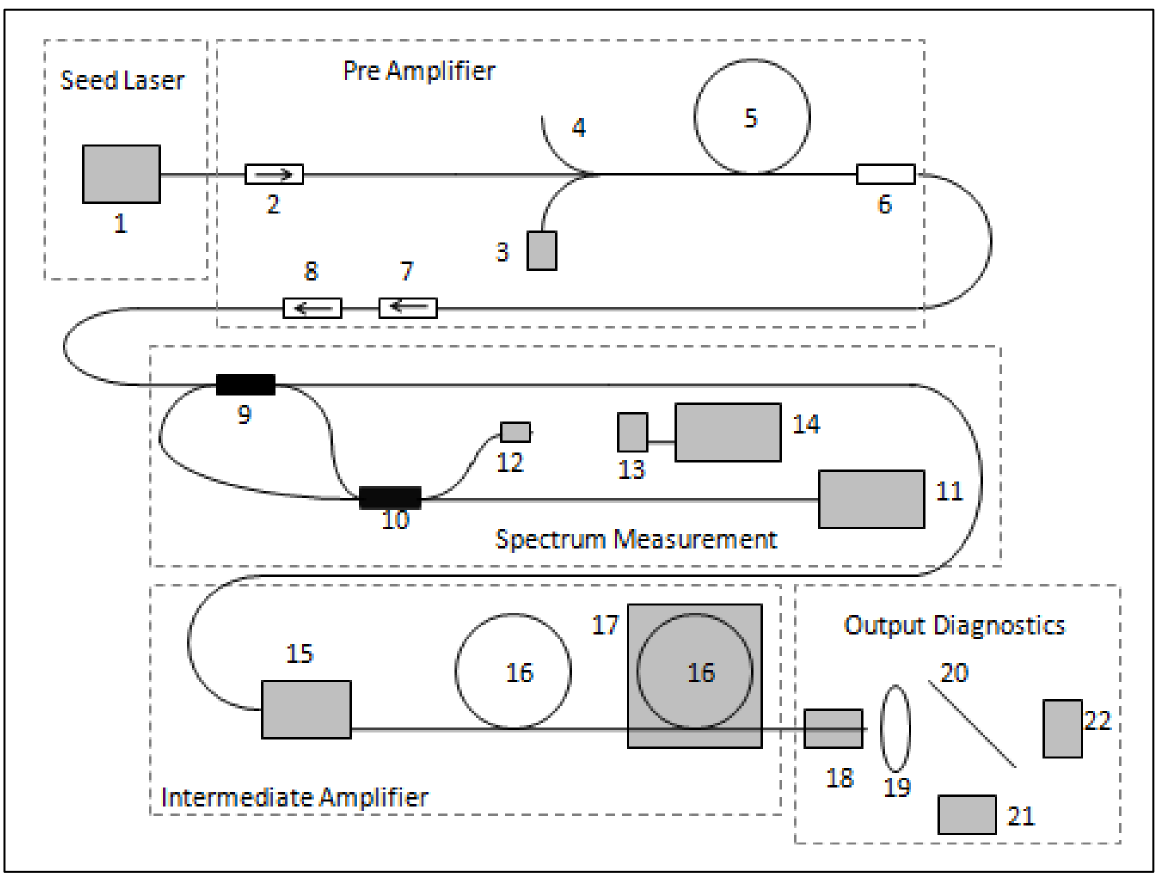

Figure A4: Low power experiment phase II detailed setup

Low Power Experiment: phase II		
Number	**Name**	**Description**
1	Seed laser	NP Photonics FLM-50-0-1064.175-1, 5kHz lindewidth
2	Isolator	Novawave tech PM1-06-P
3	Pre amplifier pump laser	Alfalight 980nm pump diode, 4007 B30386, 1.2-2.5W
4	Tapered fiber bundle	OFS tapered fiber bundle (6 legs)
5	Pre amplifier fiber	Nufern PLMA-YDF-6/125μm, 7.5m
6	Mode field adaptor	6μm to 10μm
7	Isolator	OFR IO-J-1064, 3W
8	Isolator	OFR IO-J-1064, 3W
9	Tap coupler	CIR 90/10
10	Tap coupler	CIR 90/10
11	Optical spectrum analyzer	Yokogawa AQ6319
12	Fiber mount	Newport 3 axis stage
13	Frequency counter	Newport 1437 26GHz detector
14	Spectrum analyzer	Agilent E4440A, 3Hz - 26.5GHz
15	Intermediate amplifier pump laser	Alfalight CPM-II 20W pump unit
16	Intermediate amplifier fiber	6/125μm PM Yb gain fiber
17	Temperature chamber	Sigma systems corporation, M10g, “temp chamber”
18	Fiber mount	Newport 3 axis stage
19	Lens	LightPath f=40mm lens
20	Dichroic	LayerTec dichroic, Rmax 976nm, Tmax 1064nm
21	Power sensor	Newport 818P 30W
22	Power sensor	Newport 818P 30W

Table A5: Low power experiment phase II equipment

Low Power Experiment: phase II	
Support Equipment	**Details**
Water chiller	Thermocube (19.2°C)
Laser diode controller	ILX Lightwave LDC-3900
Fiber cleaver	PKTech FK12
Laser diode controller	ILX Lightwave LDX 36000
Power backup	APC 500
Temperature chamber controller	Sigma systems Corporation, C4, controller
Data collection software	Labview 8.0
Data collection hardware	National Instruments I/O box
Piping	Plastic tubes (1/4”)
Fiber viewing	Edmund optics, “microscope adapter”
Fiber viewing	CIDTEC, camera-video
Fiber cleaving	Vytran, LDC-200, cleaver
Fiber fusing	Vytran, FFS-2000 splicer
Fiber fusing	Vytran, GPX 3000, splicer
Ultrasonic cleaner	Branson 200
Optical power measurement	Newport 2835-C
Optical power measurement	Newport 2935-C

Table A6: Low power experiment phase II support equipment

10 Appendix B: High Power Experiment Output Power and SBS Curves

Data collected from the high power experiment for output power and SBS power is presented here. It is arranged starting at 80C and ending at -100C

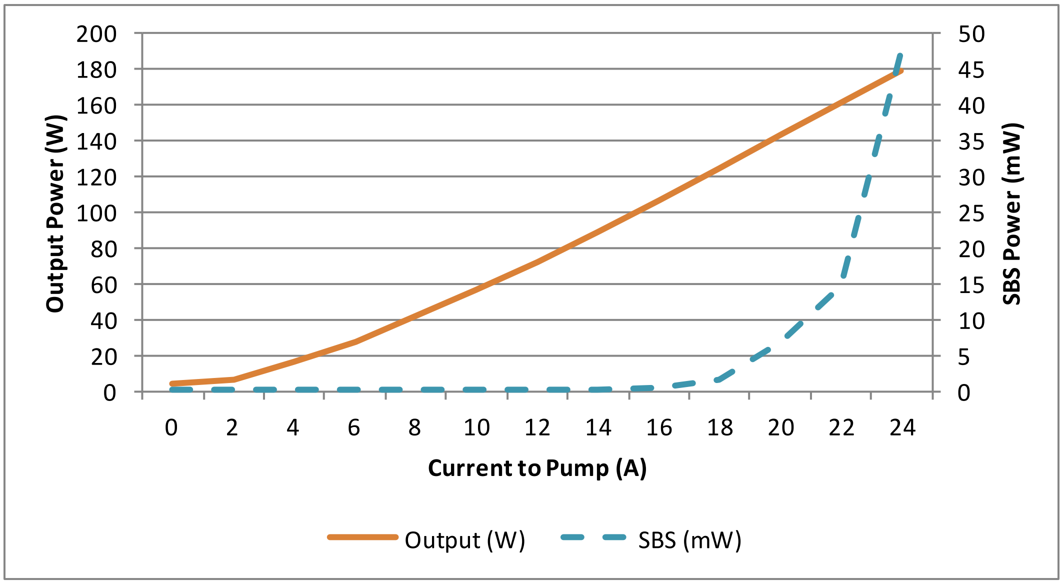

Figure B1: Output power and SBS versus current to pump at 80˚C

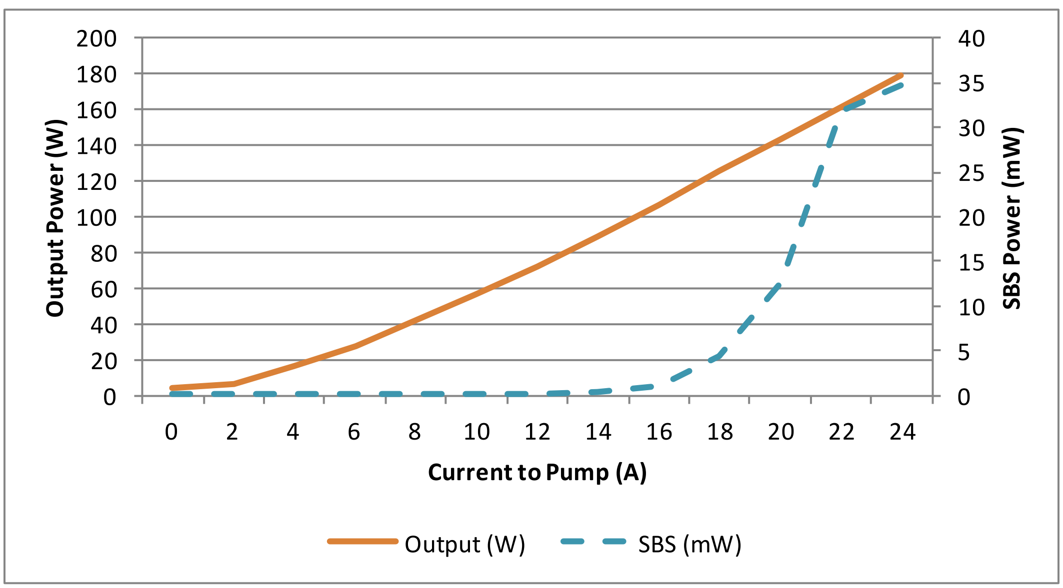

Figure B2: Output power and SBS versus current to pump at 60˚C

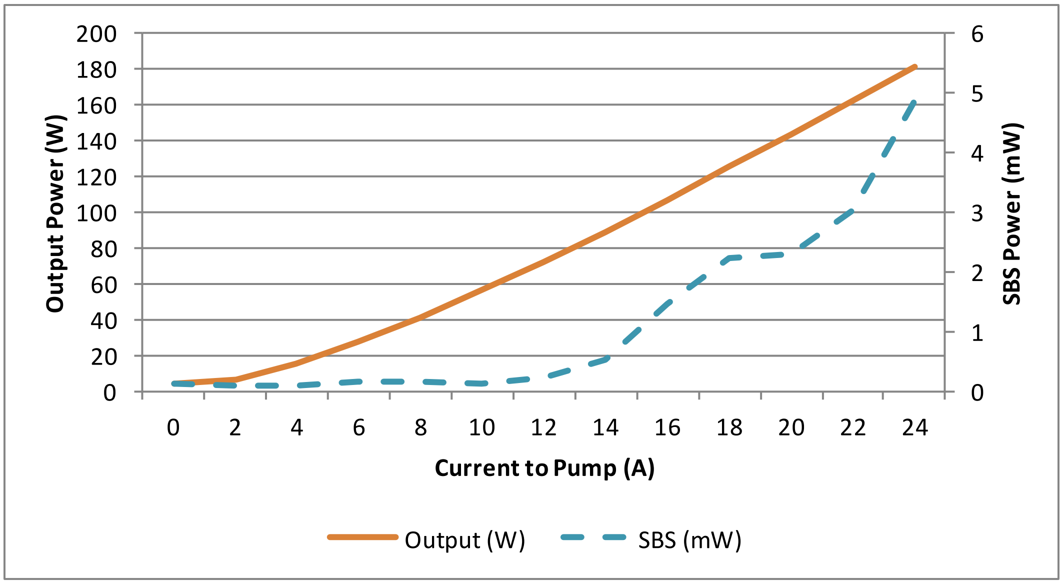

Figure B3: Output power and SBS versus current to pump at 40˚C

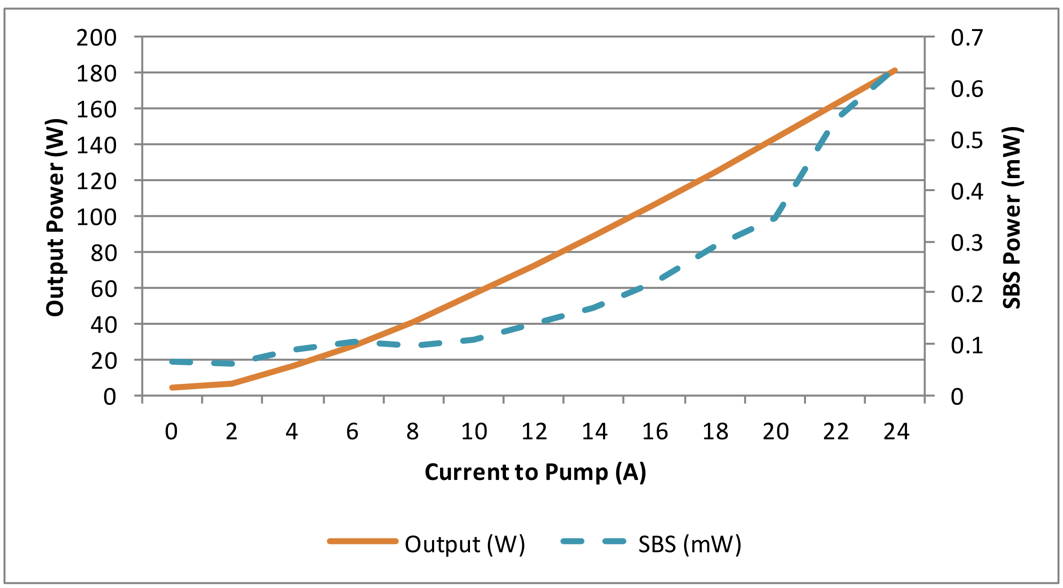

Figure B4: Output power and SBS versus current to pump at 20˚C

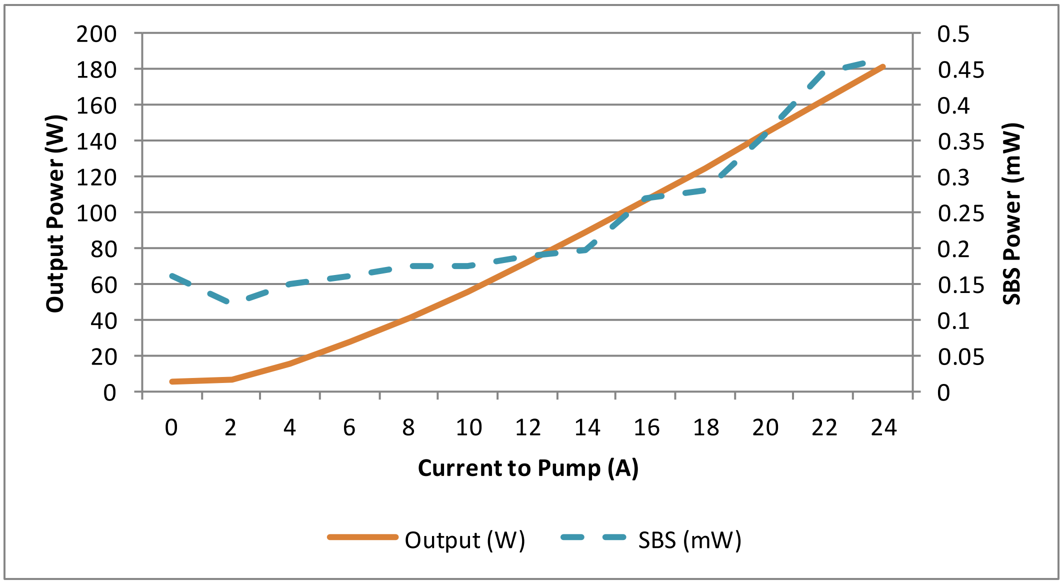

Figure B5: Output power and SBS versus current to pump at 0˚C

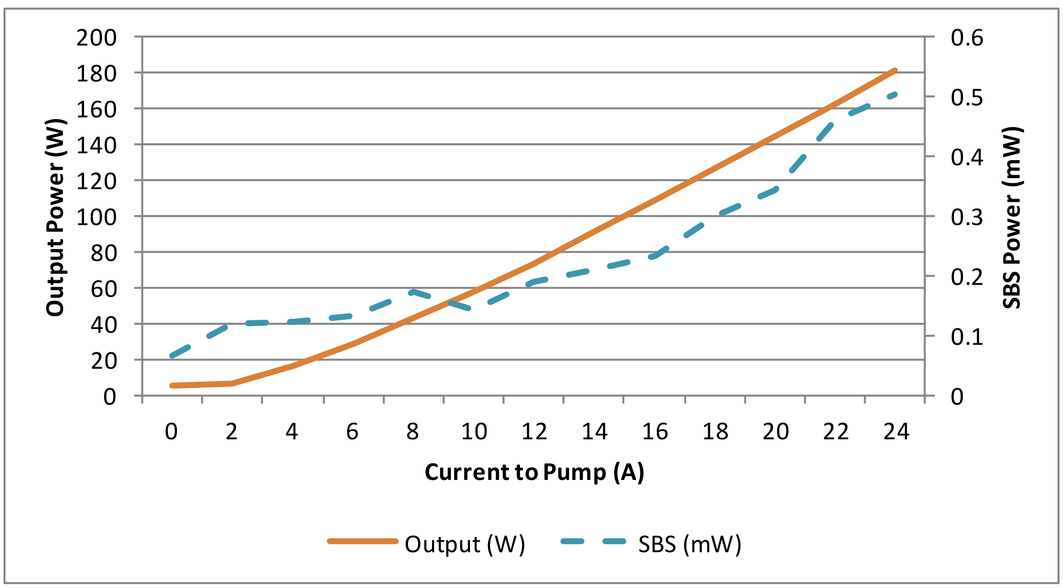

Figure B6: Output power and SBS versus current to pump at -20˚C

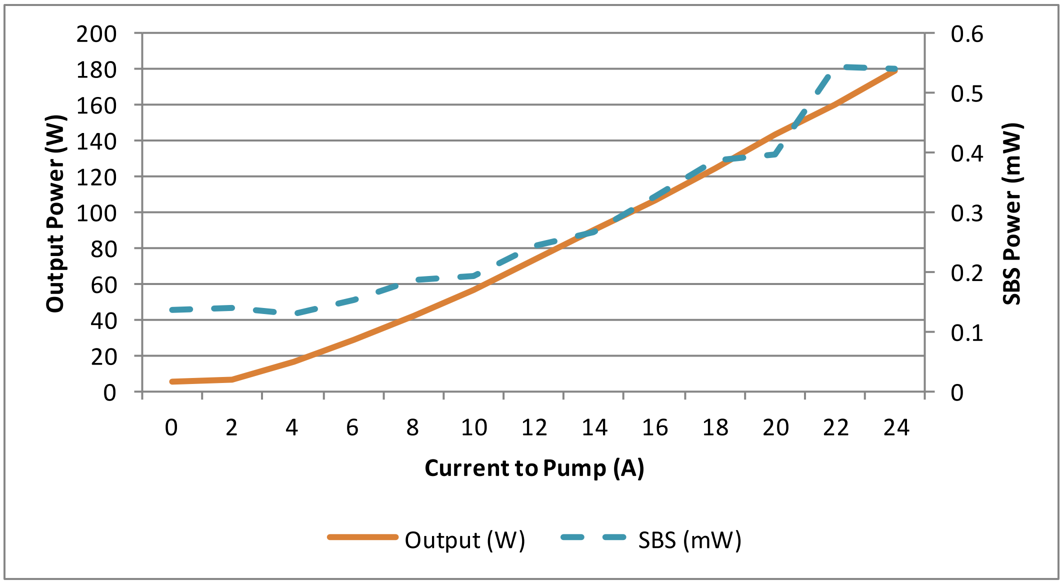

Figure B7: Output power and SBS versus current to pump at -40˚C

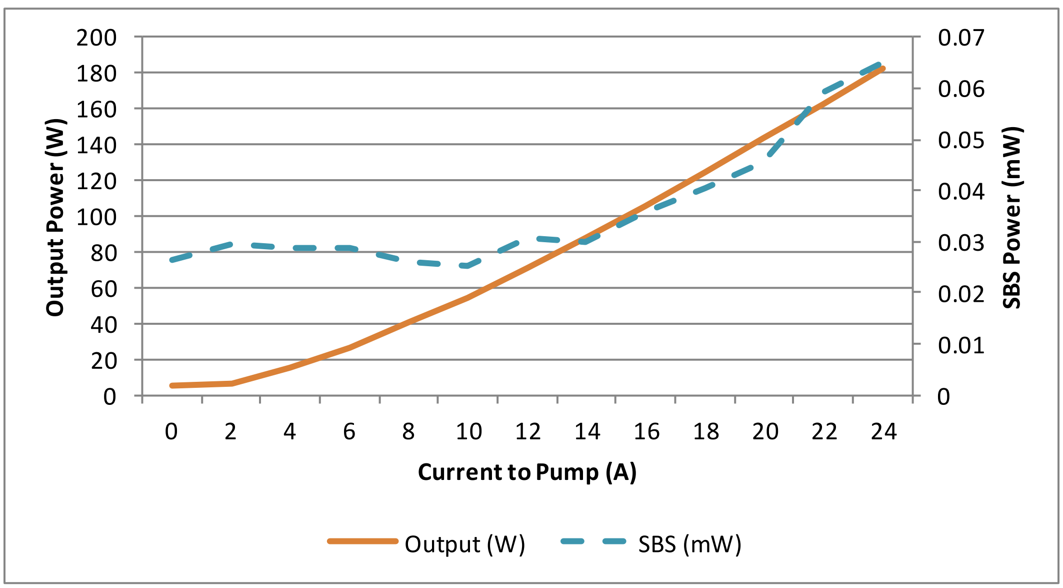

Figure B8: Output power and SBS versus current to pump at -60˚C

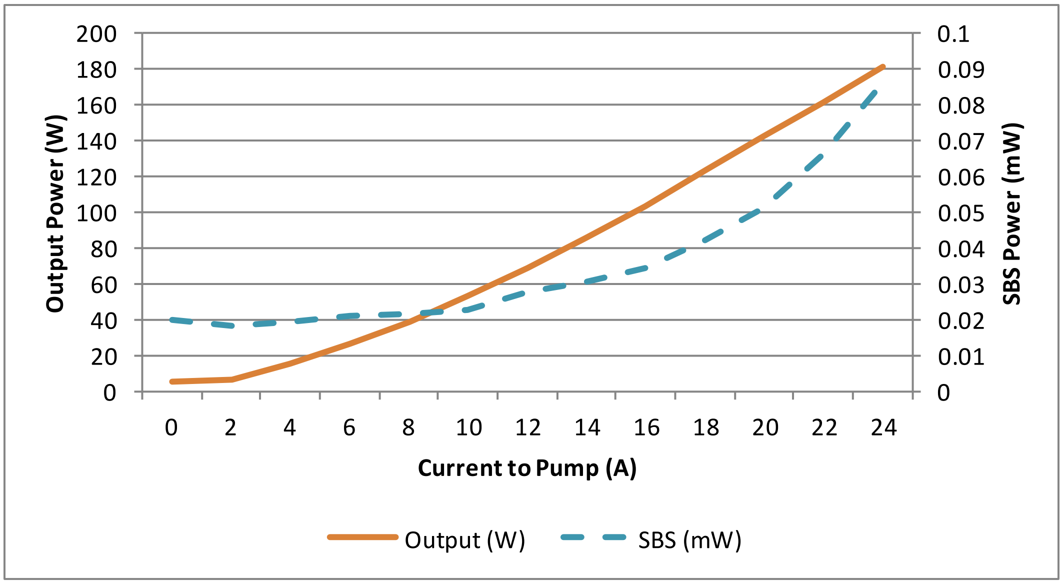

Figure B9: Output power and SBS versus current to pump at -80˚C

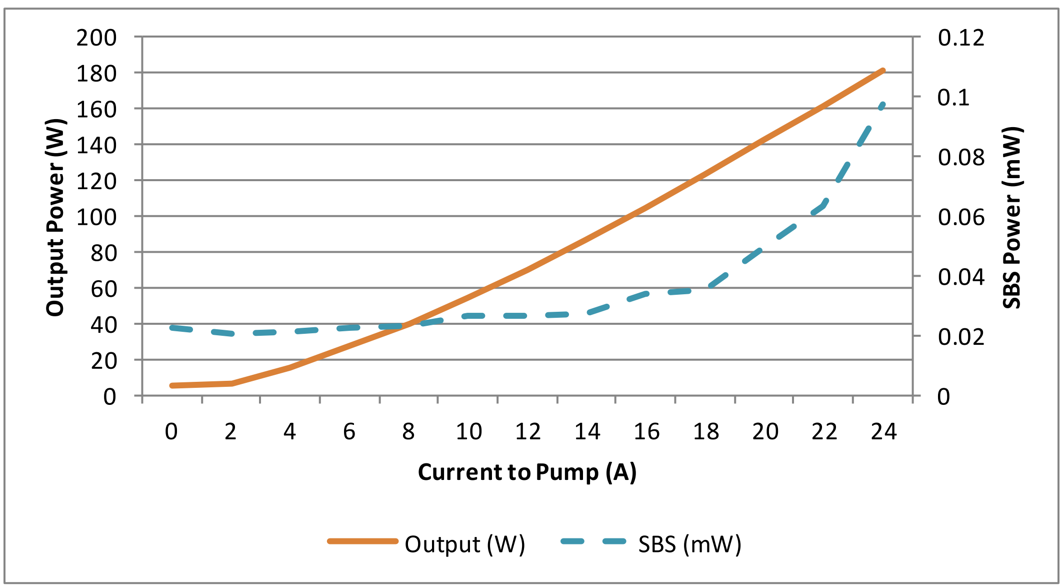

Figure B10: Output power and SBS versus current to pump at -100˚C

11 Appendix C: High Power Experiment Spectrum Data

Data collected from the high power experiment for SBS spectrums are presented here. It is arranged starting at 80C and ending at -100C. Each series corresponds to measurements taken at current to pump laser settings of 8, 12, 16, 20, or 24 Amps. Power on the left of each figure is due to Rayleigh scattering. Power on the right of each figure is due to stimulated Brillioun scattering.

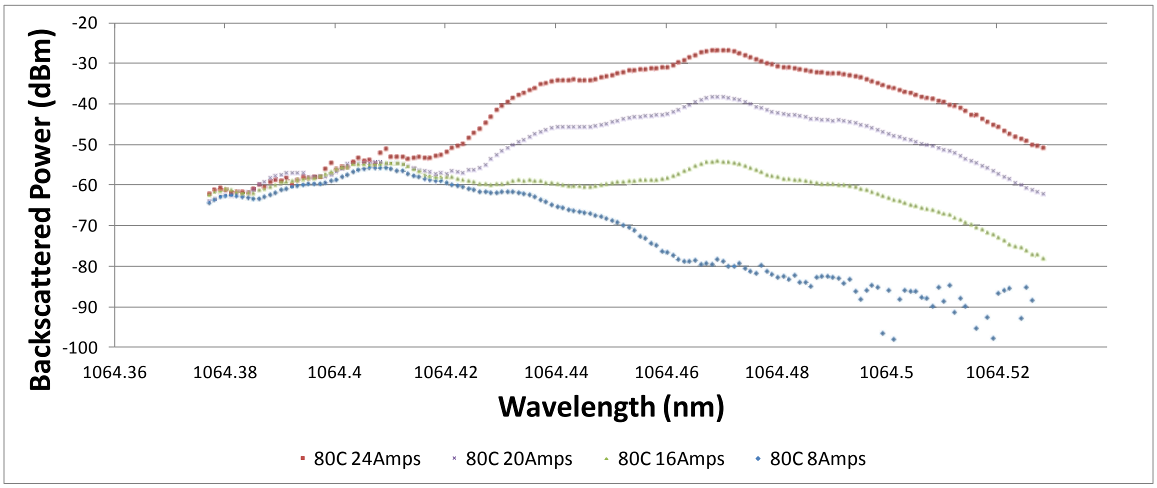

Figure C1: Power versus wavelength at 80˚C

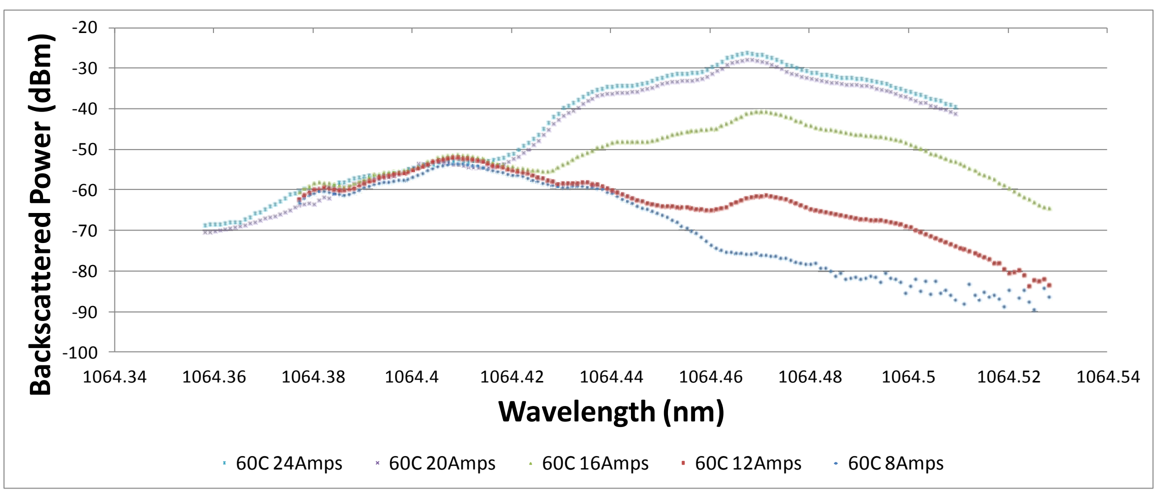

Figure C2: Power versus wavelength at 60˚C

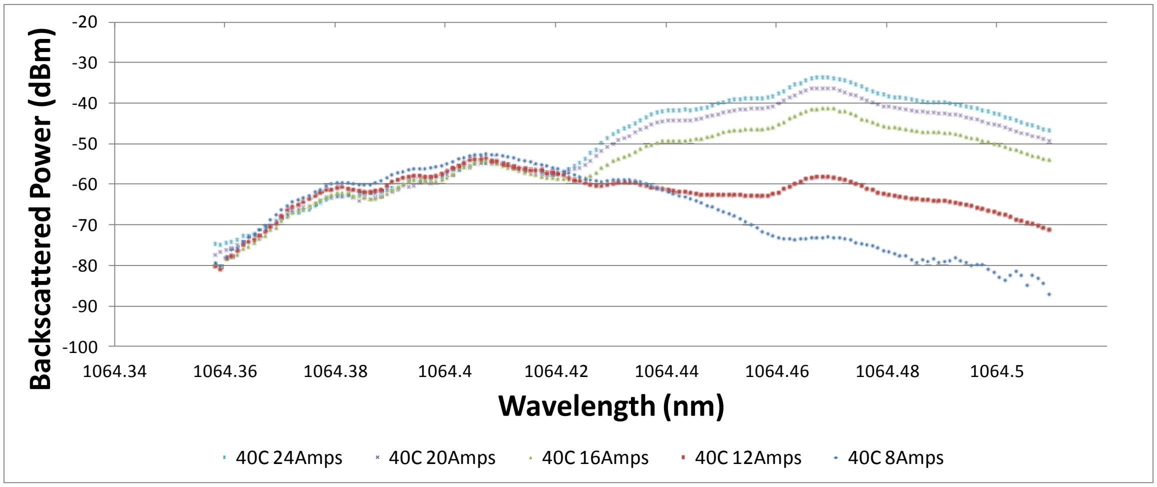

Figure C3: Power versus wavelength at 40˚C

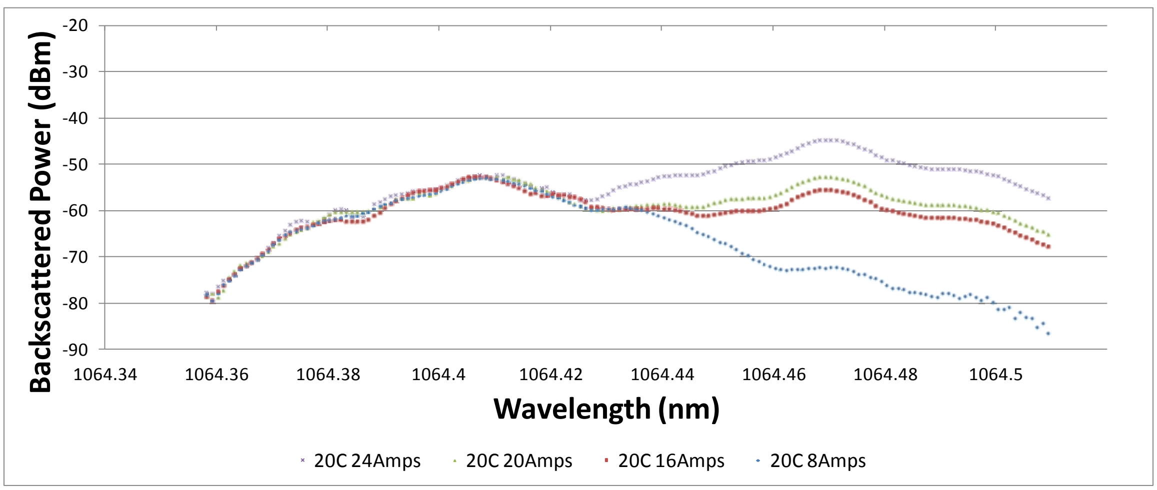

Figure C4: Power versus wavelength at 20˚C

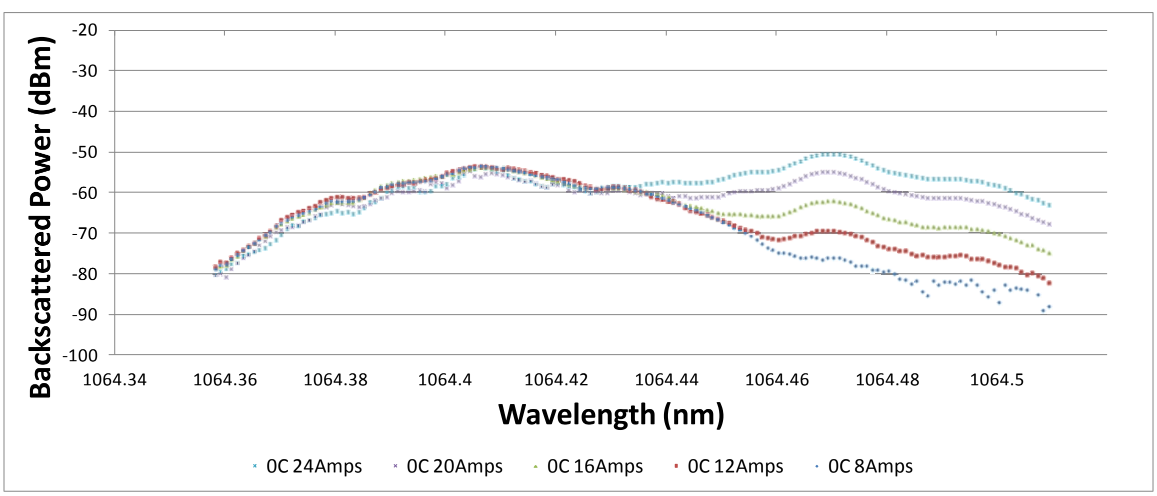

Figure C5: Power versus wavelength at 0˚C

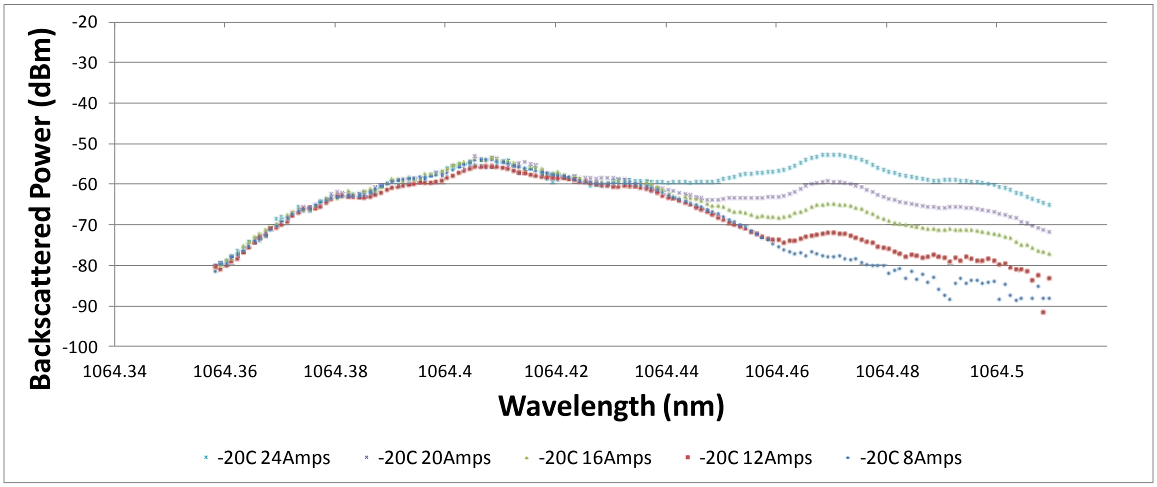

Figure C6: Power versus wavelength at -20˚C

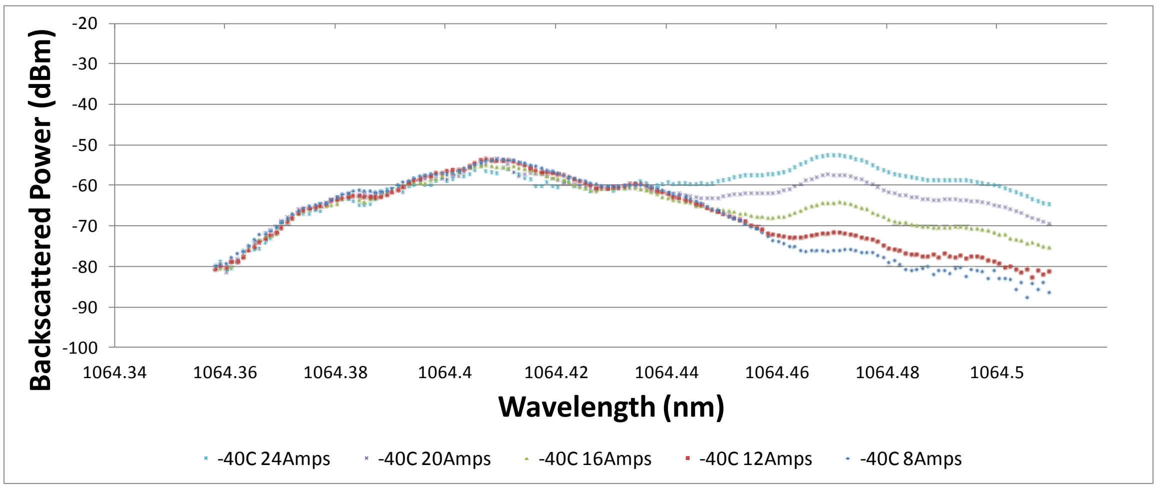

Figure C7: Power versus wavelength at -40˚C

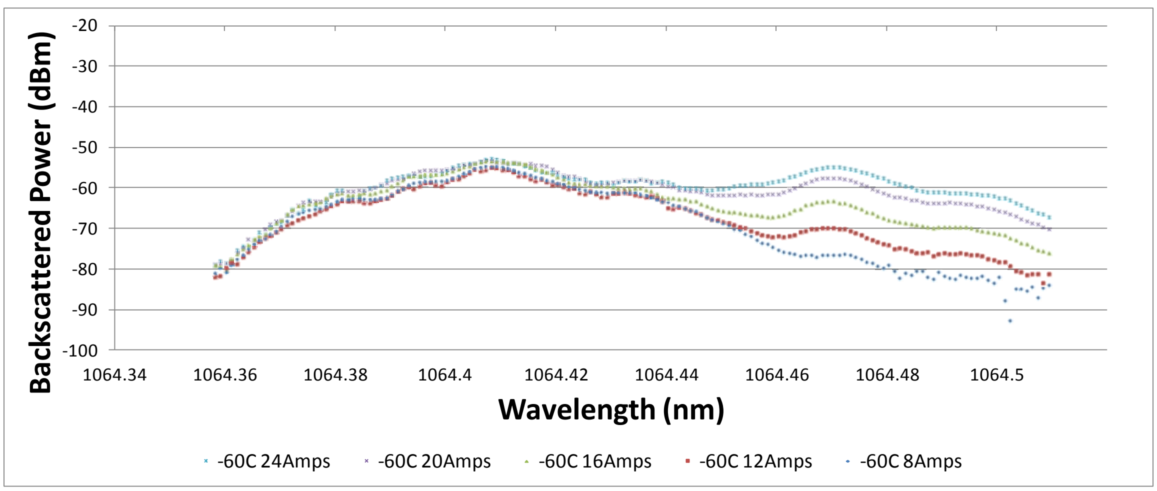

Figure C8: Power versus wavelength at -60˚C

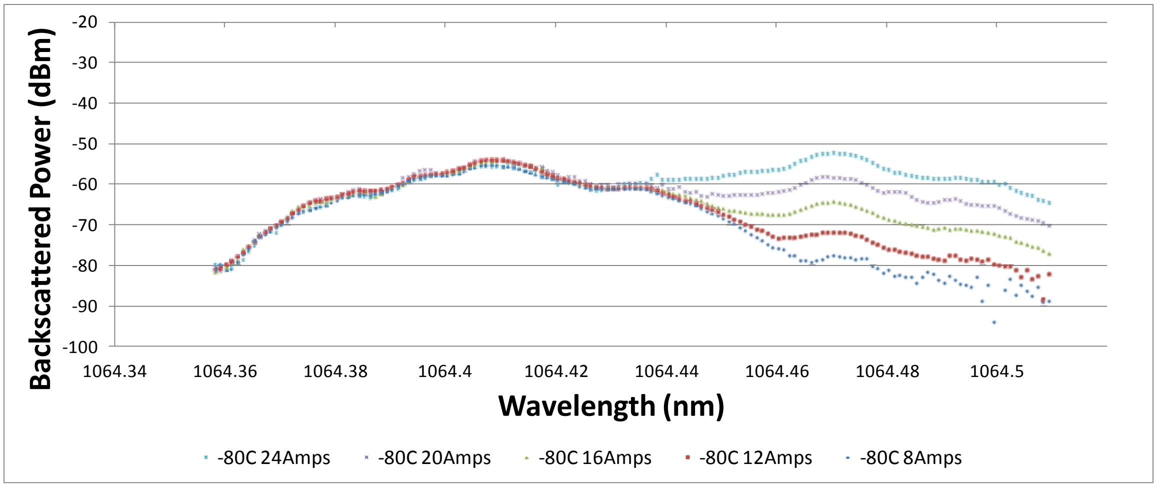

Figure C9: Power versus wavelength at -80˚C

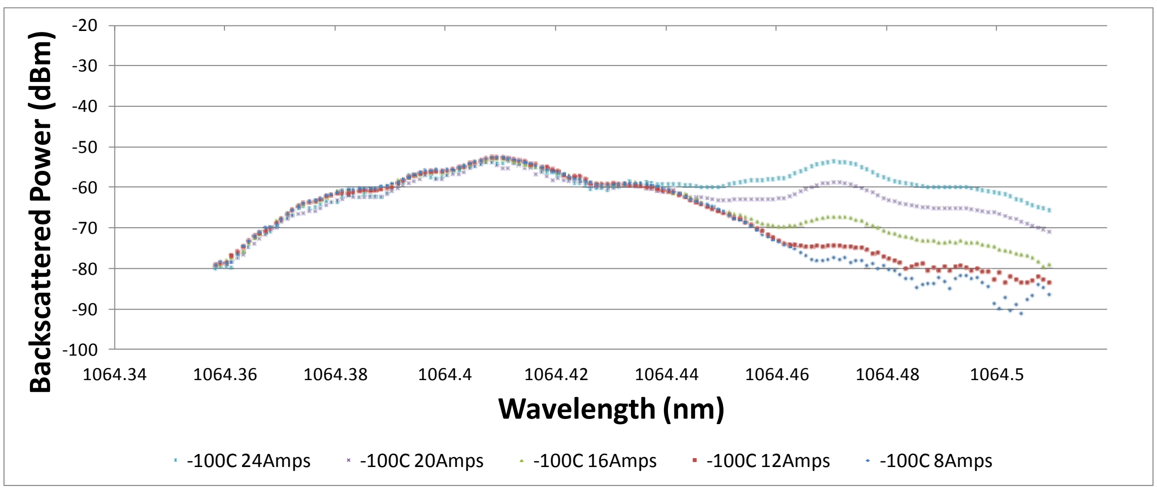

Figure C10: Power versus wavelength at -100˚C

12 Appendix D: Low Power Experiment Phase I Data

Data collected from the low power experiment phase I are presented here. It is arranged starting at 80C and ending at -100C

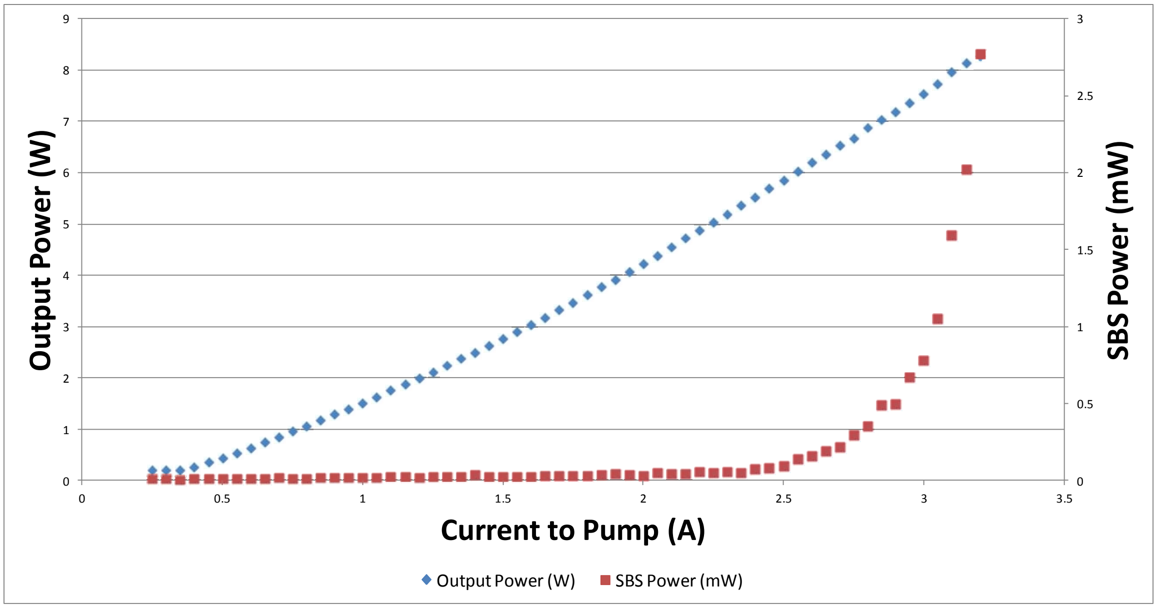

Figure D1: Output and SBS power versus current to pump at 80˚C

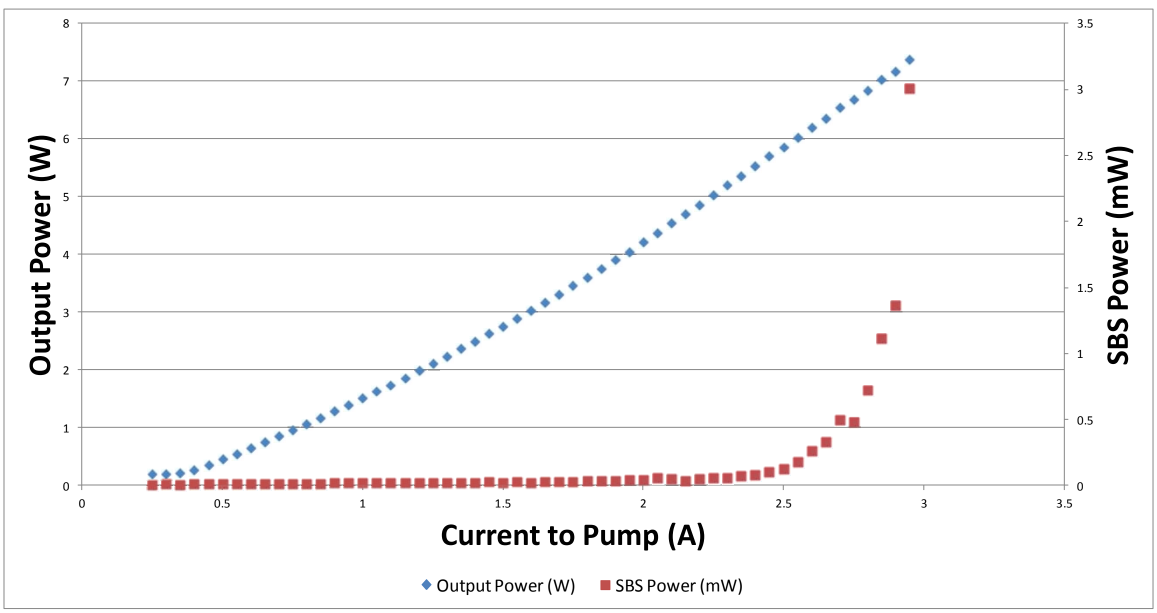

Figure D2: Output and SBS power versus current to pump at 60˚C

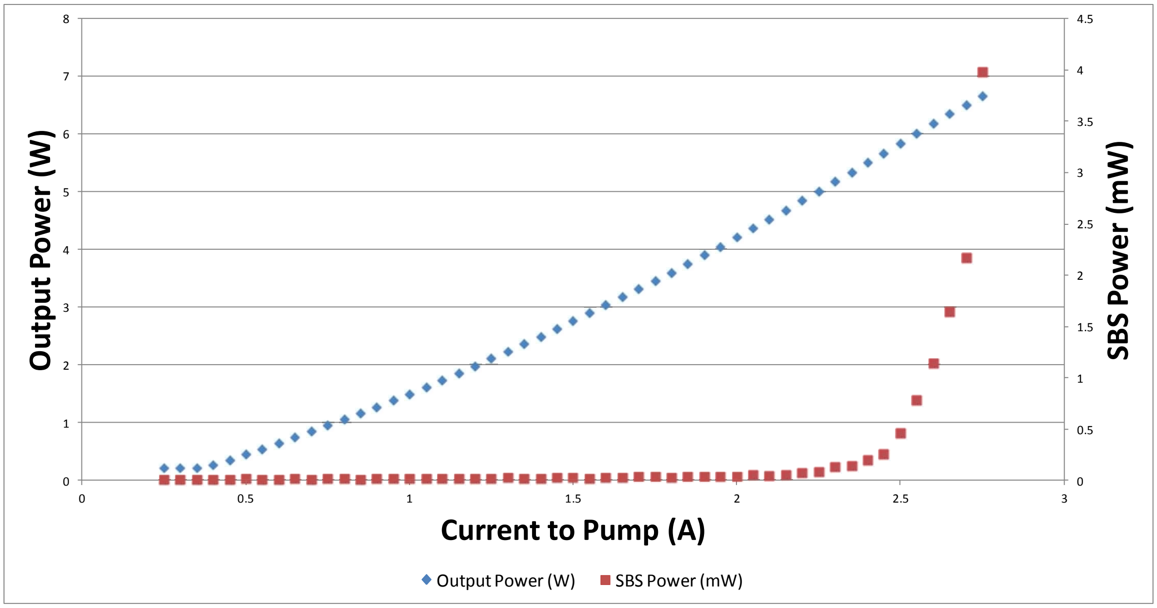

Figure D3: Output and SBS power versus current to pump at 40˚C

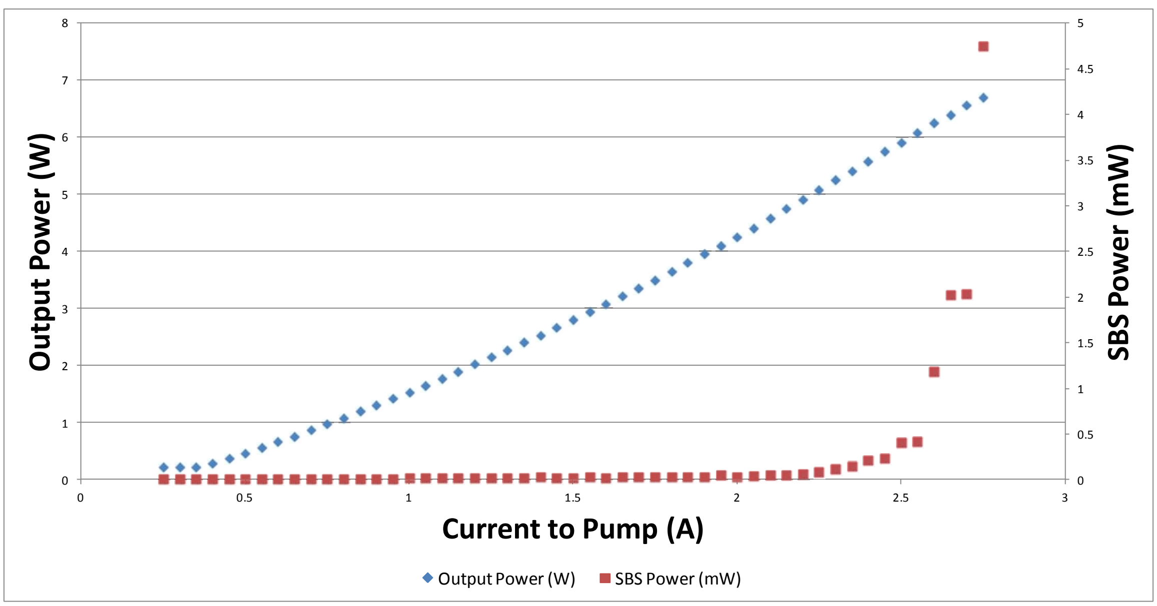

Figure D4: Output and SBS power versus current to pump at 20˚C

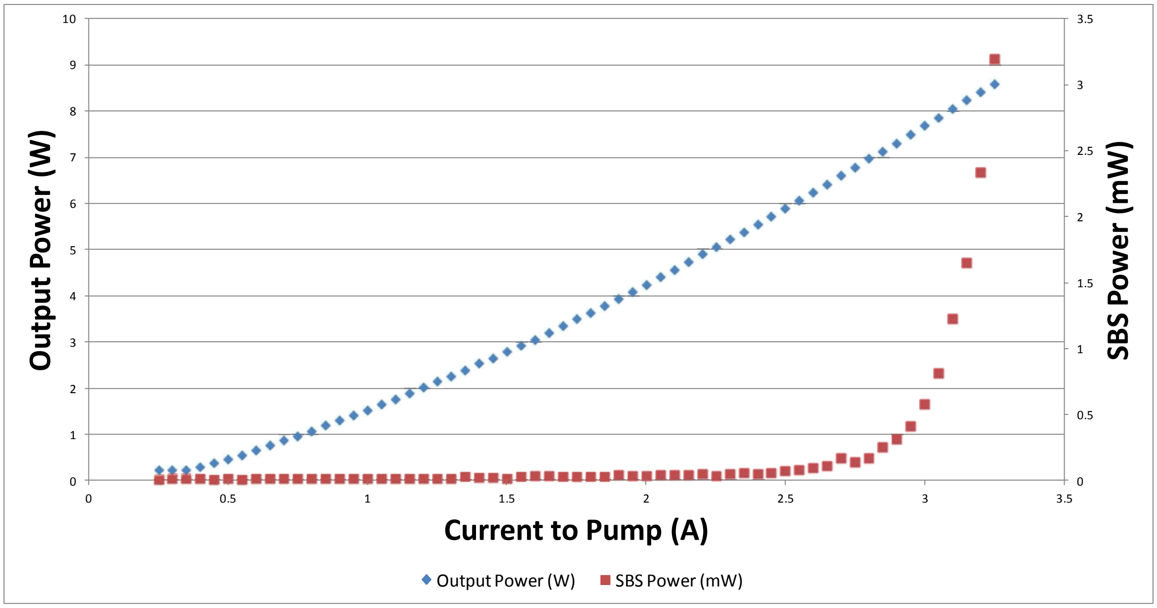

Figure D5: Output and SBS power versus current to pump at 0˚C

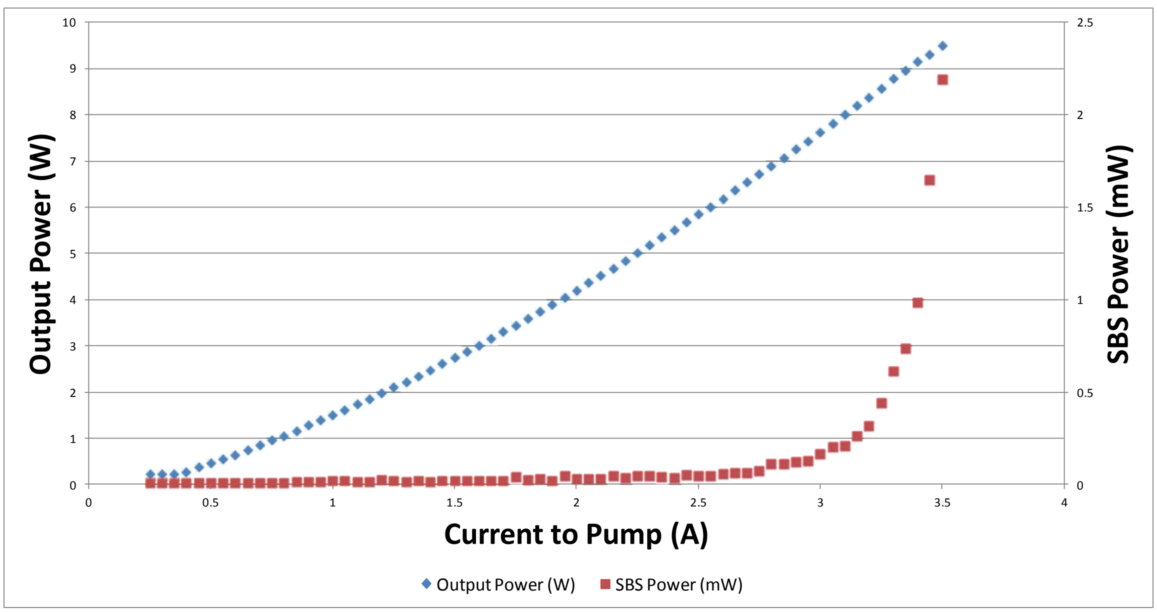

Figure D6: Output and SBS power versus current to pump at -20˚C

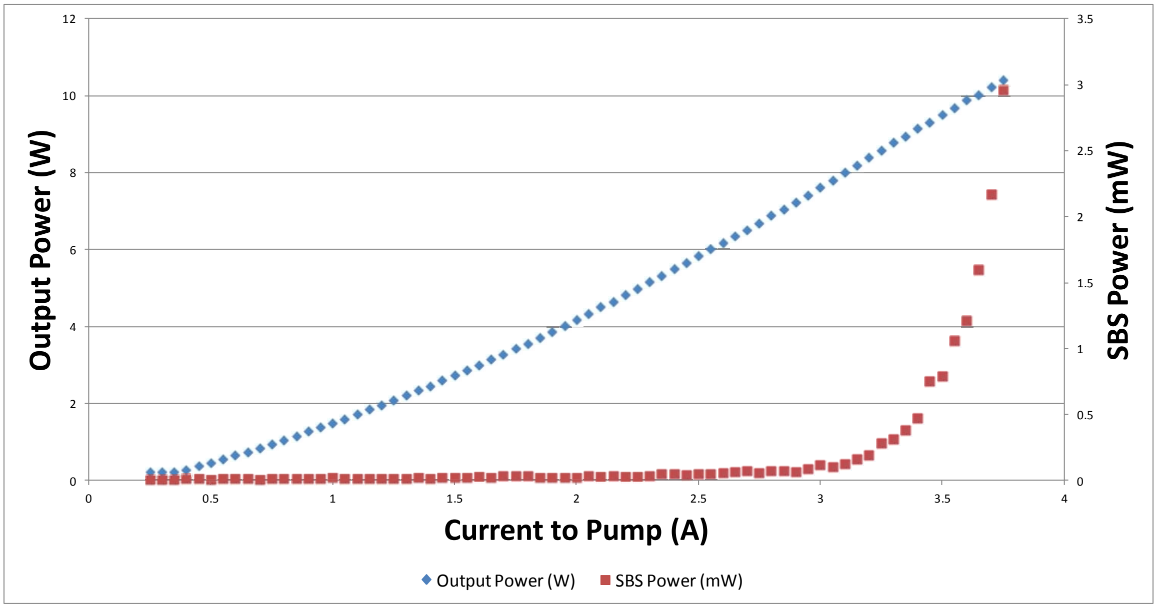

Figure D7: Output and SBS power versus current to pump at -40˚C

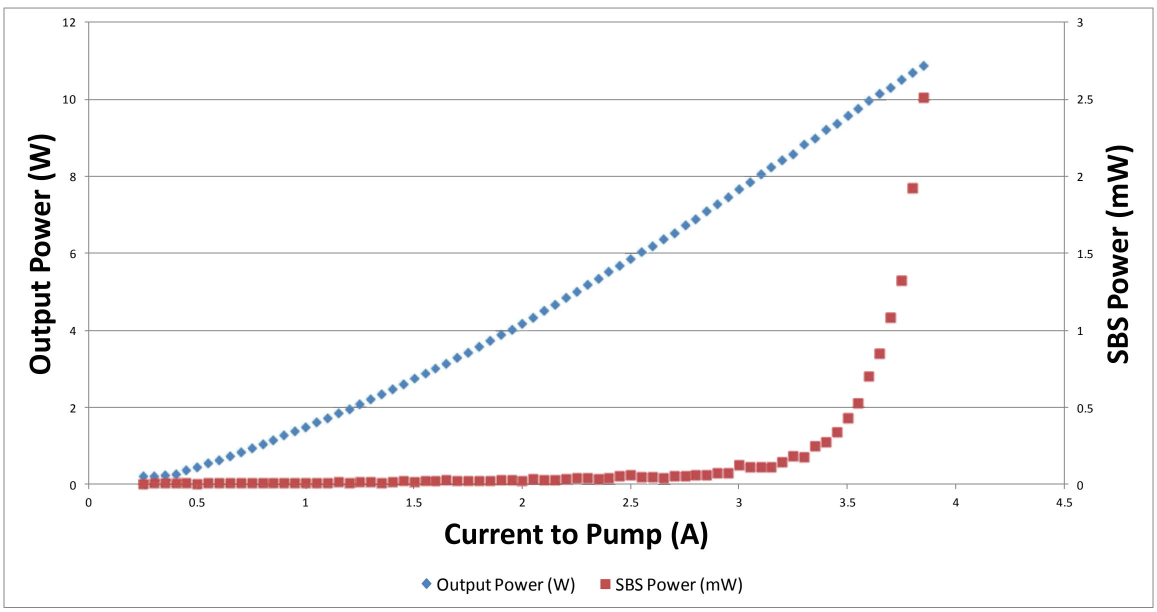

Figure D8: Output and SBS power versus current to pump at -60˚C

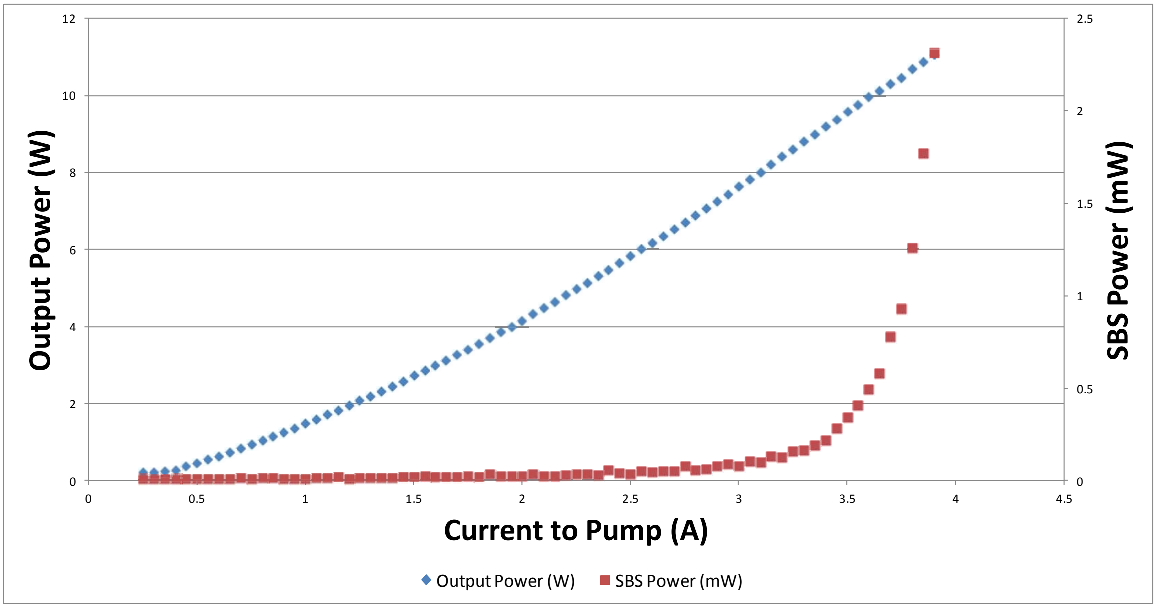

Figure D9: Output and SBS power versus current to pump at -80˚C

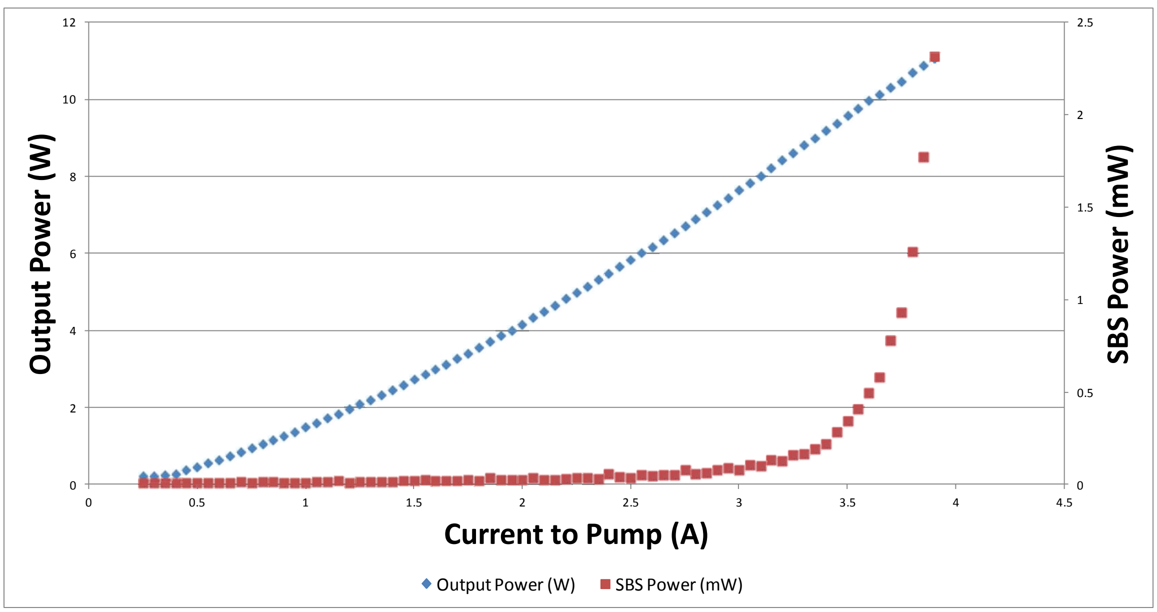

Figure D10: Output and SBS power versus current to pump at -100˚C

13 Appendix E: Low Power Experiment Phase II Data

Data collected from the low power experiment phase II is presented here. It is arranged starting at 90C and ending at -120C.

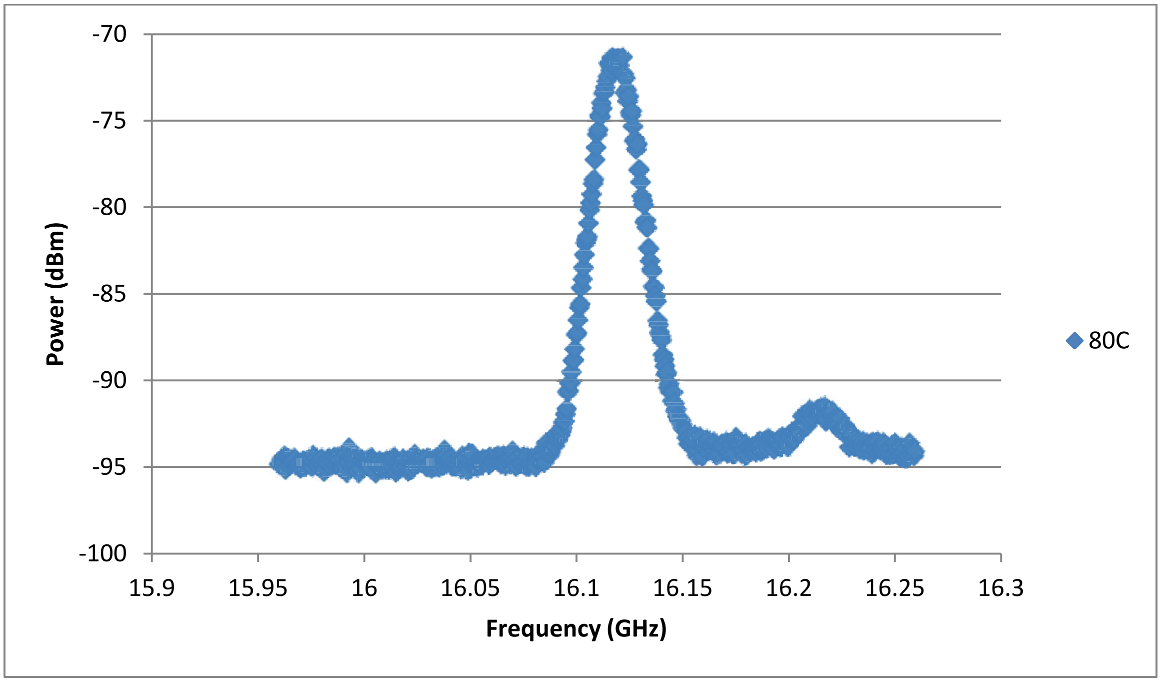

Figure E1: Beat note power versus frequency at 90˚C

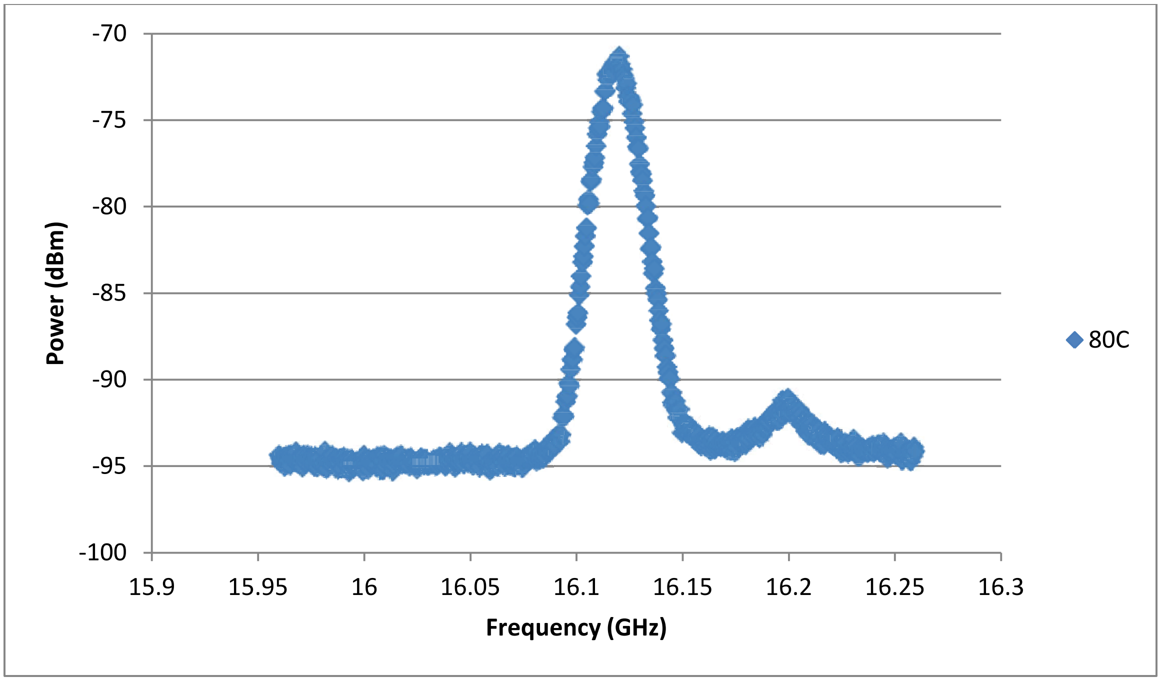

Figure E2: Beat note power versus frequency at 80˚C

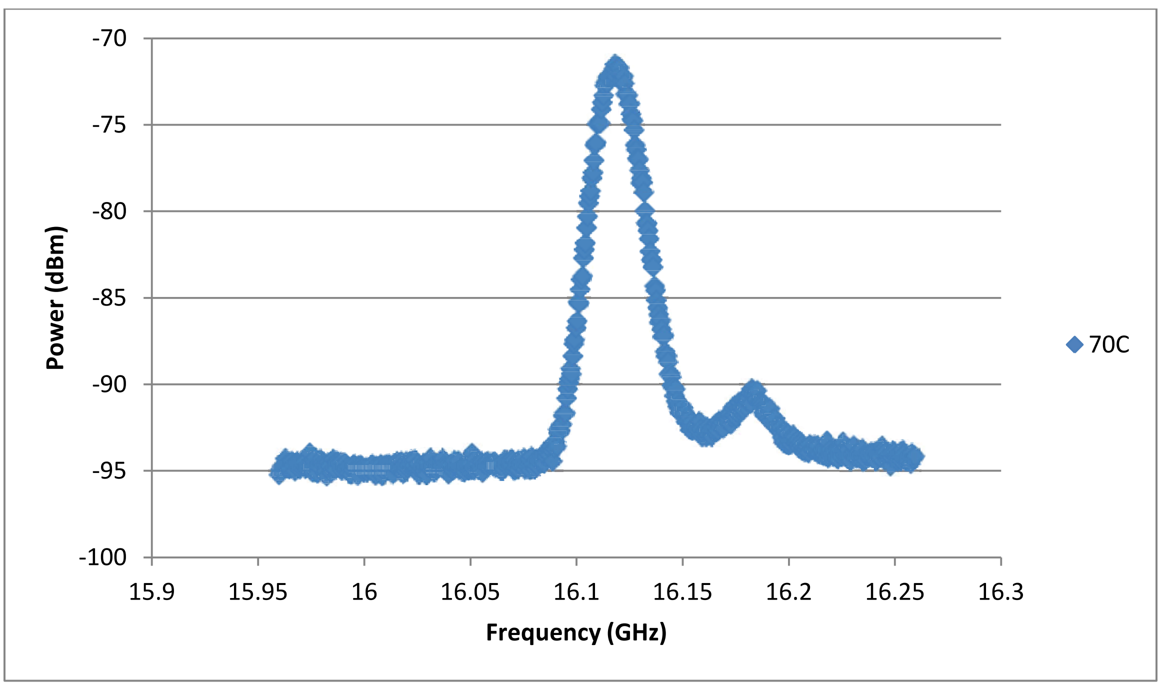

Figure E3: Beat note power versus frequency at 70˚C

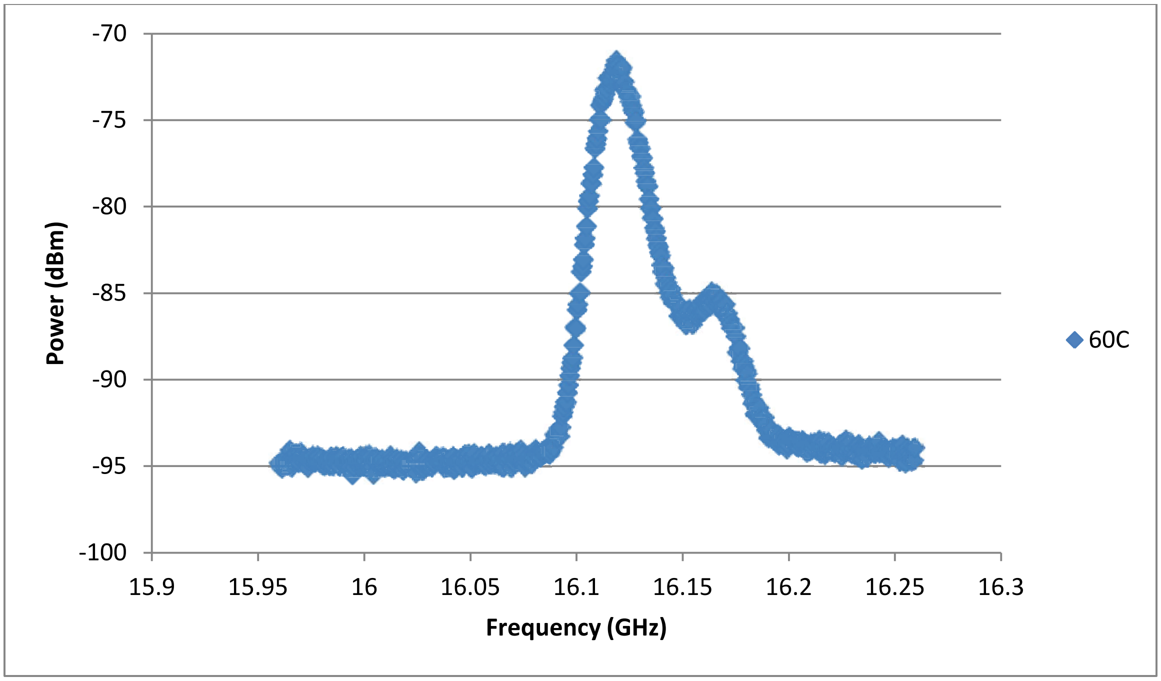

Figure E4: Beat note power versus frequency at 60˚C

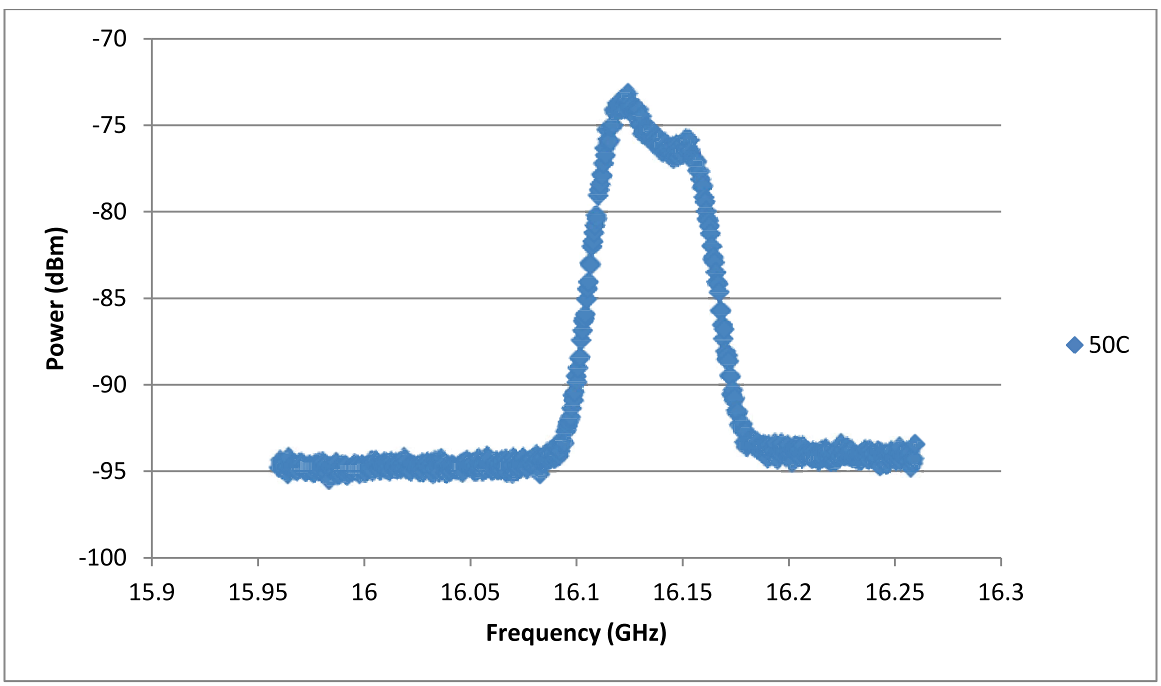

Figure E5: Beat note power versus frequency at 50˚C

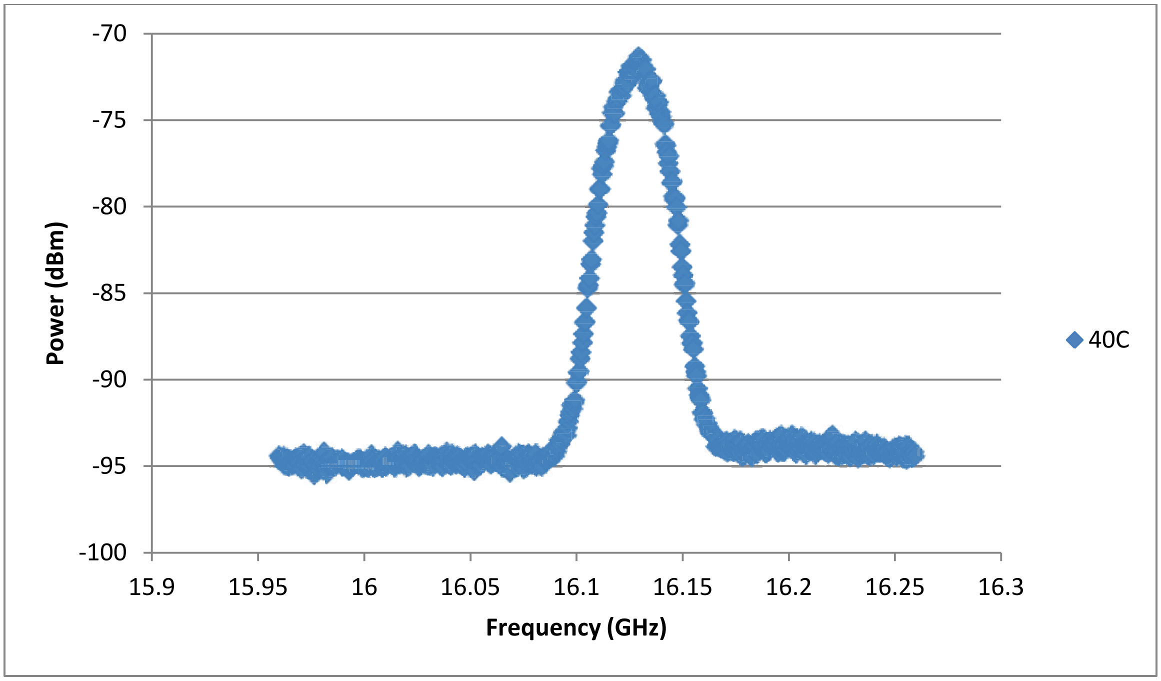

Figure E6: Beat note power versus frequency at 40˚C

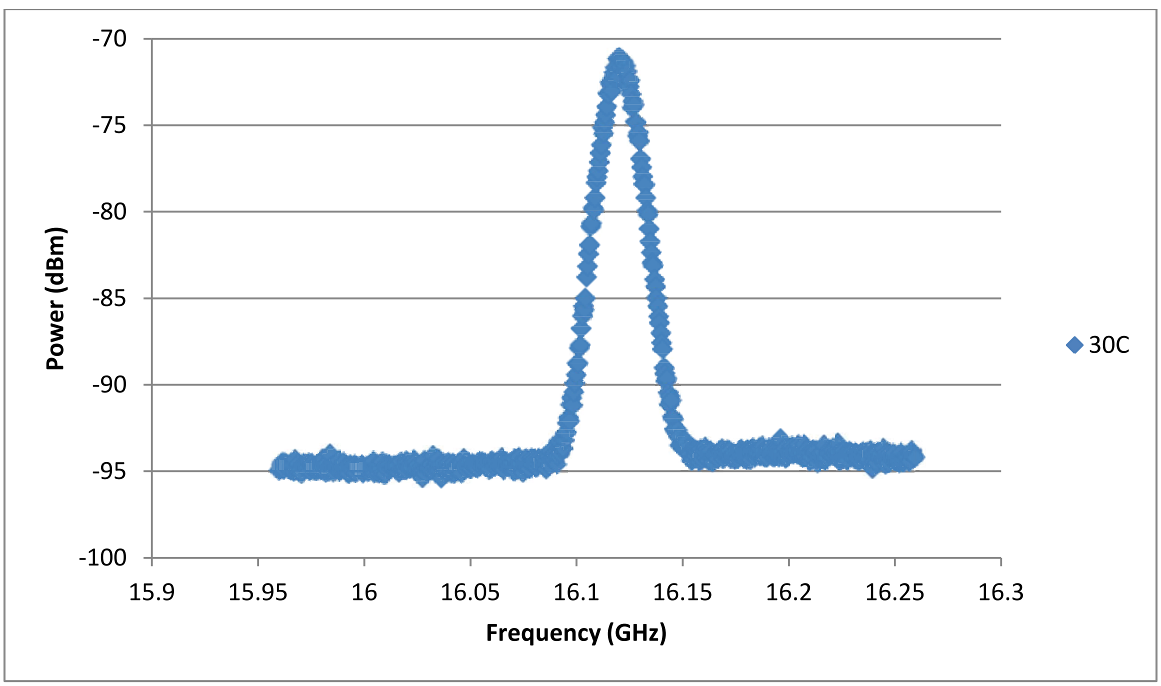

Figure E7: Beat note power versus frequency at 30˚C

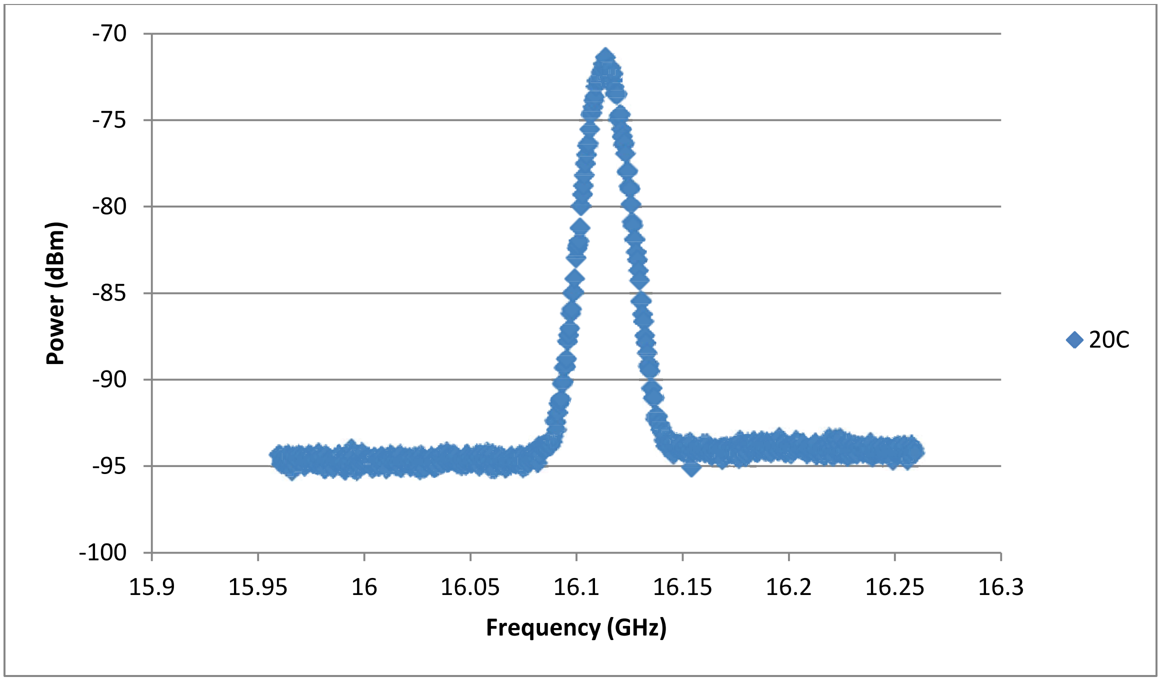

Figure E8: Beat note power versus frequency at 20˚C

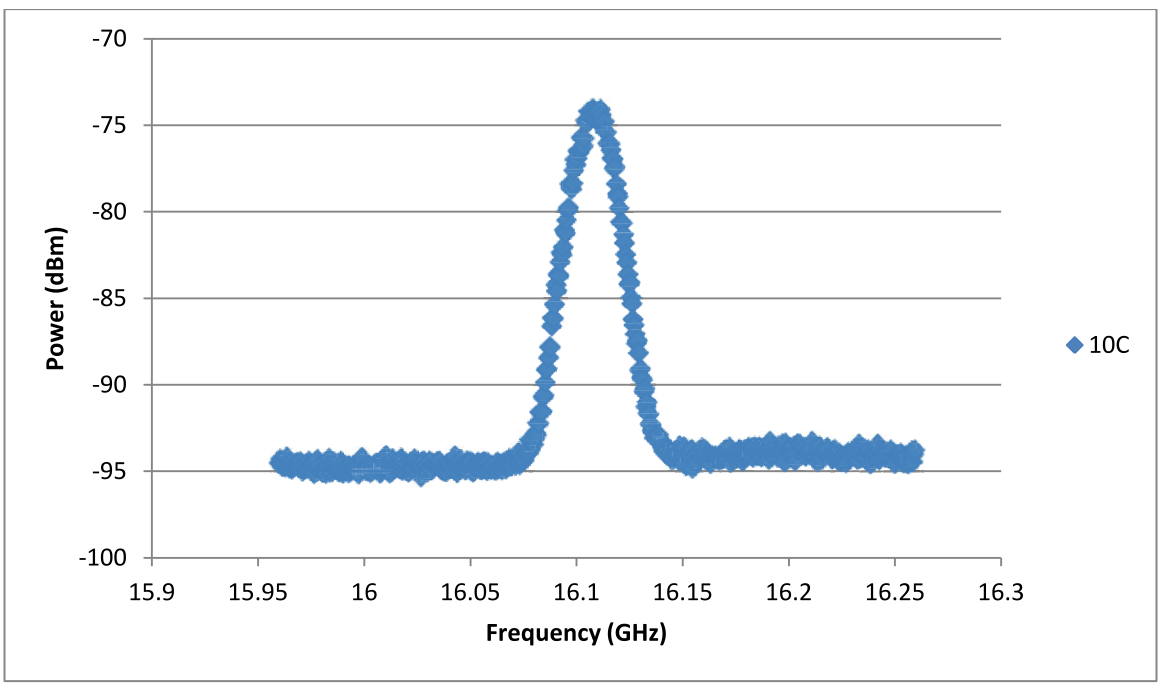

Figure E9: Beat note power versus frequency at 10˚C

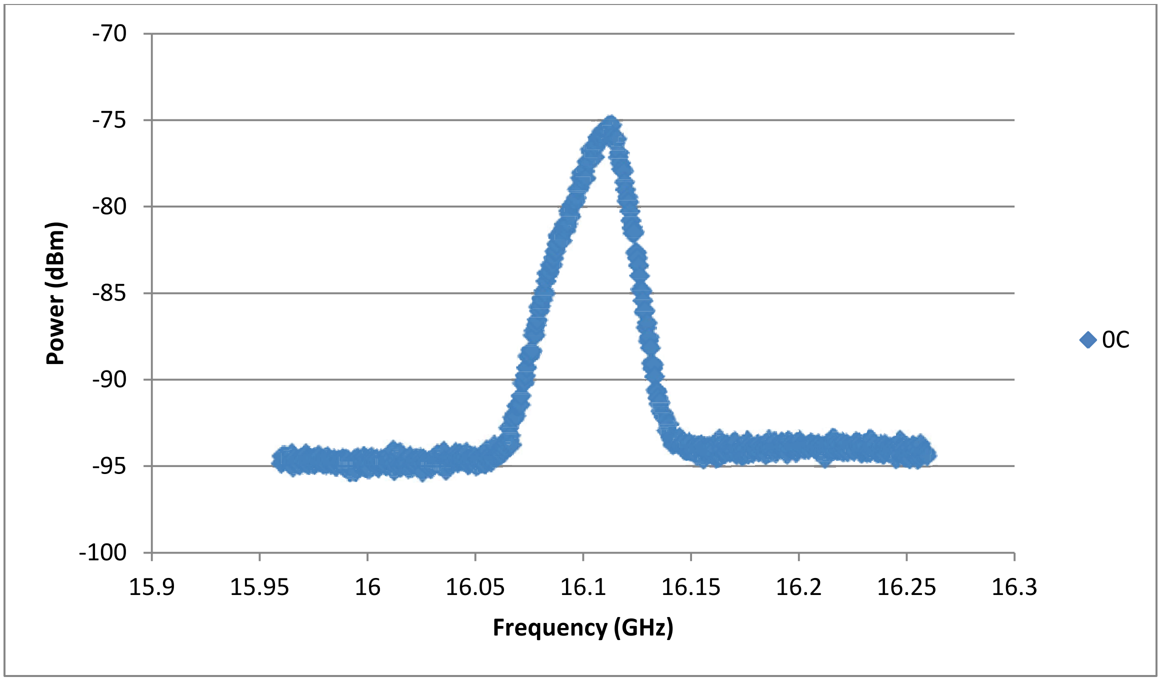

Figure E10: Beat note power versus frequency at 0˚C

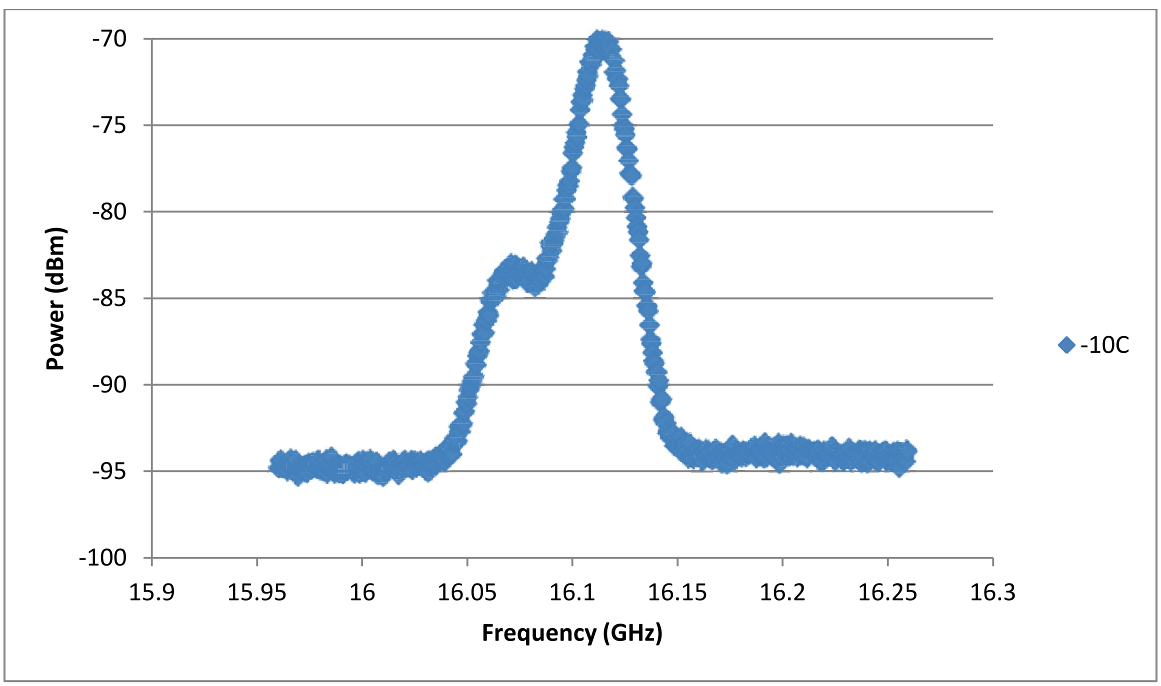

Figure E11: Beat note power versus frequency at -10˚C

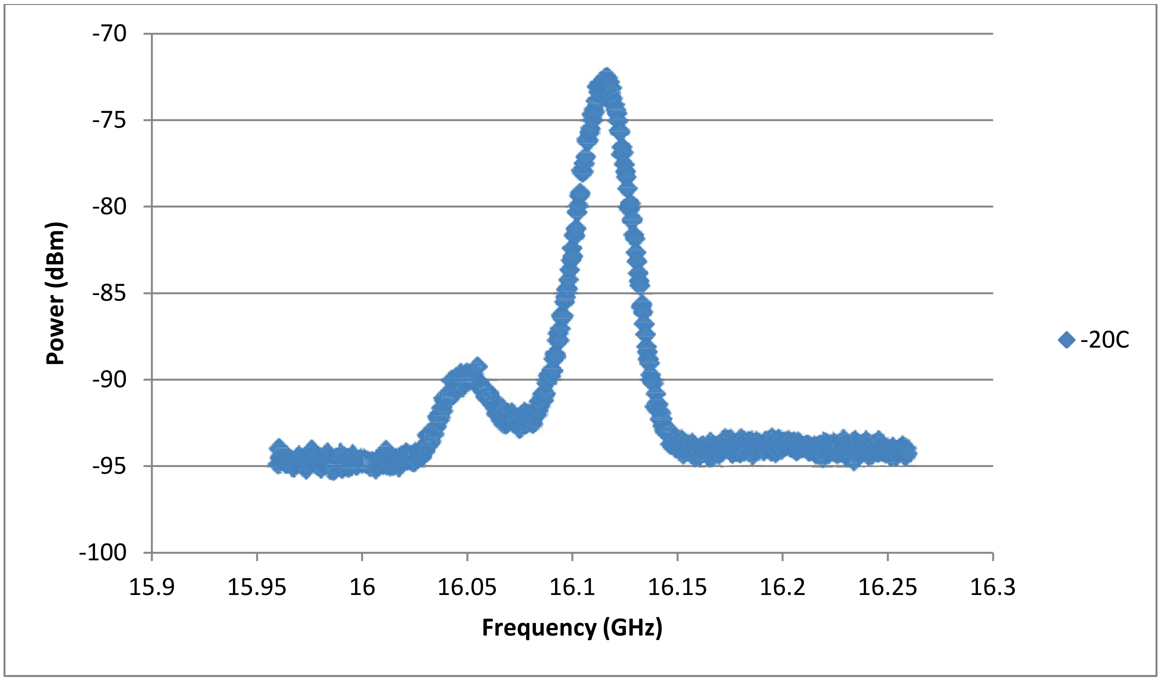

Figure E12: Beat note power versus frequency at -20˚C

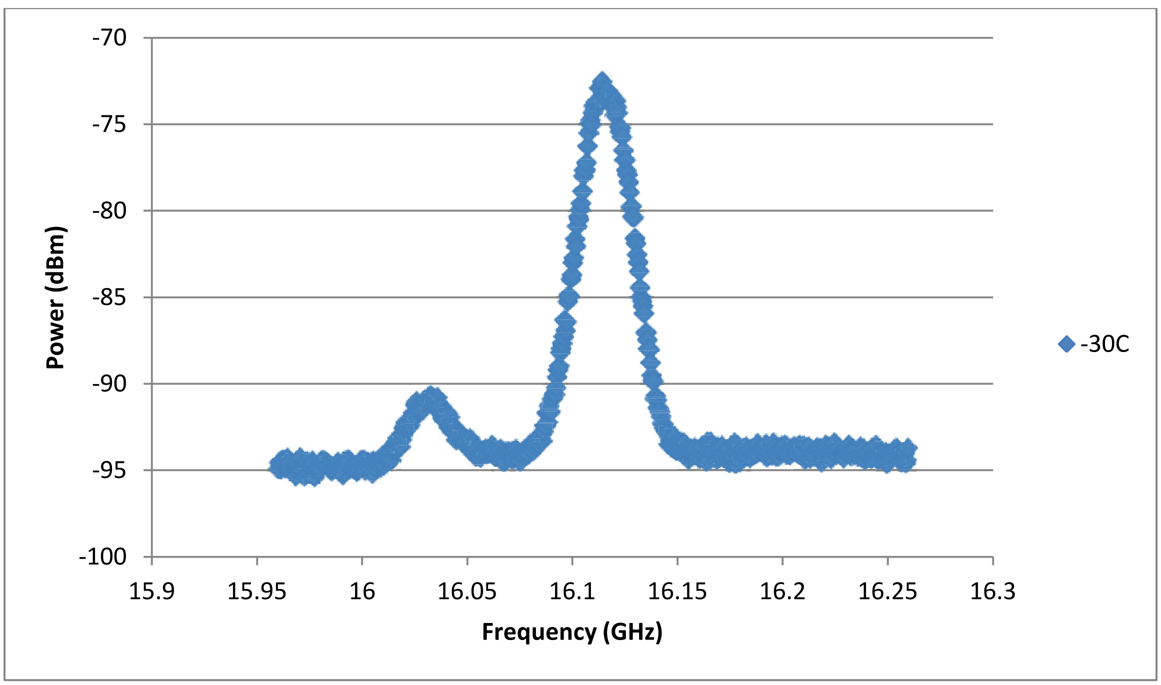

Figure E13: Beat note power versus frequency at -30˚C

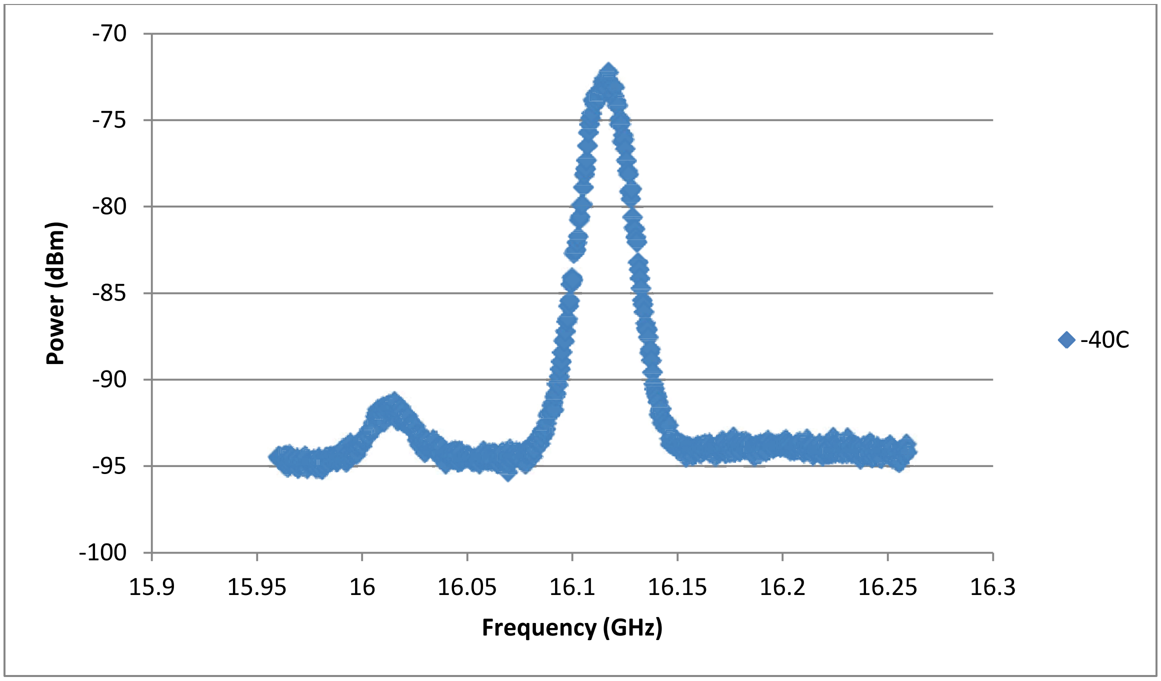

Figure E14: Beat note power versus frequency at -40˚C

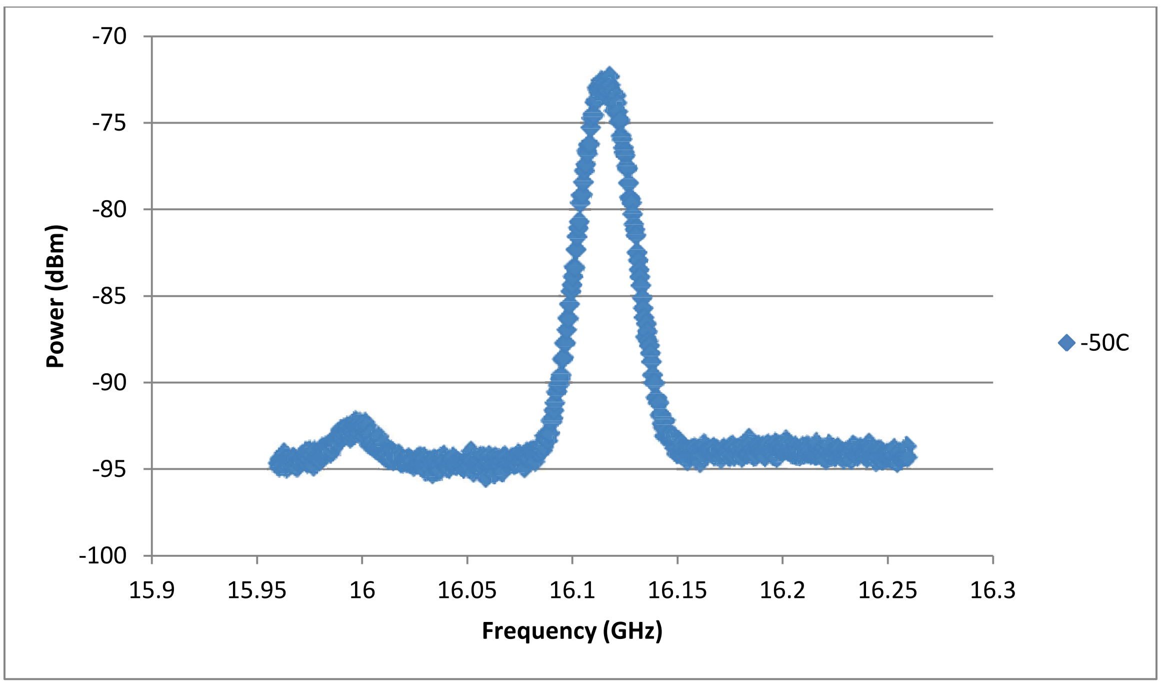

Figure E15: Beat note power versus frequency at -50˚C

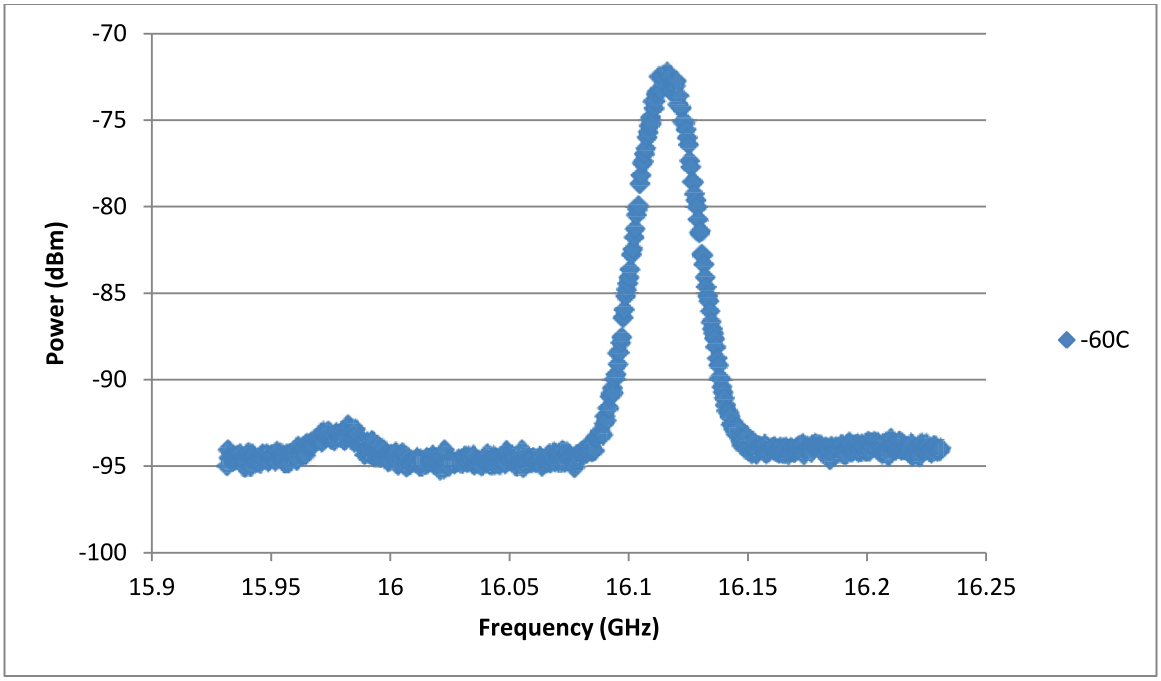

Figure E16: Beat note power versus frequency at -60˚C

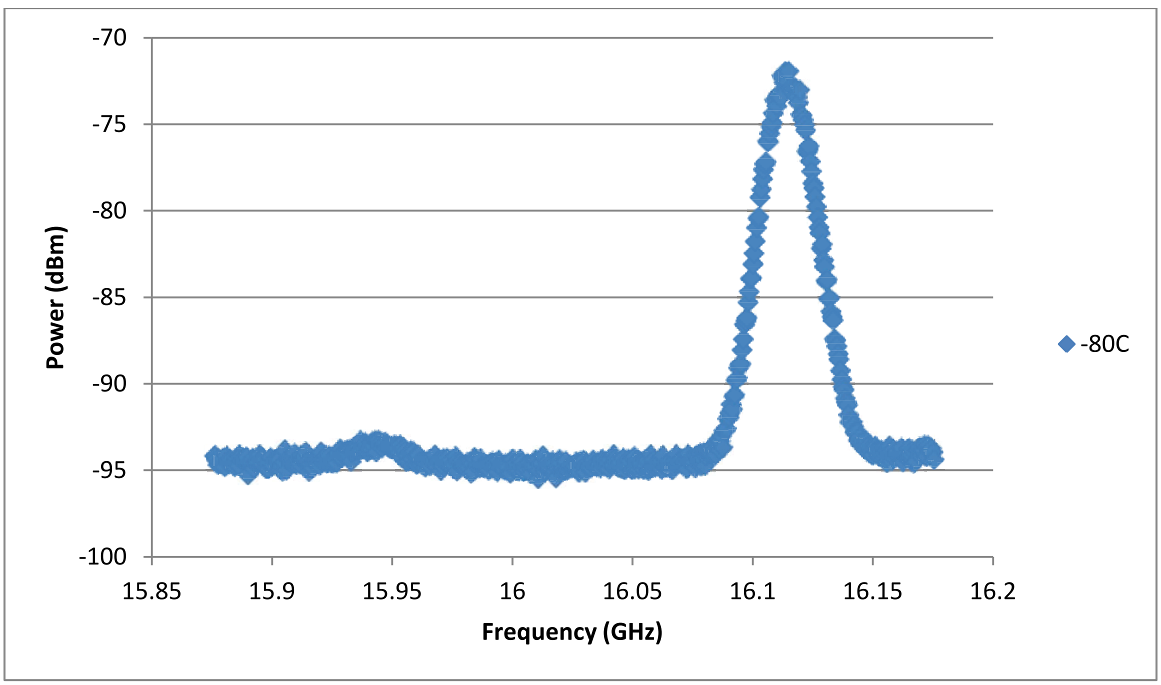

Figure E17: Beat note power versus frequency at -80˚C

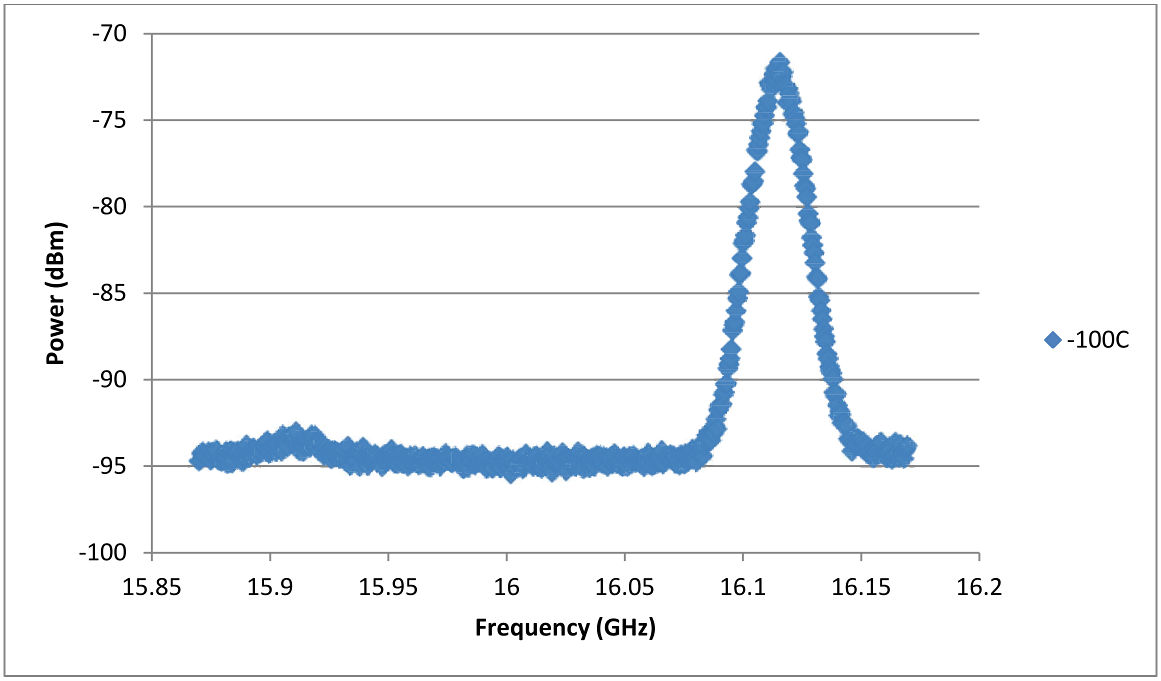

Figure E18: Beat note power versus frequency at -100˚C

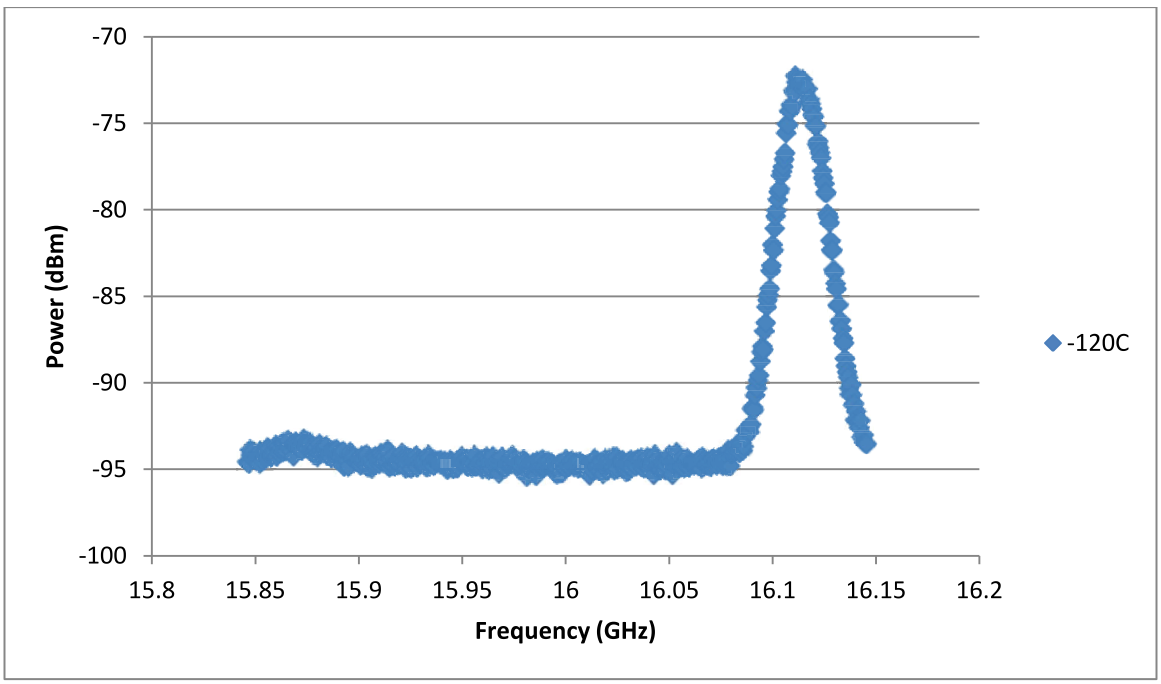

Figure E19: Beat note power versus frequency at -120˚C

14 References

Boyd, R. W. (2008). *Nonlinear Optics*. Burlington, MA: Academic Press.

Chiao, R. Y., Townes, C. H., and Stoicheff, B. P., (1964). Stimulated Brillouin Scattering and Coherent Generation of Intense Hypersonic Waves. *Physical Review Letters,* 21(12), 592-595. Doi:10.1103/PhysRevLett.12.592

Dajani, I., Zeringue, C., Bronder, T. J., Shay, T., Gavrielides, A., Robin, C. (2008). A theoretical treatment of two approaches to SBS mitigation with two-tone amplification. *Optics Express*, 18(16), 14233-14247. doi:10.1364/OE.16.014233

Fellay, A., Thevenaz, L., Garcia, J. P., Facchini, M., Scandale, W., Robert, P. (2002). Brillouin-based temperature sensing in optical fibres down to 1 K. *Optical Fiber Sensors*, 1, 301-304. doi:10.1109/OFS.2002.1000562

Galvanauskas, A. (2004, July). High Power Fiber Lasers. *Optics & Photonics News*, 42-47. doi:10.1364/OPN.15.7.000042

Hansryd, J., Dross, F., Westlund, M., Andrekson, P. A., & Knudsen, S. N. (2001). Increase of the SBS Threshold in a Short Highly Nonlinear Fiber by Applying a Temperature Distribution. *Journal of Lightwave Technology*, 11(19), 1691-1697. Retrieved from http://www.opticsinfobase.org/jlt/abstract.cfm?URI=jlt-19-11-1691

Hildebrandt, M., Buesche, S., Weßels, P., Frede, M., Kracht, D. (2008). Brillouin scattering spectra in high-power single-frequency ytterbium doped fiber amplifiers. *Optics Express*, 20(16), 15970-15979. doi:10.1364/OE.16.015970

Imai, Y., Shimada, N. (1993). Dependence of Stimulated Brillouin Scattering on Temperature Distribution in Polarization-Maintaining Fibers. *IEEE Photonics Technology Letters*, 11(5), 1335-1337. doi: 10.1109/68.250061

Ippen, E. P., Stolen, R. H. (1972). Stimulated Brillouin scattering in optical fibers. *Applied Physics Letters*, 11(21), 539-541. doi:10.1063/1.1654249

Jeong, Y., Nilsson, J., Sahu, J. K., Soh, D. B. S., Alegria, C., Dupriez, P., Codemard, C. A., Payne, D. N., Horley, R., Hickey, L. M. B., Wanzcyk, L., Chryssou, C. E., Alvarez-Chavez, J. A., Turner, P. W. (2005). Single-frequency, single-mode, plane-polarized ytterbium-doped fiber master oscillator power amplifier source with 264W of output power. *Optics Letters*, 5(30), 459-461. doi:10.1364/OL.30.000459

Keiser, G. (2000). WDM Concepts and Components. *Optical Fiber Communications* (399-402). Boston, MA: McGraw-Hill Higher Education.

Key, P. Y., Harrison, R. G. (1972). Role of Electrostriction, Absorption, and the electrocaloric Effect in the Stimulated Scattering of Light. *Physical Review A*, 5(4), 1839-1846. doi:10.1103/PhysRevA.5.1839

Kovalev, V. I., Harrison, R. G. (2006). Suppression of stimulated Brillouin scattering in high-power single-frequency fiber amplifiers. *Optics Letters*, 2(31), 161-163. doi:10.1364/OL.31.000161

Kurashima, T., Horiguchi, T., Tateda, M. (1990). Thermal effects on the Brillouin frequency shift in jacketed optical silica fibers. *Applied Optics*, 15(29), 2219-2222. doi:10.1364/AO.29.002219

Le Floch, S., Cambon, P. (2003). Study of Brillouin gain spectrum in standard single-mode optical fiber at low temperatures (1.4-370 K) and high hydrostatic pressures (1-250 bars). *Optics Communications*, 219, 395-410. doi:10.1016/S0030-4018(03)01296-3

Massey, S. M. (2008). Stimulated Brillouin Scattering Phase Conjugation in Fiber Optic Waveguides (Doctoral dissertation, Air Force Institute of Technology). Retrieved from http://oai.dtic.mil/oai/oai?verb=getRecord&metadataPrefix=html&identifier=ADA487254

Nikles, M., Thevenaz, L., & Robert, P. A. (1997). Brillouin Gain Spectrum Characterization in Single-Mode Optical Fibers. *Journal of Lightwave Technology*, 10(15), 1842-1851. doi: 10.1109/50.633570

Smith, R. G. (1972). Optical Power Handling Capacity of Low Loss Optical Fibers as Determined by Stimulated Raman and Brillouin Scattering. *Applied Optics*, 11(11), 2489-2494. doi:10.1364/AO.11.002489

Stolen, R. H. (1980). Nonlinearity in Fiber Transmission. *Proceedings of the IEEE*, 68(10), 1232-1236. doi:10.1109/PROC.1980.11837

Tang, C. L. (1966). Saturation and Spectral Characteristics of the Stokes Emission in the Stimulated Brillouin Process. *Journal of Applied Physics*, 37(8), 2945-2955. doi: 10.1063/1.1703144

Zhang, L., Liao, Y., Dai, Z., Ou, Z., Liu, Y., Peng, Z. (2006). Demodulated method of optical fiber stokes temperature sensors. *Optoelectronics Letters*,5(2), 345-347. doi: 10.1007/BF03033519